Detector Development & High-Z Sensor Characterisation at PSI

J. Mulvey, D. Greiffenberg, M. Anastasi, B. Schmitt, A. Bergamaschi, M. Brückner, M. Carulla, R. Dinapoli, S. Ebner, K. Ferjaoui, E. Fröjdh, V. Gautam, S. Hasanaj, V. Hinger, M. Hürst, V. Kedych, T. King, S. Li, L. Lunin C. Lopez Cuenca, A. Mazzoleni, D. Mezza, K. Moustakas, A. Mozzanica, M. Müller, C. Ruder, S. Silletta, D. Thattil, X. Xie, J. Zhang

PSI Center for Photon Science, 5232 Villigen PSI, Switzerland

University of Birmingham, 15th July 2026

PSI Center for Photon Science

Introduction to PSI

- **Science at PSI**
- **User Facilities – SLS, SwissFEL, etc.**
- **Photon Science Detector Group – How we support user facilities**

High-Z Characterisation at PSI

- Overview of High-Z materials
- GaAs
- CZT

High-Z Future & Applications

- Photon Science
- Medical Physics
- Astronomy

The Paul Scherrer Institut

PSI - Swiss federal research facility

- Largest Swiss research institute for natural and engineering sciences
- Hosts large scale research infrastructure including:
- SINQ – Neutron scattering
- SμS – Muons
- COMET – Proton therapy
- CHRISP – Particle Physics

SLS2.0

- SLS since 2001
- SLS2.0 since 2025

SwissFEL

- Since 2016
- First user operation in 2019

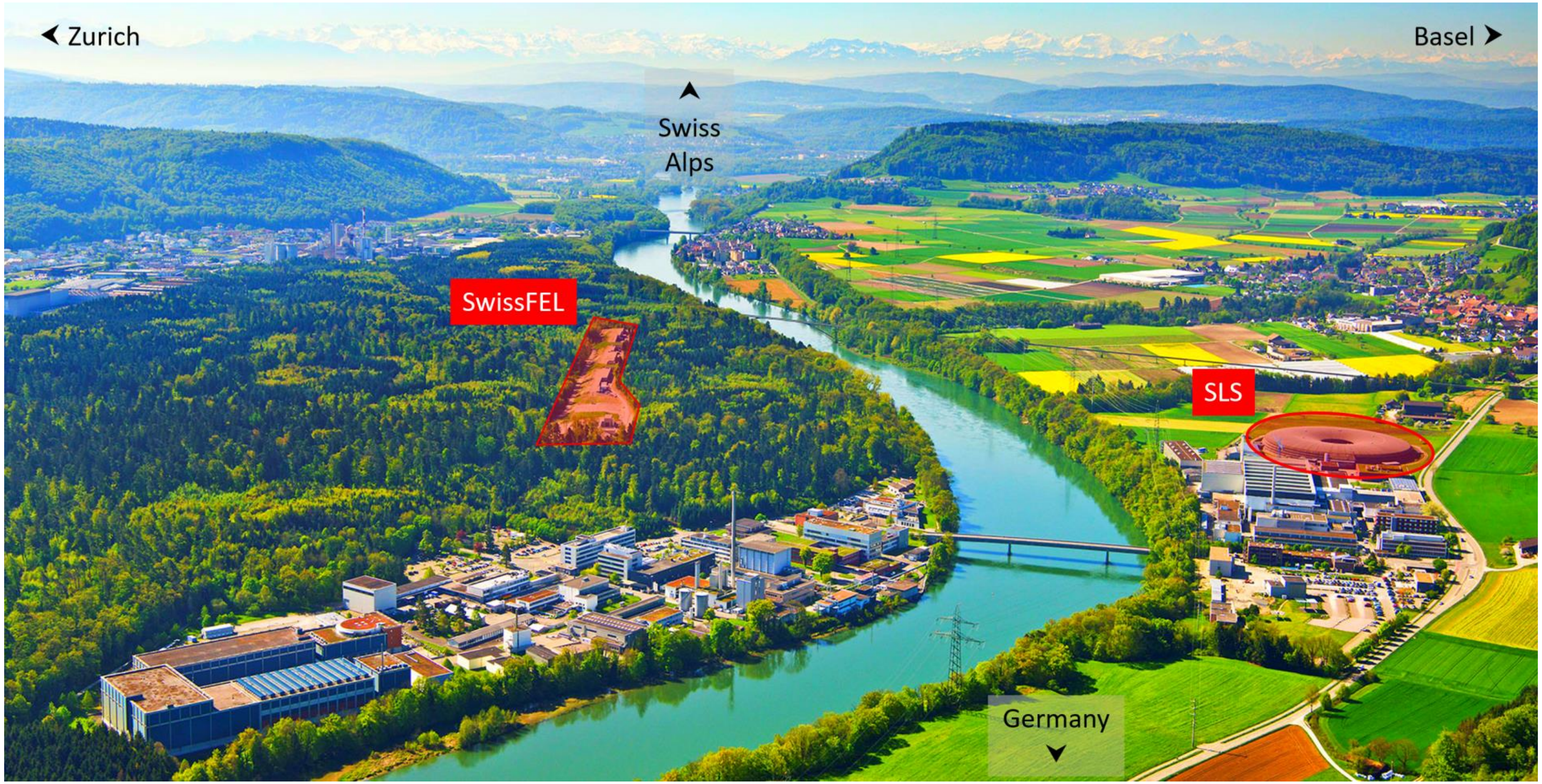

~ 2200 Employees | ~320 PhD Students | ~200 Postdocs

Swiss Light Source 1.0 (SLS)

➢ Electron accelerator	← 2.4 GeV electrons in 12 ps bunches
➢ 3rd generation synchrotron source	← 288m circumference
➢ Utilizes Bremsstrahlung to generate X-rays	← 5.4 keV median energy
➢ Multiple electron bunches in circulation	← 400 mA total current (< 10 mA per bunch)
➢ Not typically coherent	← partially with undulators
➢ X-ray energy selected through a monochromator	← 100 eV up to 40 keV (> 100 keV for SLS2.0)

M. Böge [1]

Mitchell et al [2]

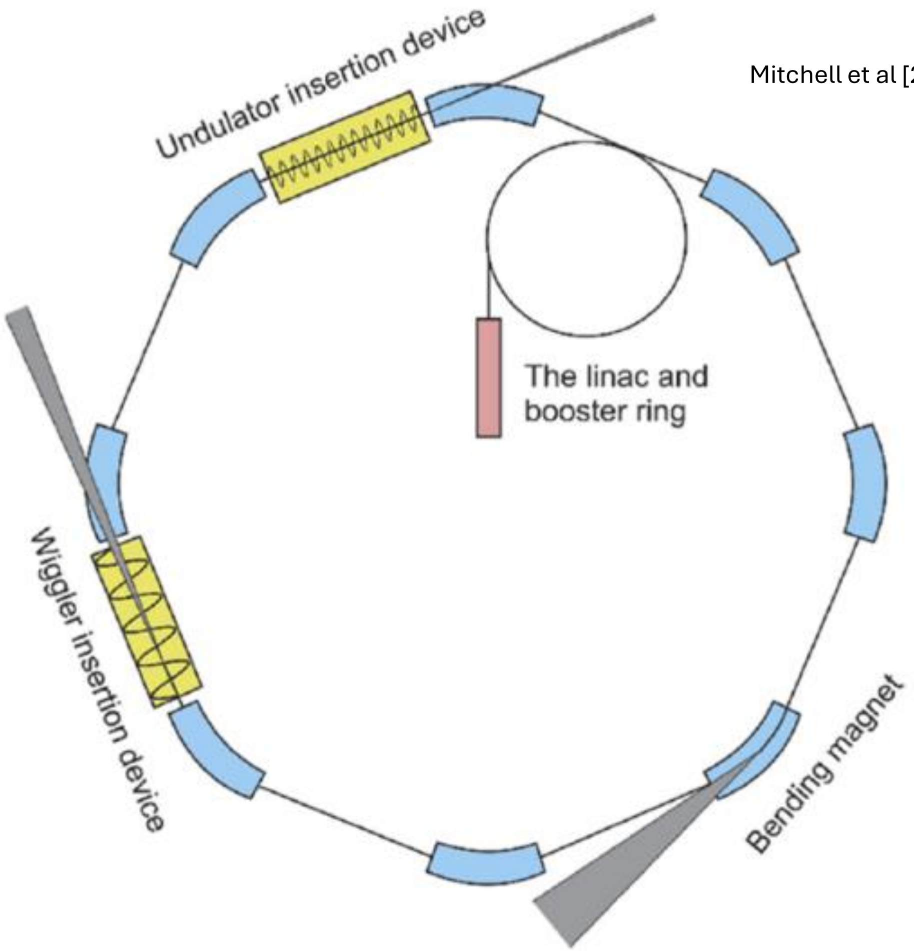

From SLS1.0 to SLS2.0

➢ SLS1.0	→ SLS2.0
➢ 3rd Generation Synchrotron light source	→ 4th Generation
➢ 2.4 GeV electrons	→ 2.7 GeV electrons
➢ 288m circumference	→ Still 288m
➢ 400 mA total current	→ Remains 400 mA
➢ 100 eV up to 40 keV	→ > 100 keV (50% higher flux at these energies)

Mitchell et al [2]

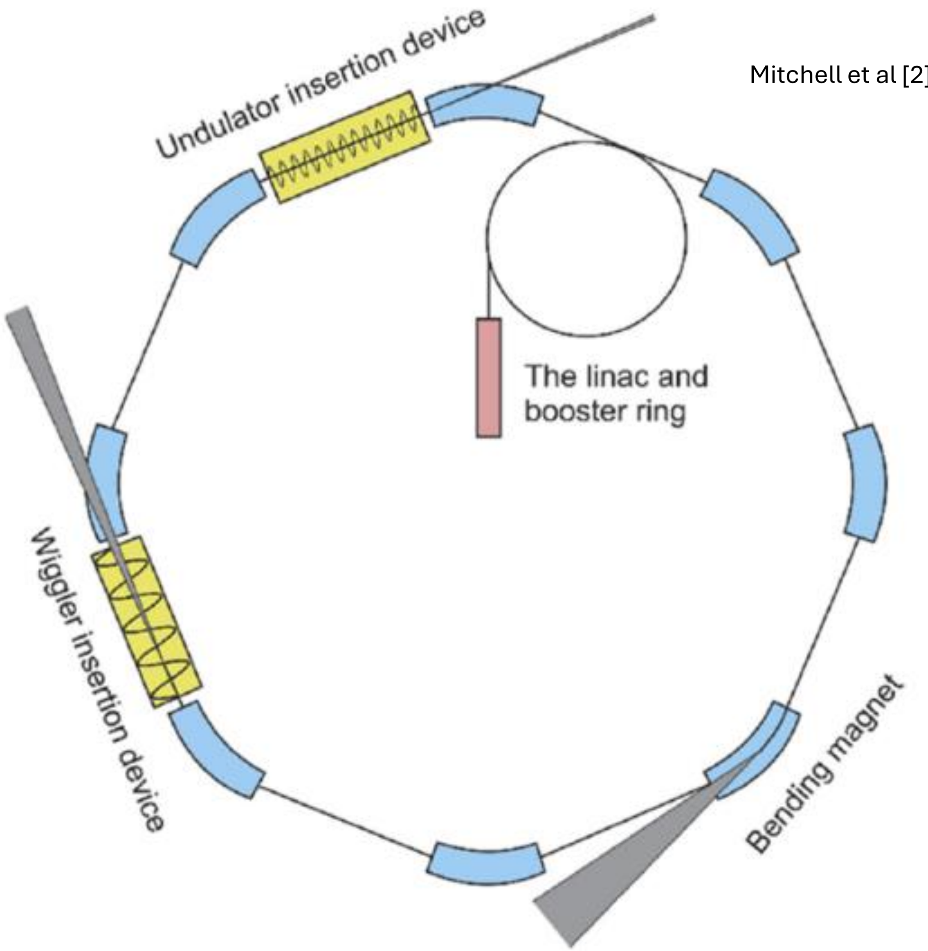

M. Böge [1, 3]

Swiss Fast Electron Laser (SwissFEL)

- High spatial and temporal coherence (laser-like)
- 2.1 - 5.8 GeV electrons
- Extremely short pulse duration (1 – 20 fs)
- 100 Hz repetition rate
- Photon energy between 0.25 and 12 keV
- Order of 10^{10} photons per 12 keV

[4]

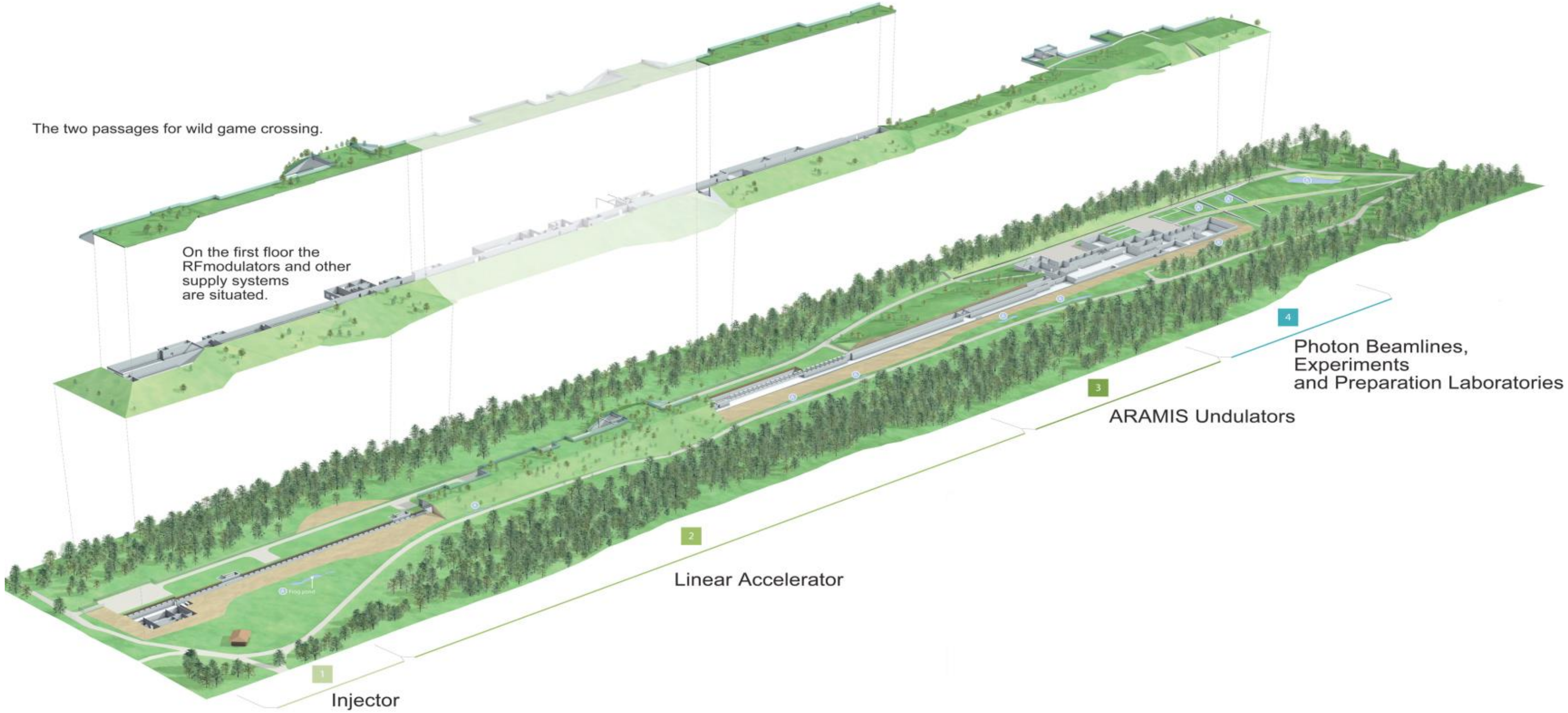

Photon Science Applications

Synchrotron

- High-res imaging (ptychography down to nm range)
- Structure determination (crystallography, X-ray diffraction)
- Absorption imaging (tomography)
- Spectroscopy (element specific)

FEL

- Ideal for probing dynamic systems on the scale of fs
- Damage-free "diffraction before destruction"
- Single-shot imaging

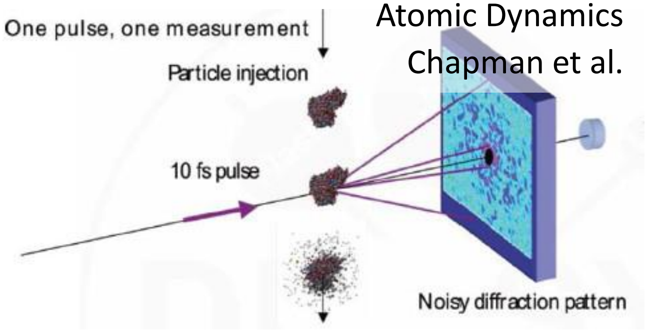

Atomic Dynamics
Chapman et al.

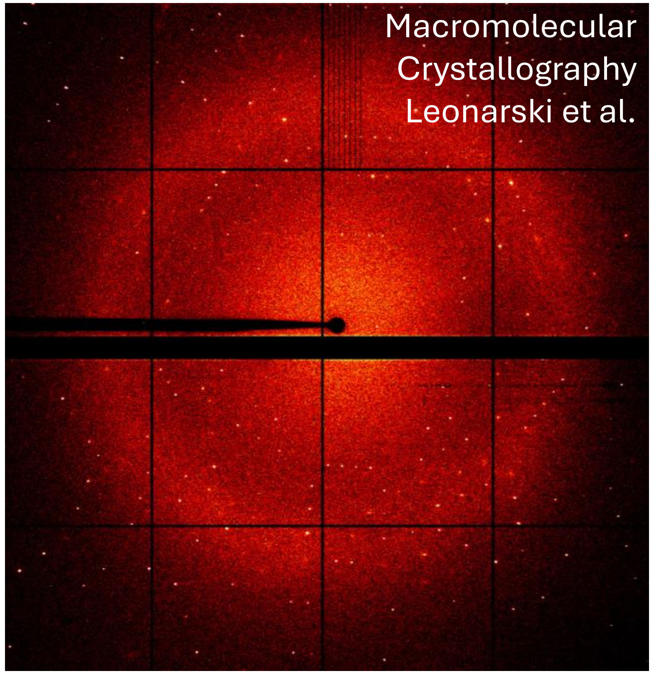
Macromolecular Crystallography
Leonarski et al.

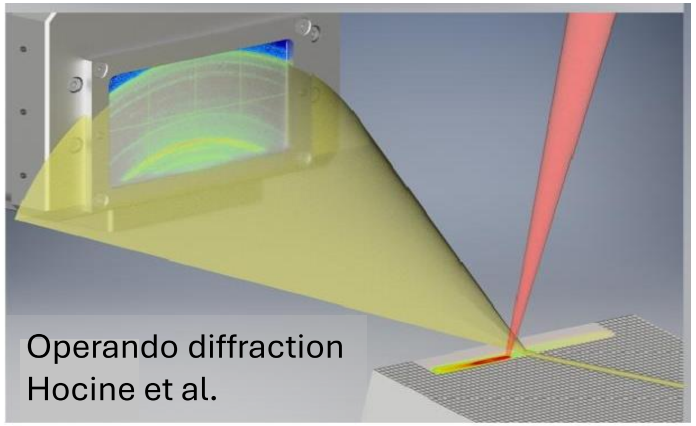
Operando diffraction
Hocine et al.

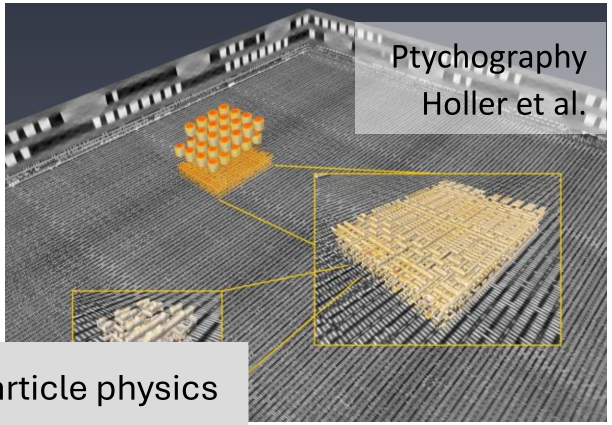
Ptychography
Holler et al.

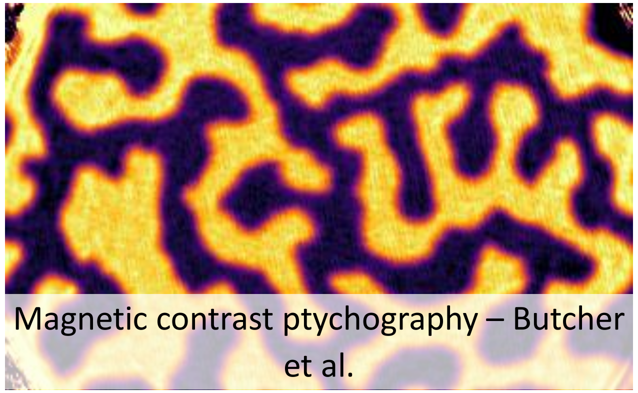
Magnetic contrast ptychography – Butcher et al.

Similarly to particle physics

- Use the diffraction pattern to work back to understand structure of crystal/protein/etc. under test

Detector Requirements

- Small pixels < 100 µm (even 5 µm)
- Energy range: eV → ~ 100 keV
- Count rate per pixel:
  - SLS 1.0: Few MHz
  - SLS 2.0: 10s MHz
  - SwissFEL: 100 THz
- Large area: 16Mpixel (32x32 cm^2)
- High frame rates: ~10 kHz

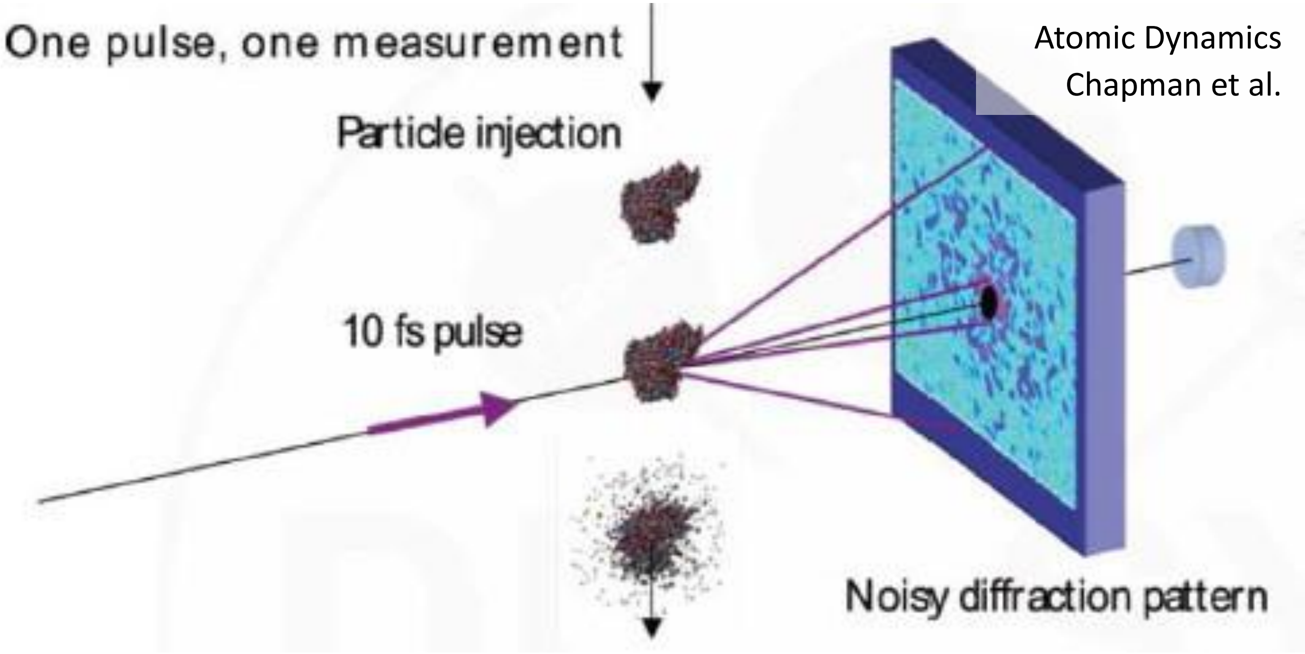

Atomic Dynamics
Chapman et al.

We've already come a long way…

W. Röntgen, 1895

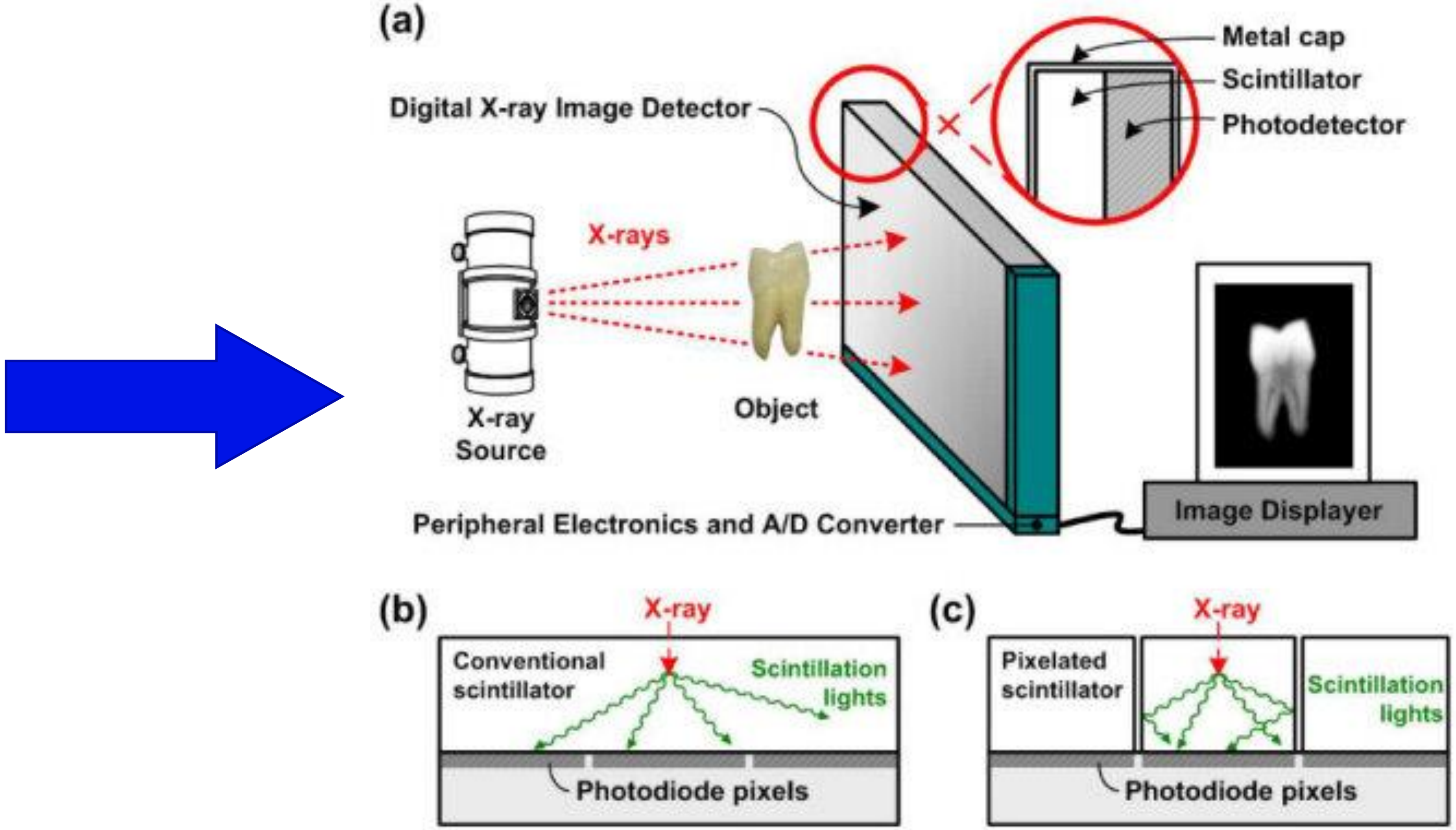

P. G. Jung [5]

Hybrid detectors – A step forward

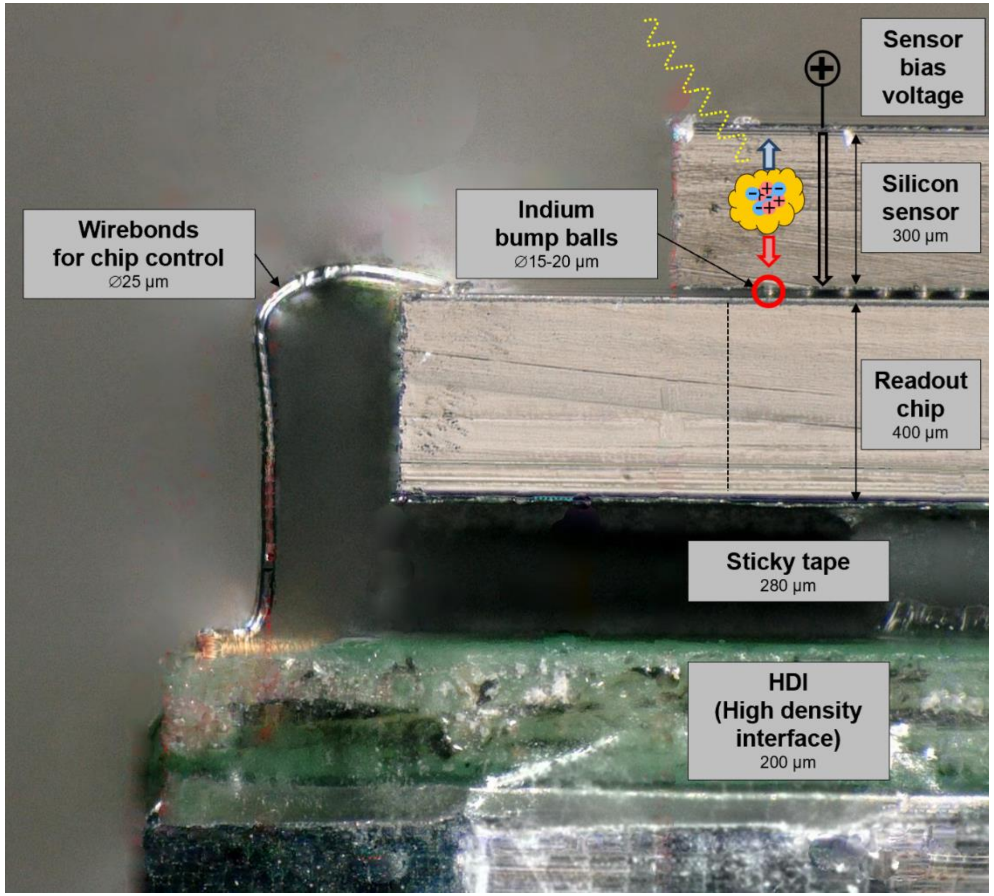

Hybrid sensors fit our requirements

- ➢ Semiconductor sensor
  - ➢ Direct conversion
- ➢ Bump bonding
  - ➢ Minimum pixel pitch ~ 20 µm
  - ➢ Noise due to input capacitance
- ➢ Versatile CMOS readout chip
  - ➢ Fast readout
  - ➢ Radiation hardness

Readout Modes

Photon counting

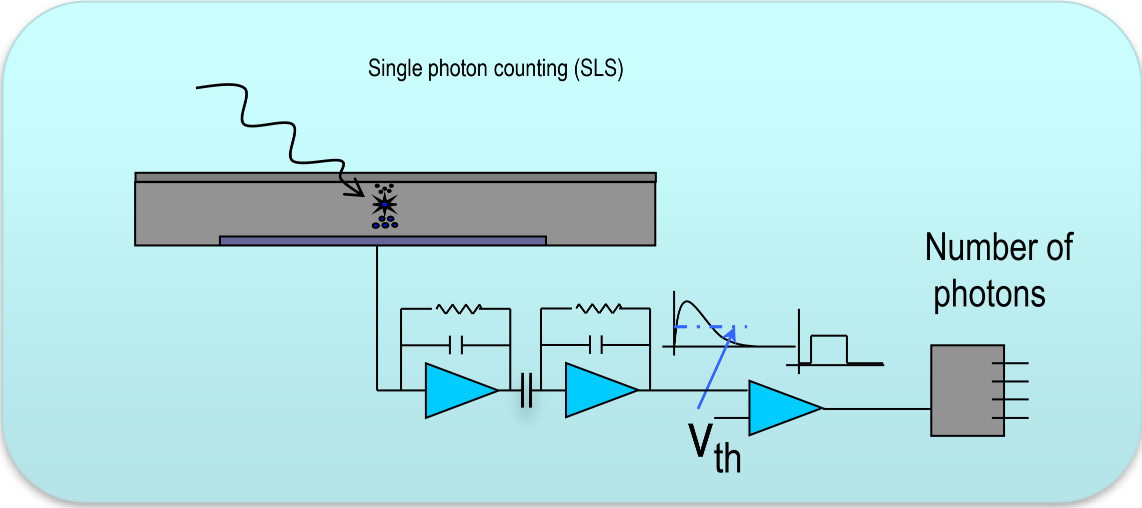

Count rate limited

Charge integrating

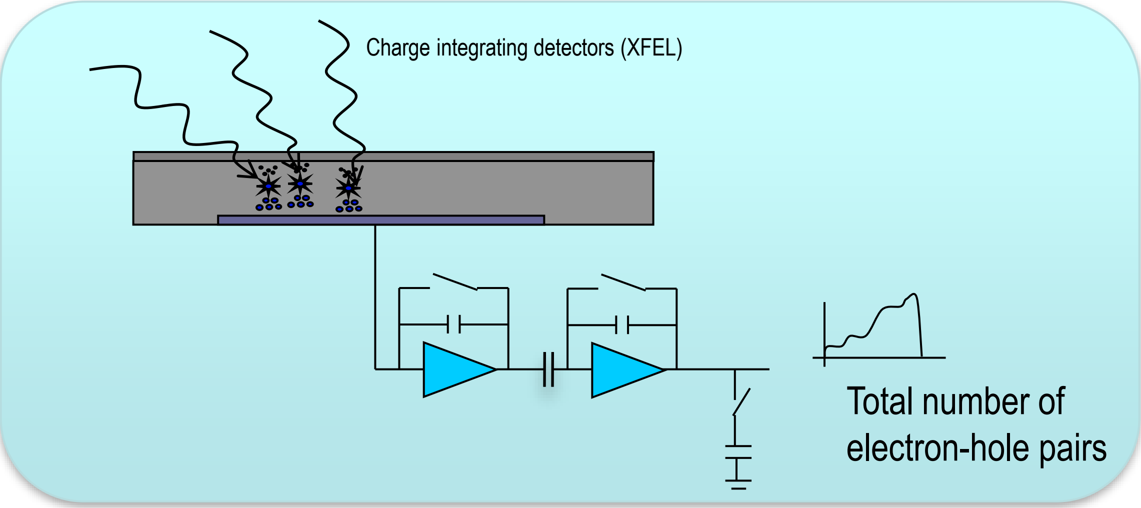

Dynamic range limited

Readout Modes

Photon counting

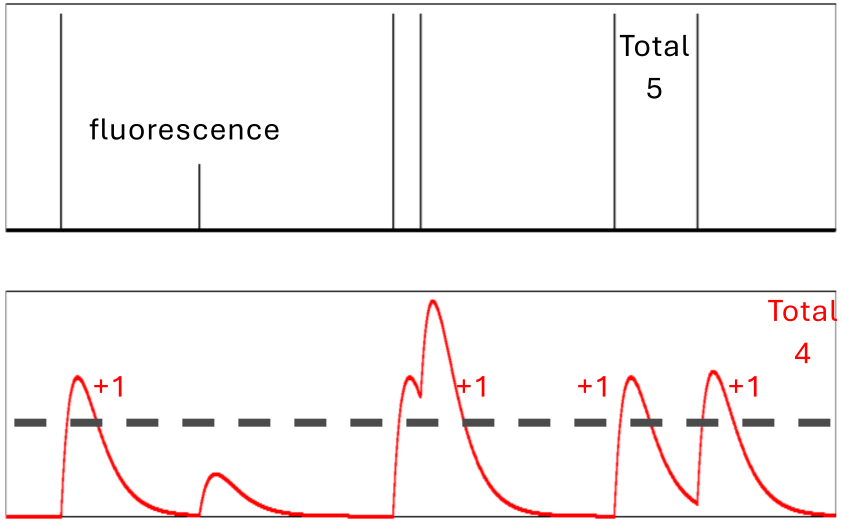

- ✓ Noiseless, very large dynamic range
- ✓ Stable operation, well established calibration
- ✓ Fluorescence suppression
- ✓ Frame rate scales with counter depth
- ✗ Pile-up ≳1MHz/pixel
- ✗ Soft X-ray detection prevented by noise

Charge integrating

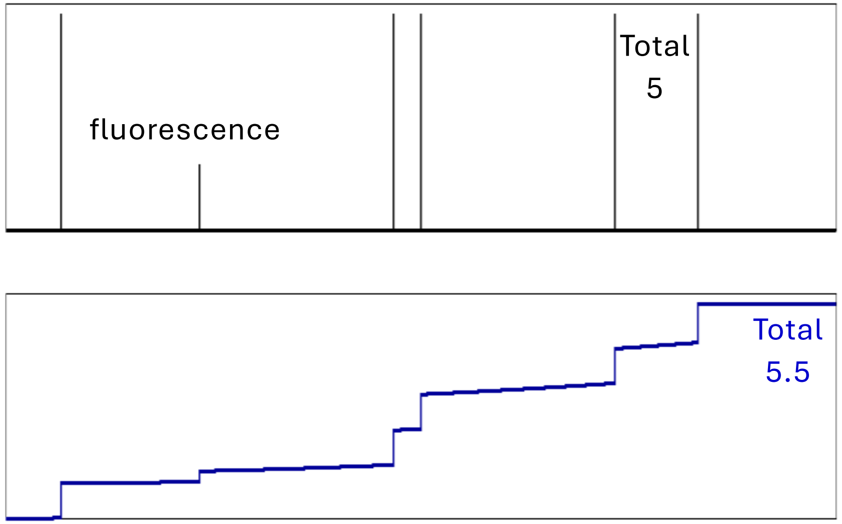

- ✓ Compromise between noise and dynamic range
- ✓ Works also at pulsed sources
- ✓ Detection of multiple soft X-rays
- ✗ Saturation for long integration times

PSI Detector portfolio

	Microstrip 1D	Pixel 2D	
	25/50 µm pitch	75 µm pitch	25 µm pitch
Single photon counting	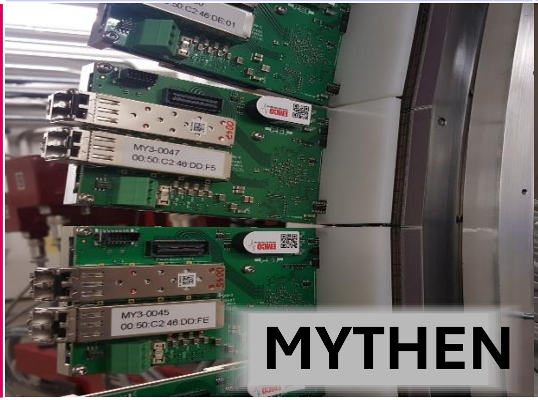		
Charge integrating			

(Almost) Everything in-house

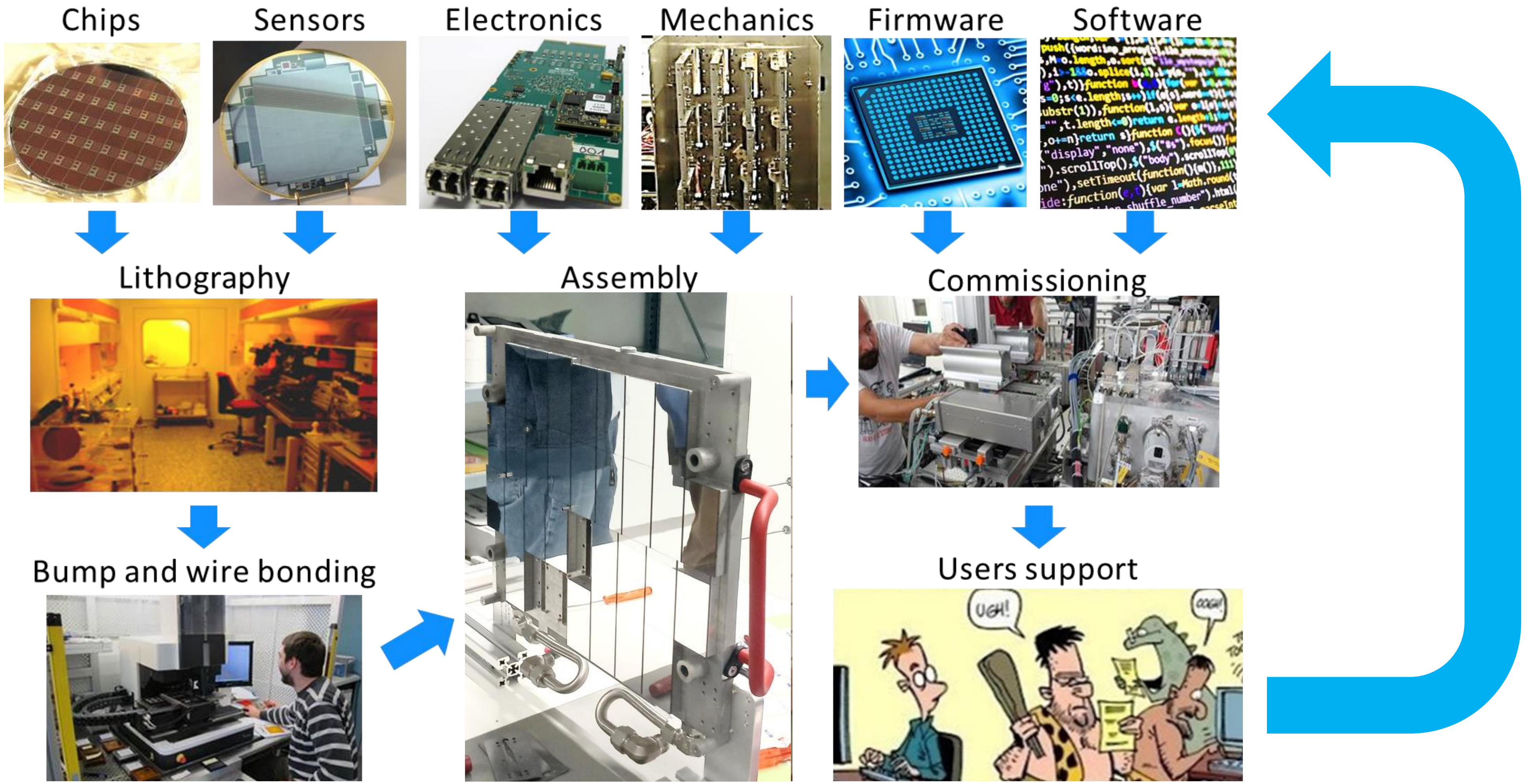

The JUNGFRAU ASIC

PSI

- **Charge integrating**
- Low noise
- Dynamic per-pixel gain switching
- **75 µm pitch**
- **256 x 256 pixels** per 2 x 2 cm^2 chip
- Can resolve single photons in highest gain

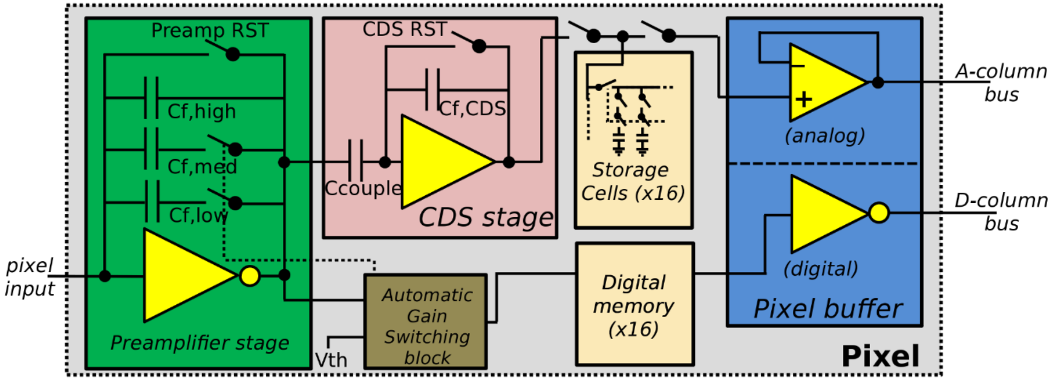

A. Mozzanica, 2014 [6]

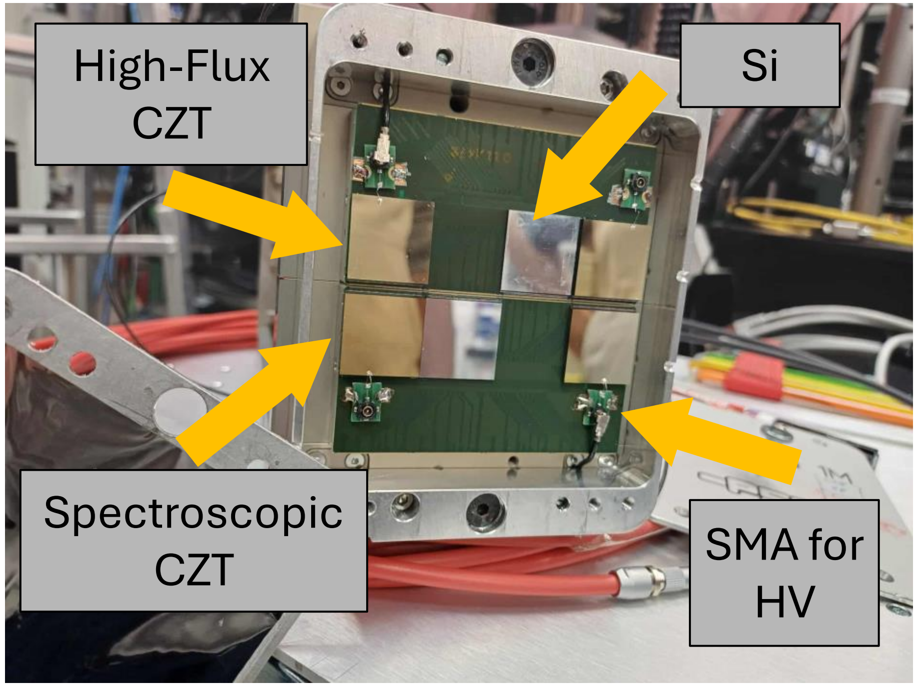

JUNGFRAU's charge integrating architecture allows us to probe sensor properties, such as the afterglow effect, in greater detail

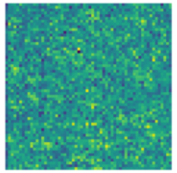

Raw Frame

Subtract Dark Image

Cluster

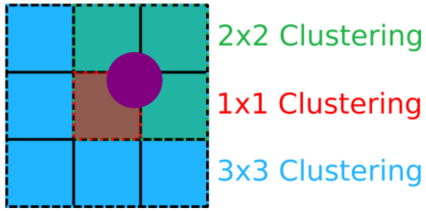

The JUNGFRAU ASIC

- **Charge integrating**
- Low noise
- Dynamic per-pixel gain switching
- **75 µm pitch**
- **256 x 256 pixels** per 2 x 2 cm^2 chip
- Can resolve single photons in highest gain

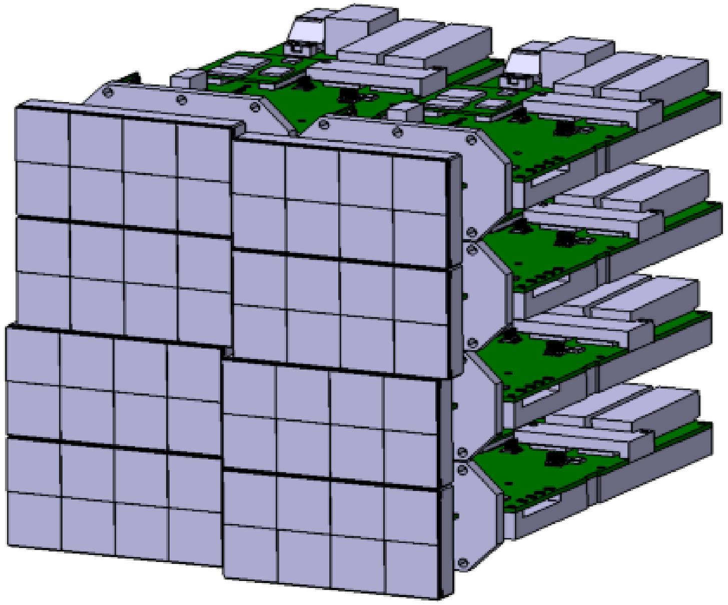

JUNGFRAU's charge integrating architecture allows us to probe sensor properties, such as the afterglow effect, in greater detail

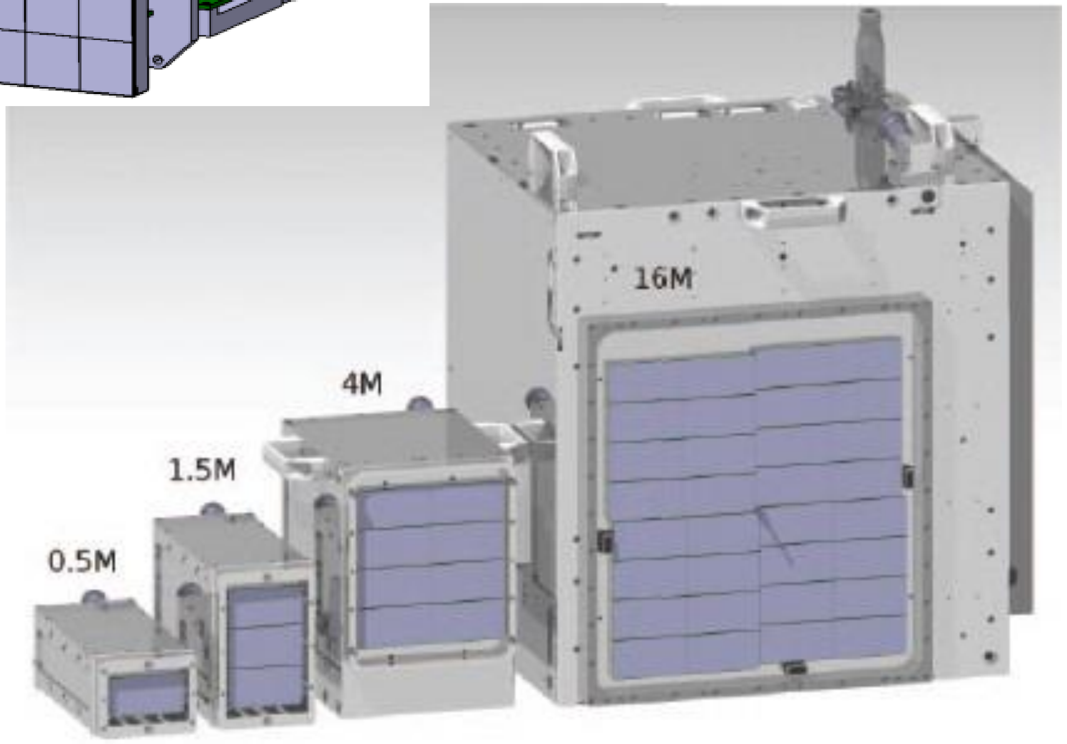

- Large areas (16Mpixels) can be achieved by tiling modules

Upgraded Light Sources: Many More Photons!

PSI

Photon counting

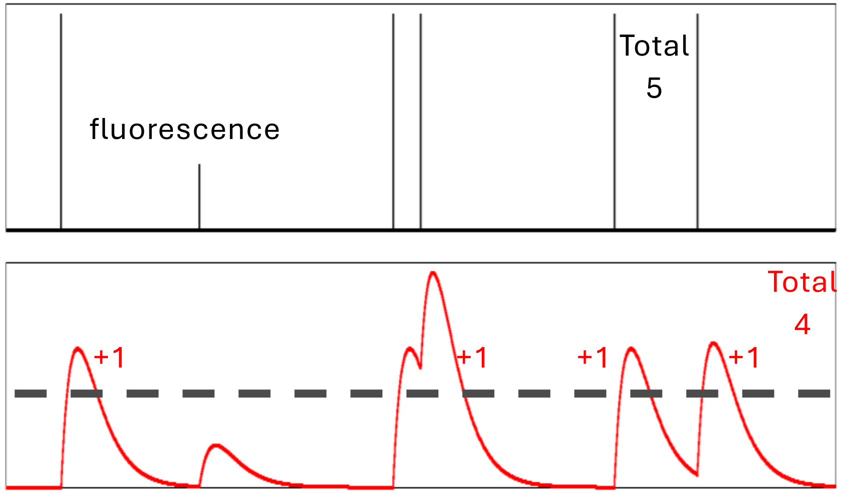

- ✓ Noiseless, very large dynamic range
- ✓ Stable operation, well established calibration
- ✓ Fluorescence suppression
- ✓ Frame rate scales with counter depth
- ✗ Pile-up ≳1MHz/pixel
- ✗ Soft X-ray detection prevented by noise

Charge integrating with adaptive gain

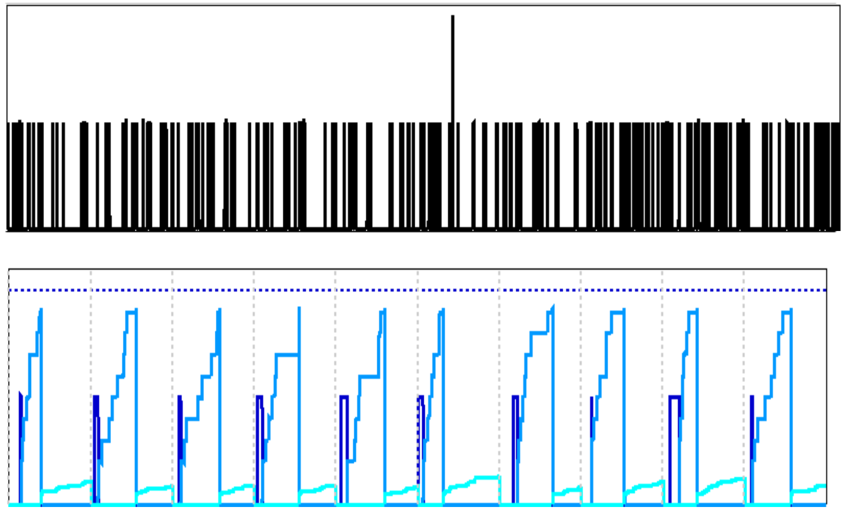

- ✓ Single photon resolution for hard/tender X-rays
  - ✓ Detection of multiple soft X-ray
- ✓ Works also at pulsed sources
- ✓ Dynamic range up to ~10^4 photons/pixel/s
- ✓ **Supported flux scales with frame rate**
- ✗ Saturations for long integration times
- ✗ **Challenging calibration and cumbersome data processing needs high throughput!**

Upgraded Light Sources: Many More Photons!

Photon counting

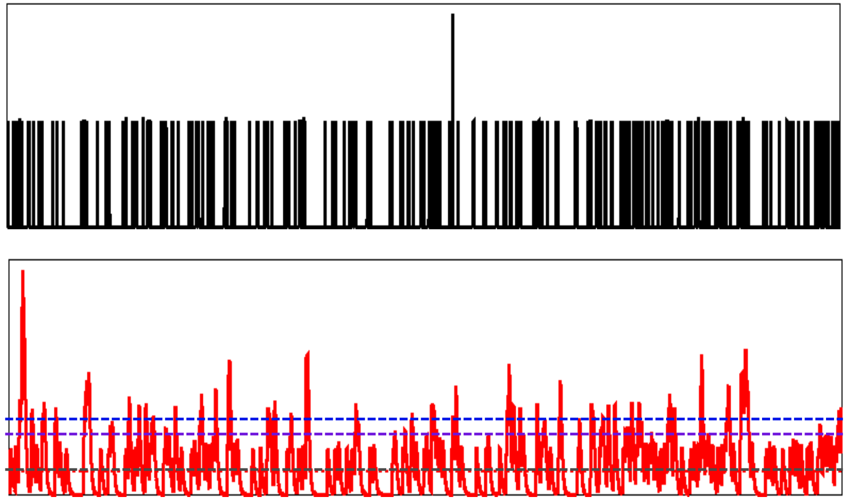

- ✓ Noiseless, very large dynamic range
- ✓ Stable operation, well established calibration
- ✓ Fluorescence suppression
- ✓ Frame rate scales with counter depth
- ✓ **Faster shaping, pile-up tracking**
- ✗ Pile-up ≳1MHz/pixel
- ✗ Soft X-ray detection prevented by noise

Charge integrating with adaptive gain

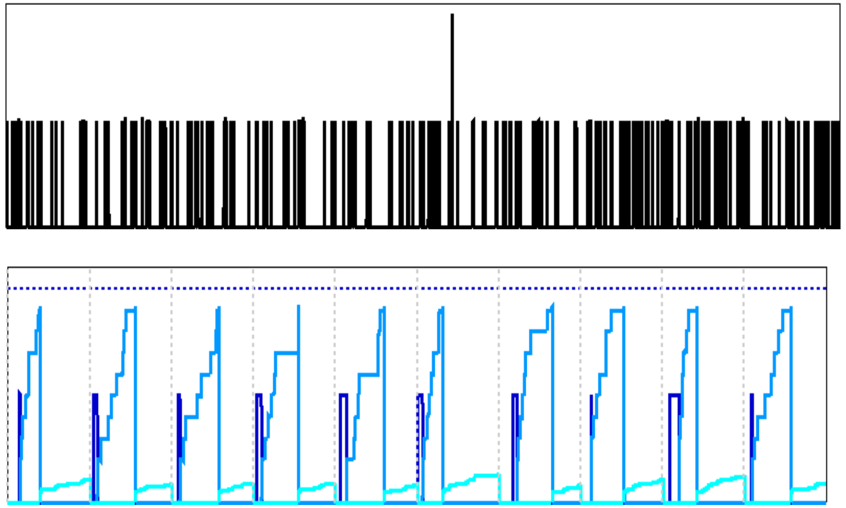

- ✓ Single photon resolution for hard/tender X-rays
  - ✓ Detection of multiple soft X-ray
- ✓ Works also at pulsed sources
- ✓ Dynamic range up to ~10^4 photons/pixel/s
- ✓ **Supported flux scales with frame rate**
- ✗ Saturations for long integration times
- ✗ **Challenging calibration and cumbersome data processing needs high throughput!**

PSI Detector portfolio

	Microstrip 1D	Pixel 2D	
	25/50 µm pitch	75 µm pitch	25 µm pitch
Single photon counting	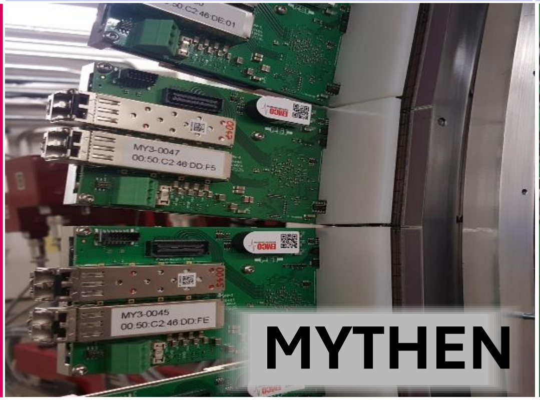	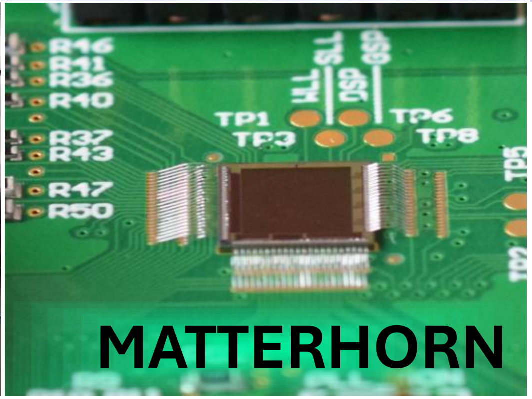	
Charge integrating			

Silicon has limits

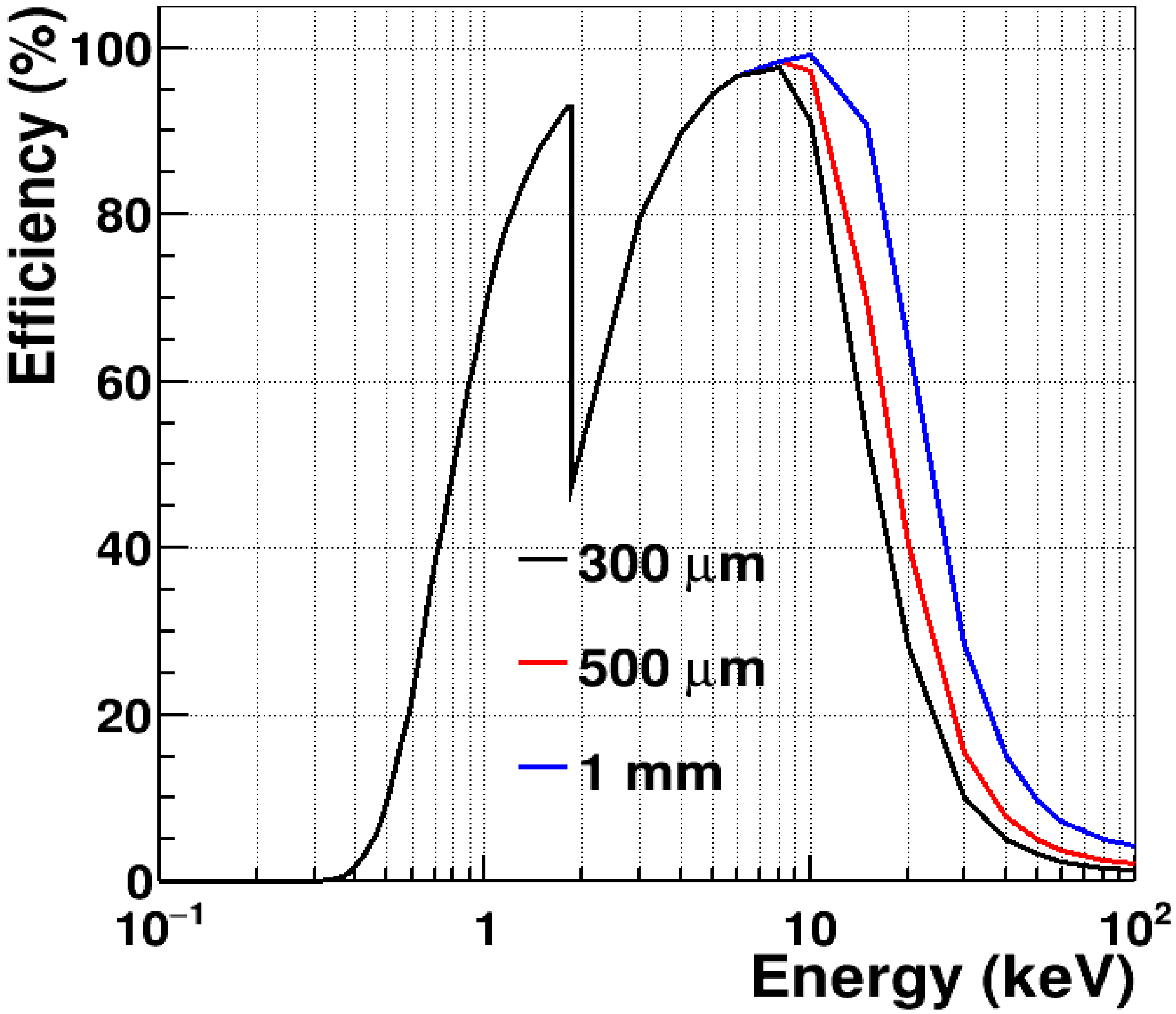

Frontiers of Photon Detectors

Silicon

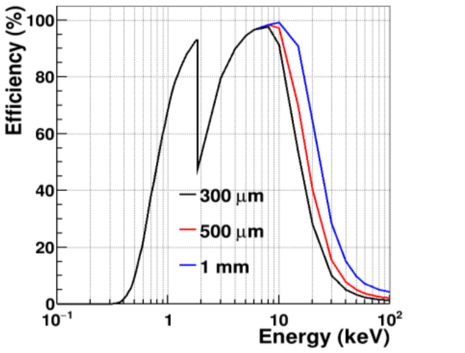

Low Energy (< 1 keV)

LGAD

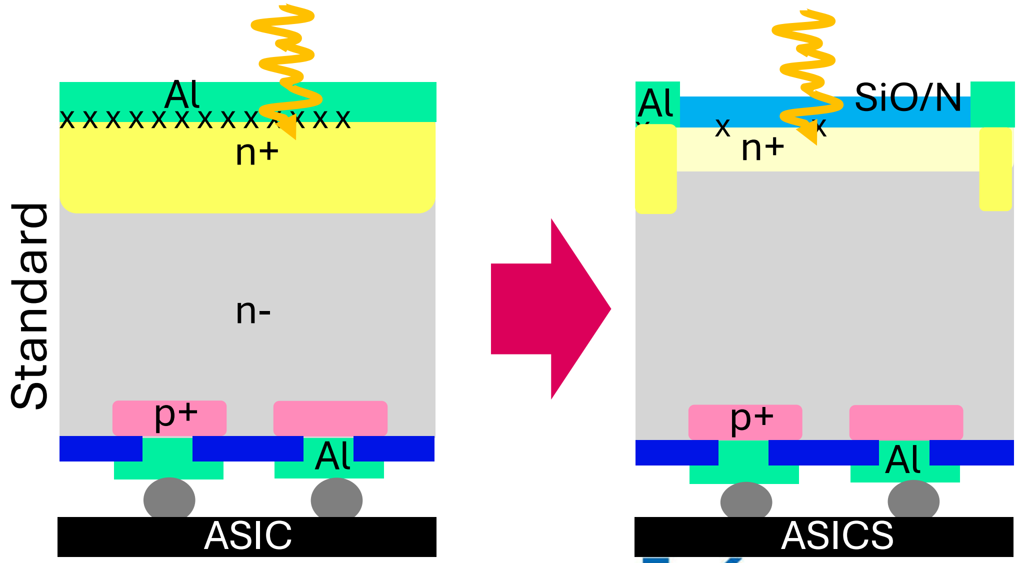

Zhang, *et al. JINST* 2022; 17(11): C11011.

FONDAZIONE BRUNO KESSLER

High Energy (> 40 keV)

High-Z

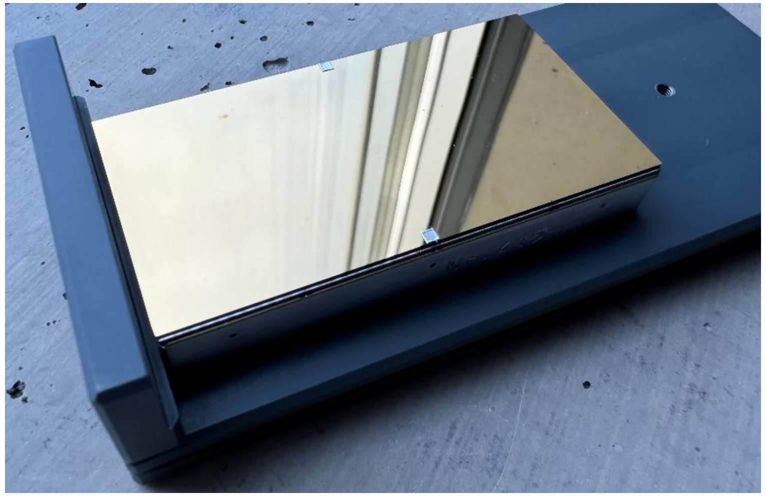

PSI Center for Photon Science

Introduction to PSI

- Science at PSI
- User Facilities – SLS, SwissFEL, etc.
- Photon Science Detector Group – How we support user facilities

High-Z Characterisation at PSI

- **Overview of High-Z materials**
- **GaAs**
- **CZT**

High-Z Future & Applications

- Photon Science
- Medical Physics
- Astronomy

The Need For A New Material

SLS 2.0 (4th gen. synchrotron)

- Increased flux for photon energies **> 20 keV**
- **Silicon** (low-Z) **inefficient** in this range

High-Z

- Higher atomic number → Stops more hard X-rays
- Three varieties we have worked with: **GaAs:Cr, CdTe, CdZnTe**
- Thinner is better for charge sharing, but stops less

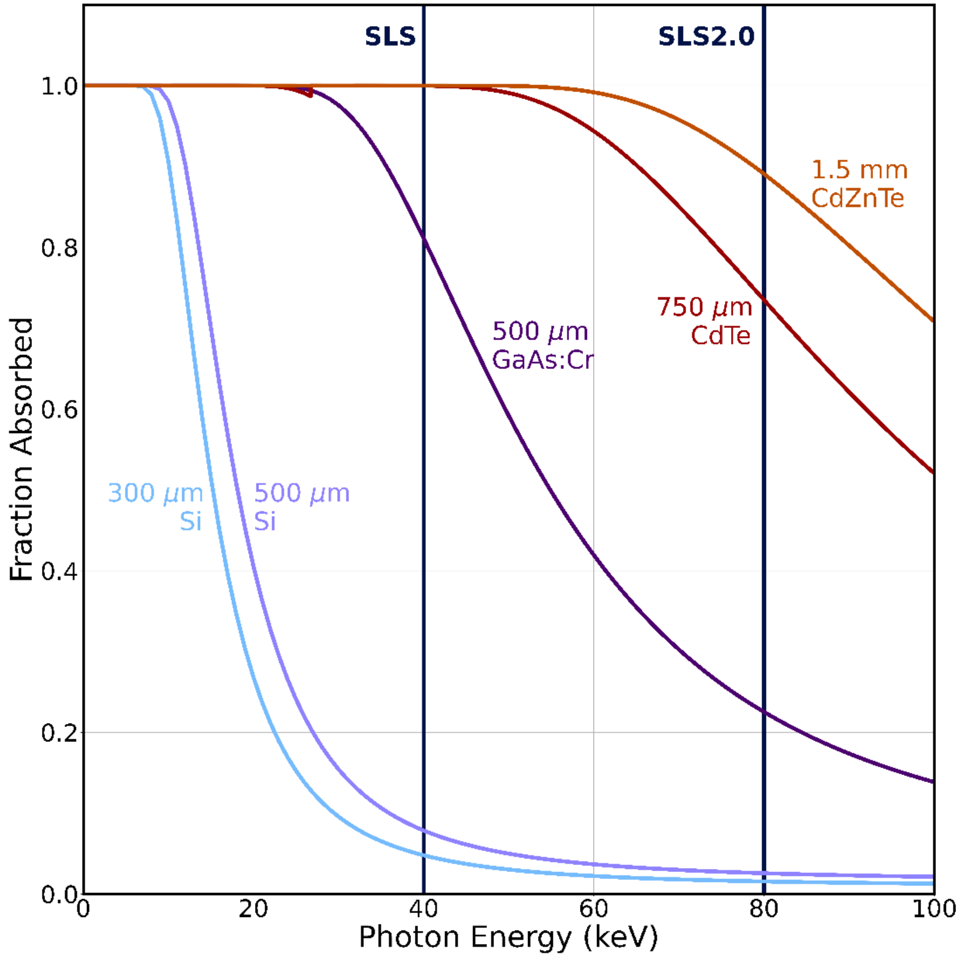

High-Z Sensors

	GaAs:Cr	CdTe (e⁻ Schottky type)	CdTe (Ohmic type)	CdZnTe (Spectroscopic/ High flux)
Raw material	Unknown commercial supplier	ACRORAD (JP)	ACRORAD (JP)	REDLEN (CA)
Processing	• ~~TSU (RU)~~ • ADVAFAB (FIN) • DECTRIS (CH)	ACRORAD (JP) (Contacts)	ACRORAD (JP) (Contacts)	REDLEN (CA)
Bump bonding	• TSU→PSI • ADVAFAB→ADVAFAB • DECTRIS→DECTRIS	ADVAFAB	ADVAFAB	ADVAFAB
Contacts	Ni/GaAs:Cr/V	Pt/CdTe/Al	Pt/CdTe/Pt	Au/CdZnTe/Au Pt/CdZnTe/Au
Thickness	500 μm	750 μm	750 μm	1500-2000 μm
Test systems	JUNGFRAU MÖNCH GOTTHARD	JUNGFRAU MYTHEN GOTTHARD	JUNGFRAU MYTHEN GOTTHARD	JUNGFRAU
Pixel pitches	25 × 25 μm^2 75 × 75 μm^2	75 × 75 μm^2	75 × 75 μm^2	75 × 75 μm^2

Courtesy of D. Greiffenberg

Material Properties

PSI

	Atomic Number, Z	Auto-fluorescence [keV]	Band Gap Energy (@RT) [eV]	$e^{-}h^{+}$ Pair Creation Energy [eV]	Resistivity [$\Omega \cdot cm$]	Electron $\mu \cdot \tau$ [cm^2/V]
Silicon	14	1.7	1.12	3.6	$< 10^4$	> 1
$Cd_{0.9}Zn_{0.1}Te$	48, 30, 52	23, 27	1.57	4.6	10^{10}	$10^{-3}..10^{-2}$
CdTe	48, 52	23, 27	1.44	4.4	10^9	3×10^{-3}
GaAs:Cr	31, 33	10	1.43	4.2	$\sim 10^9$	$< 5 \times 10^{-4}$

Courtesy of D. Greiffenberg

PSI Center for Photon Science

CZT

CZT Variants

PSI

CZT manufactured by Redlen Technologies

- 1.5 mm thick
- 2 x 2 cm^2 single chip samples
- Operated at -500 V (But rated for -900 V)
- Two variants

Spectroscopic (SP)

- The original (**Standard**) variety.
- Efficient for energies upto 120 keV

High-Flux (HF)

- Optimised for high flux environments (10^{-10} ph s^{-1} mm^{-2}) in medical and security applications
- Increased hole lifetime
- Afterglow performance is also improved

Thicker material tested by STFC

	$\mu_e\tau_e$ ($\times 10^{-4}$ cm^2V^{-1})	μ_e ($cm^2V^{-1}s^{-1}$)	τ_e ($\times 10^{-6}$ s)	$\mu_h\tau_h$ ($\times 10^{-4}$ cm^2V^{-1})	μ_h ($cm^2V^{-1}s^{-1}$)	τ_h ($\times 10^{-6}$ s)
2 mm Thick — High Flux CdZnTe	11 ± 6	940 ± 190	1.2 ± 0.8	2.9 ± 1.4	114 ± 22	2.5 ± 1.4
10 mm Thick — Standard CdZnTe	100	1100	11	0.2	88	0.2

By STFC:

B. Thomas, 2017 [7]

Dark Frame

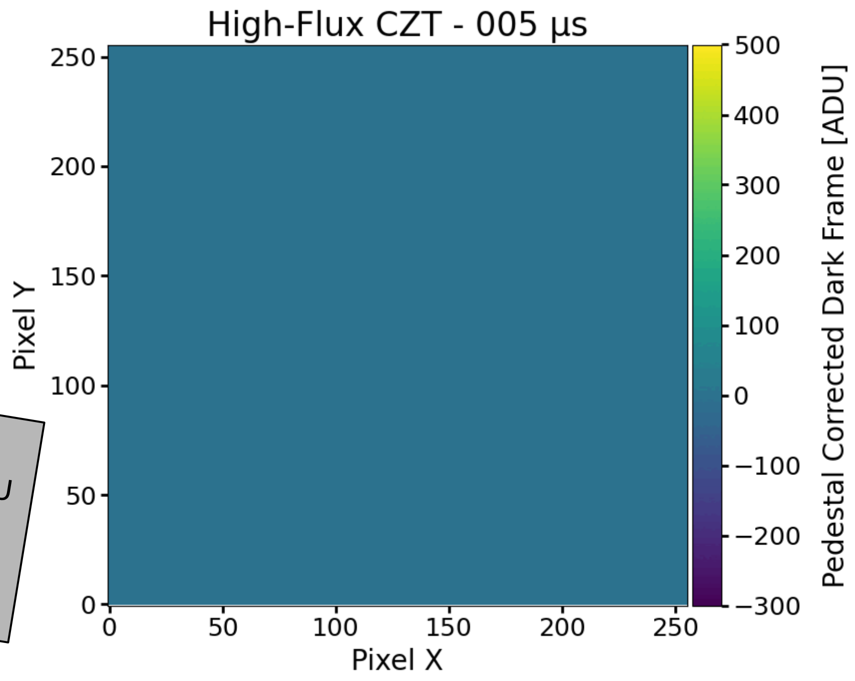

Average dark frame (raw ADU values) as integration time increases

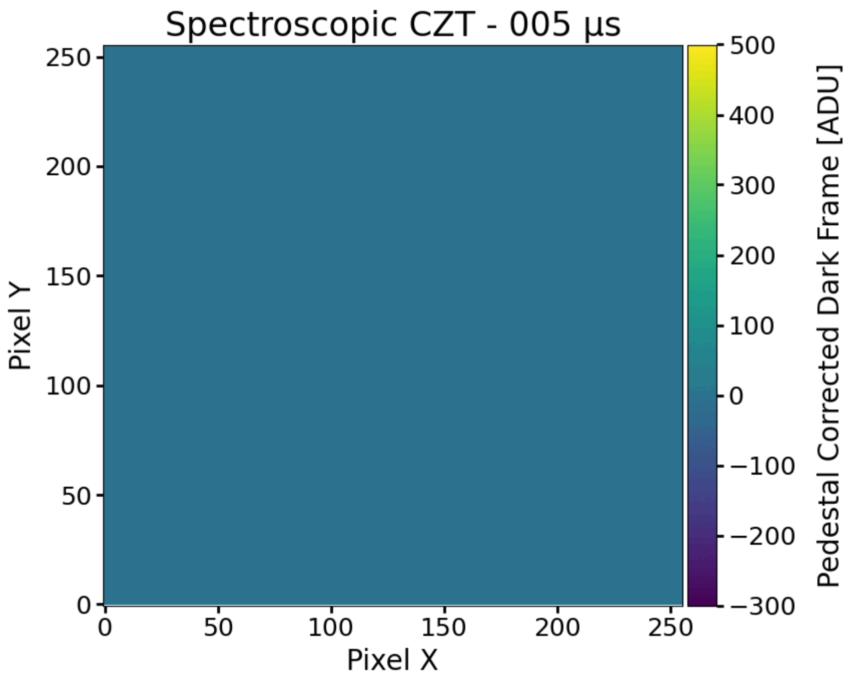

5 µs baseline (Pedestal Correction)

Lots of **scratches** in **both variants**

- ➢ Increased ADU
- ➢ From polishing on pixelated surface
- ➢ **No major defects in High-Flux**

Spectroscopic has many defects by comparison

- ➢ Significant elevation in ADU
- ➢ But only **one device** of each variant tested

Leakage Current

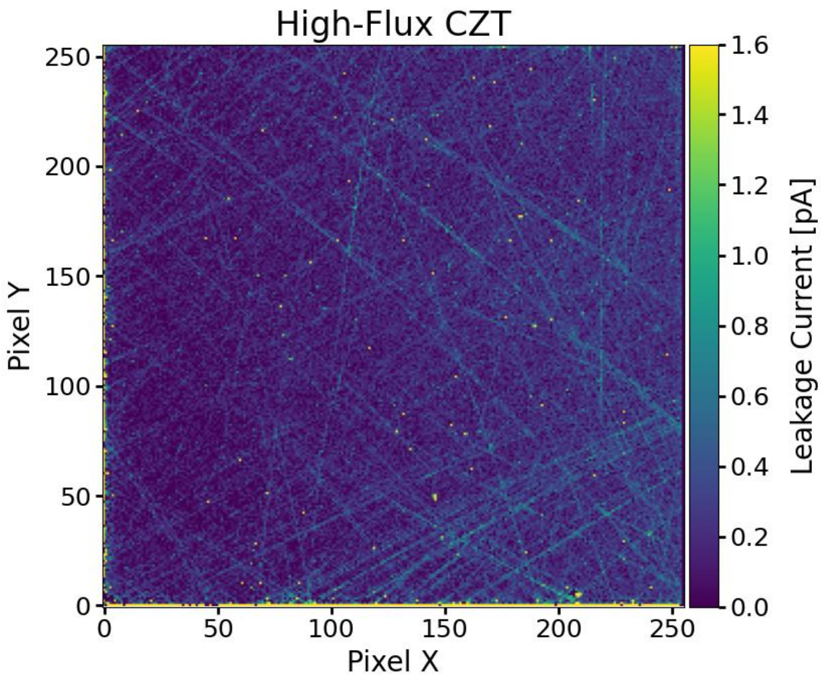

15 °C

-500 V Bias

Material	MPV Pixel Leakage Current
High-Flux CZT	~ 0.18 pA
Standard CZT	~ 0.49 pA
Silicon	~ 2 pA
GaAs	~ 190 pA [8]

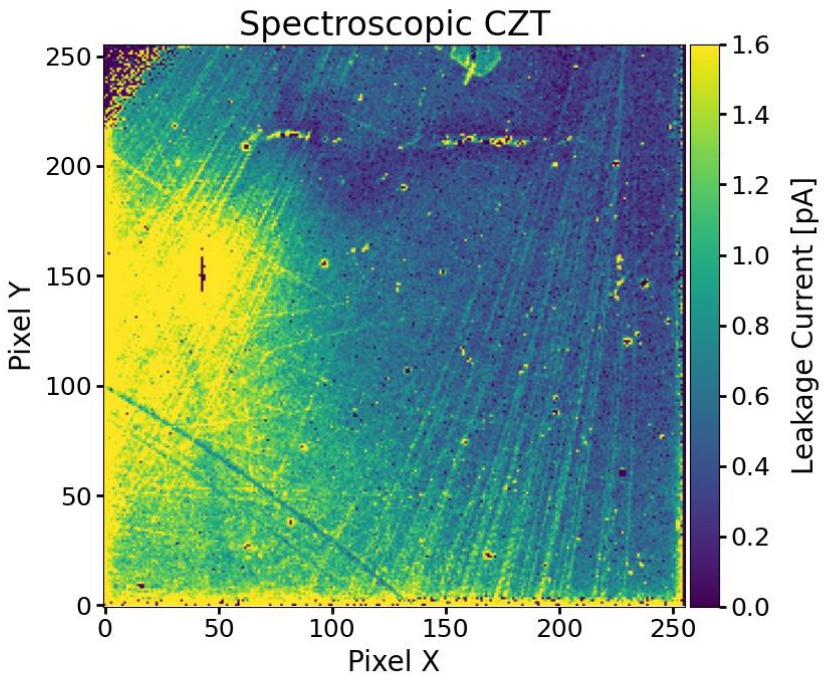

Similar to dark frames

- ➢ But now we can quantify the **low current**
- ➢ Even in defect region **< 8 pA per pixel**
- ➢ All measurements at **15 °C**

2-3 orders of magnitude improvement over GaAs

- ➢ Better than silicon

Noise

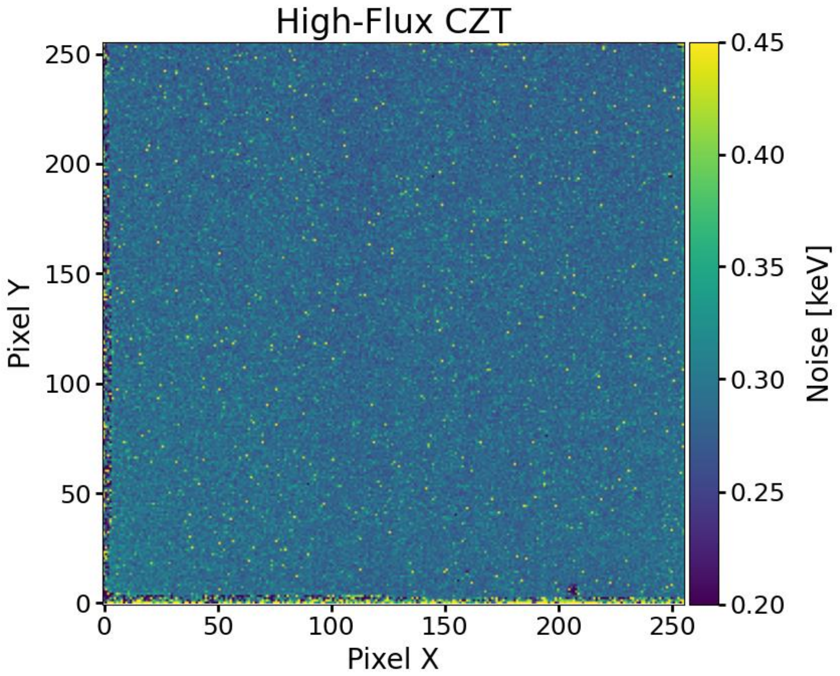

15 °C	-500 V Bias	5 µs Int. Time

Material	Average Pixel Noise
High-Flux CZT	~ 0.28 keV
Standard CZT	~ 0.29 keV
Silicon	~ 0.3 keV [9]
GaAs	~ 0.41 keV [8]

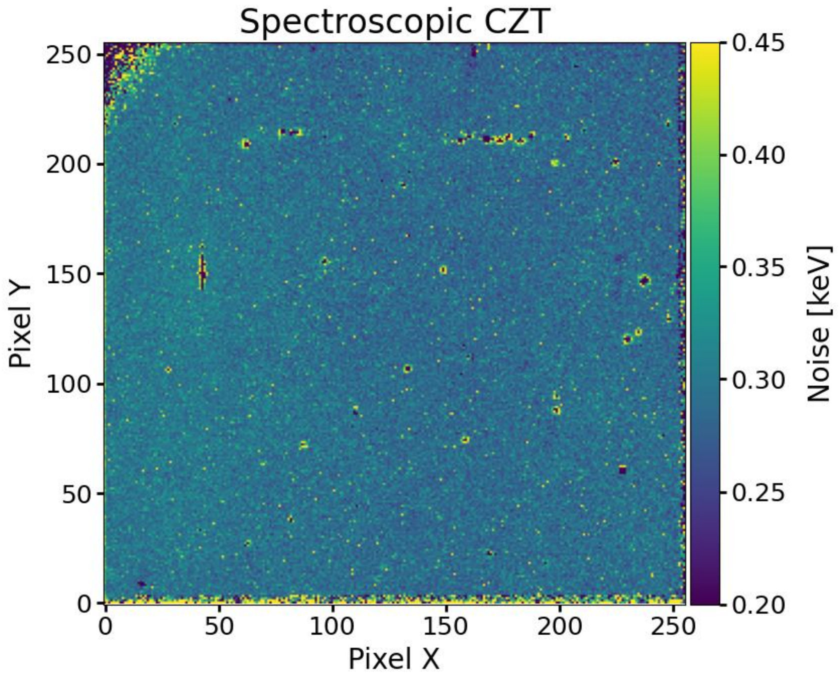

Generally flat distribution across sensor area

- **5 µs** integration time
- Reasonably consistent across sensor material

Noisy pixels everywhere

- But generally corresponds to hot spots

Otherwise, **better than GaAs** and **comparable to silicon**

Am241 Spectra

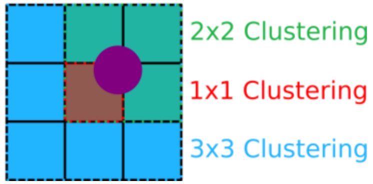

15 °C

-500 V Bias

5 µs Int. Time

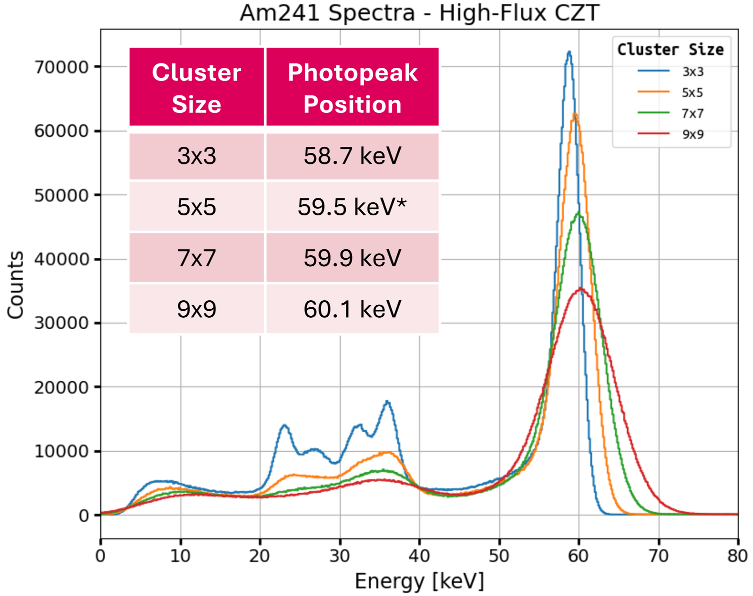

Cluster Size	Photopeak Position
3x3	58.7 keV
5x5	59.5 keV*
7x7	59.9 keV
9x9	60.1 keV

Cluster Size (Virtual Pitch)	FWHM [keV] (Energy Resolution)	
	High-Flux	Spectroscopic
3x3 (225 µm)	5.8%	6.5%
5x5 (375 µm)	8.2%	9.0%
7x7 (525 µm)	11.9%	13.7%
9x9 (675 µm)	16.7%	20.0%

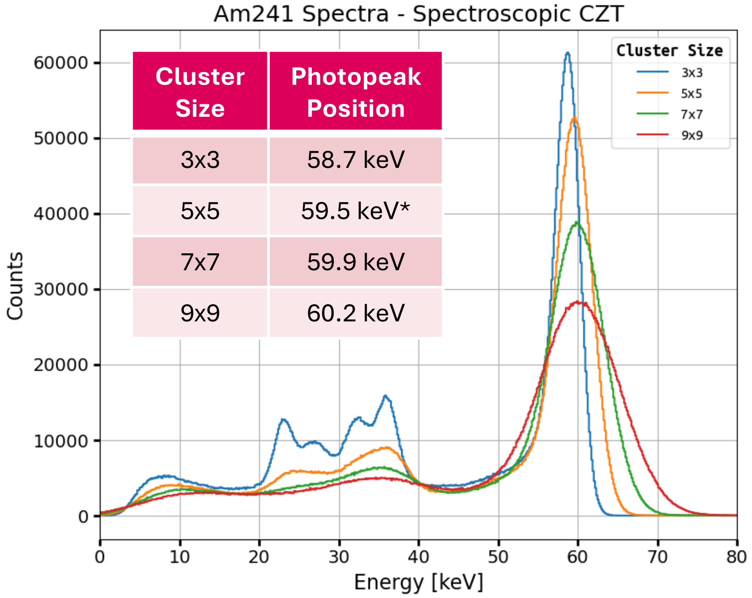

Cluster Size	Photopeak Position
3x3	58.7 keV
5x5	59.5 keV*
7x7	59.9 keV
9x9	60.2 keV

Similar spectra for High-Flux and Spectroscopic

5x5 cluster required to collect all charge

- ➢ Slight shift in photopeak between 3x3 and 5x5

Spectral resolution is the **ratio of FWHM and peak position** (59.5 keV)

- ➢ Comparable with GaAs (especially earlier generations) [8]
- ➢ Would likely be improved by a pixel-by-pixel calibration

*Assumed to be Am241's 59.5 keV photopeak

Hecht Scans

$$Q(U) = Q_0 \cdot \underbrace{\left[\exp\left(-\frac{(d-D)\cdot d}{\mu\cdot\tau\cdot(U-U_0)}\right)\right]}_{\text{Charge trapping}} \cdot \underbrace{\left[\frac{\mu\cdot\tau\cdot(U-U_0)}{D\cdot d}\cdot\left[1-\exp\left(-\frac{D\cdot d}{\mu\cdot\tau\cdot(U-U_0)}\right)\right]\right]}_{\text{Signal induction}}$$

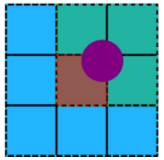
2x2 Clustering
1x1 Clustering
3x3 Clustering

PSI

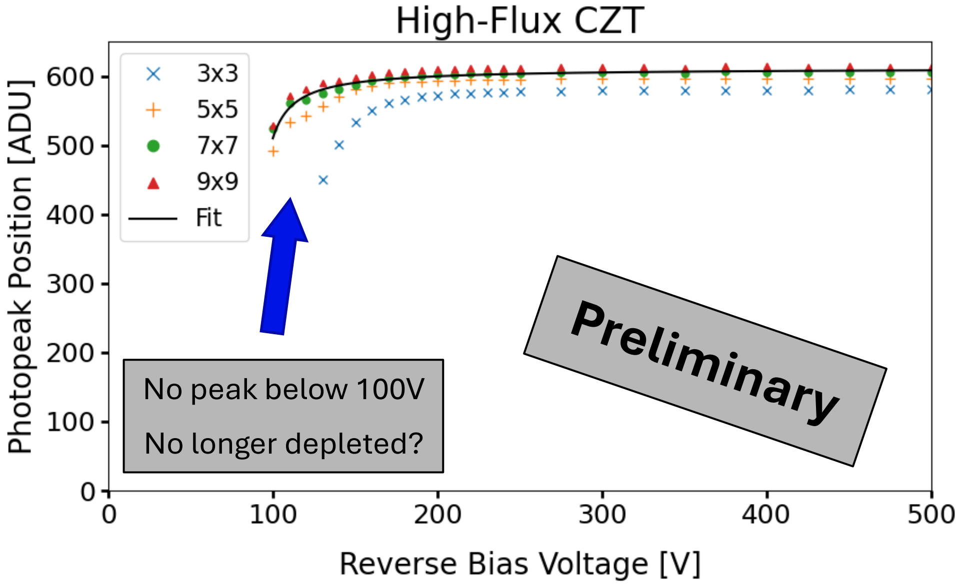

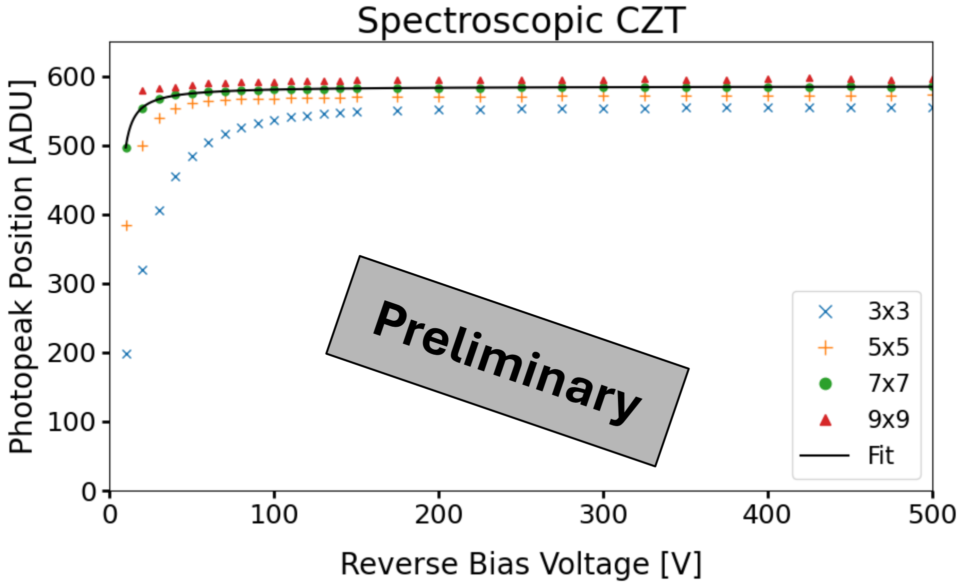

15 °C

5 μs Int. Time

Mo Peak (17.5 keV)

Mo (17.5 keV) is ideal for Hecht

- Absorption depth only ~ 15 μm

Extract $\mu_e \cdot \tau_e$ by fitting with 7x7

- Charge loss in 3x3 is not purely trapping → Charge sharing dominates for low sensor bias and small cluster sizes
- $\mu_e \cdot \tau_e$ for High-Flux CZT is **better than GaAs and CdTe** (~ 0.4 x 10^{-3} cm^2/V [8] and 1 x 10^{-3} cm^2/V [10])

Cluster Size (Virtual Pitch)	$\mu_e \cdot \tau_e$ [x10^{-3} cm^2/V]	
	High-Flux	Spectroscopic
3x3 (225 μm)	9.7 ± 0.8	4.41 ± 0.13
5x5 (375 μm)	9.6 ± 1.2	14.0 ± 0.6
7x7 (525 μm)	10.0 ± 1.1	13.96 ± 0.6
9x9 (675 μm)	11.9 ± 0.9	13.1 ± 0.7

$\mu_e \cdot \tau_e$ 3x3 is untrustworthy
(Curve dominated by charge loss)

Charge Collection Efficiency

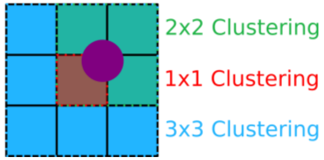

PSI

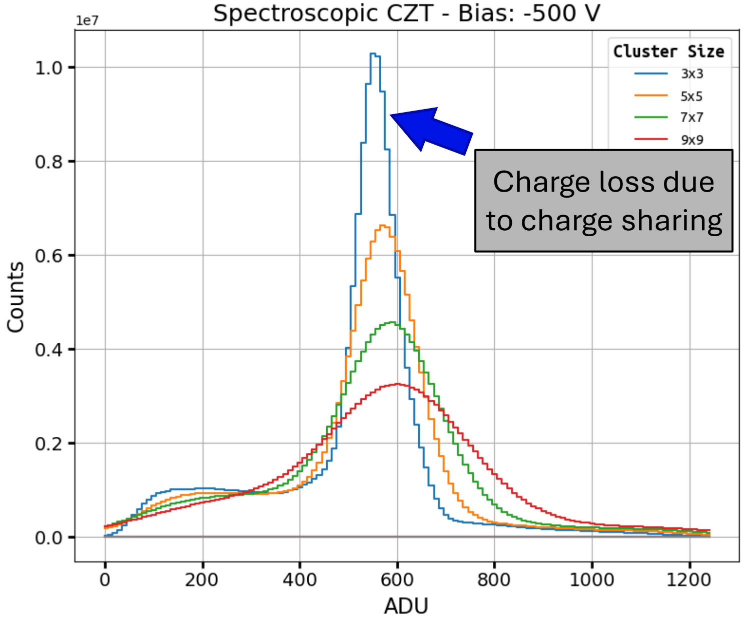

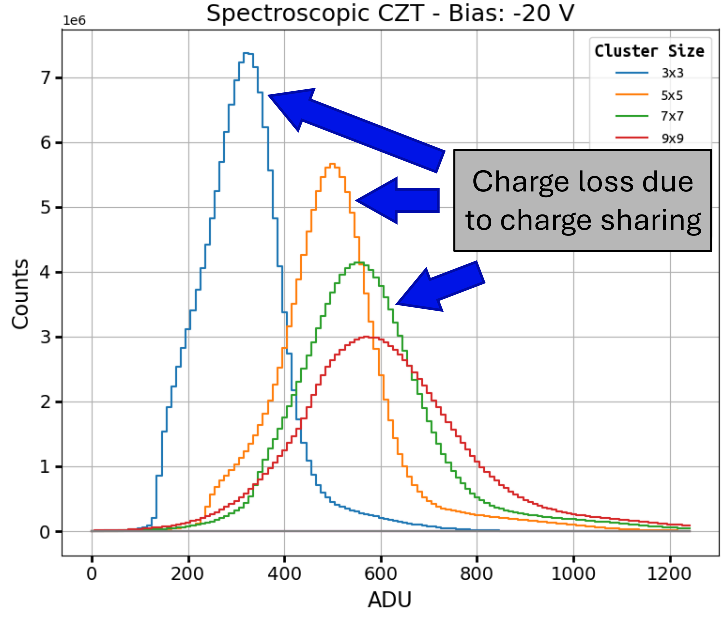

15 °C

5 µs Int. Time

Mo Peak (17.5 keV)

Charge sharing lowers 3x3 peak even at -500 V

- ➢ 7x7 is affected at -20 V
- ➢ Only trapping contributes to the 9x9 peak (lower at -20 V compared to -500 V)

Spectroscopic can still collect a majority of charge (> 97% CCE) at -20 V!

- ➢ (Where High-Flux needs **over 100 V** to start collecting charge)
- ➢ Charge collection efficiency (CCE) at 500 V is **over 99%** for both variants

Cluster Size (Virtual Pitch)	Charge collection efficiency	
	Spectroscopic @ -20V	Spectroscopic @ -500 V
3x3 (225 µm)	55.8%	97.1%
5x5 (375 µm)	86.6%	99.4%
7x7 (525 µm)	94.4%	99.9%
9x9 (675 µm)	97.0%	99.9%

PSI Center for Photon Science

GaAs:Cr

Results by Kirsty A. Paton

Dark Current, Noise & Dynamic Range

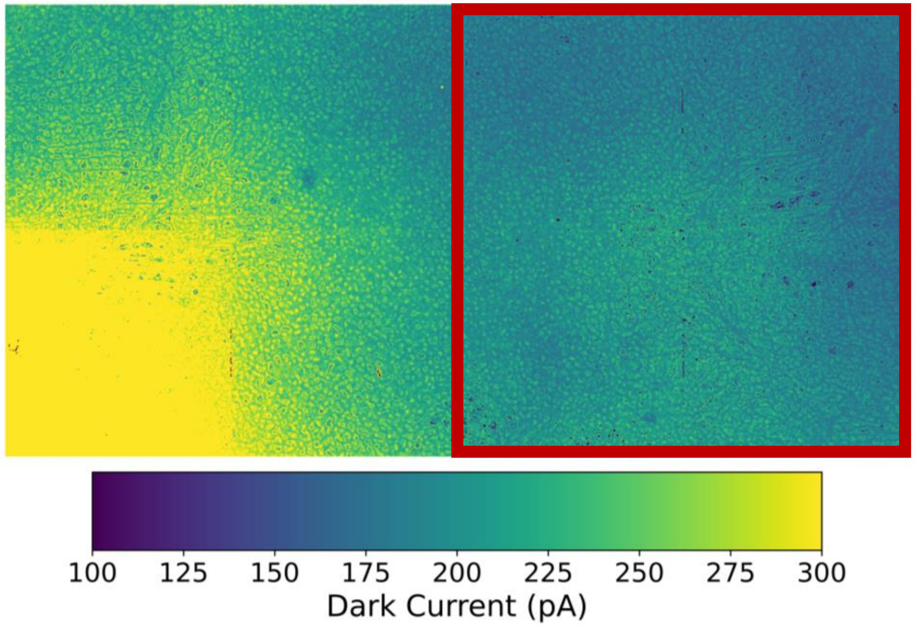

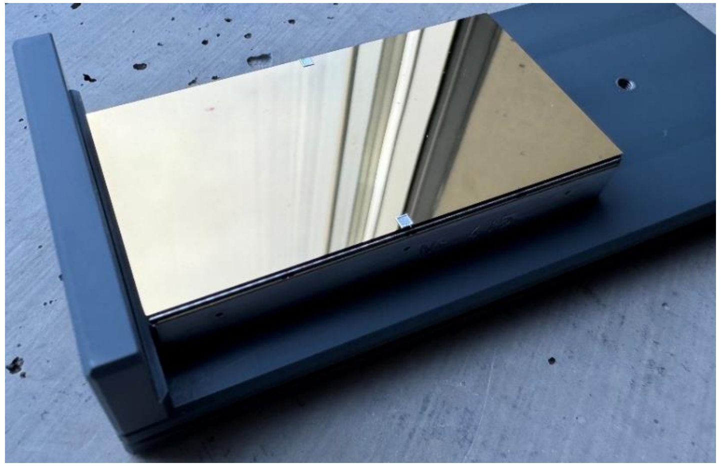

~~TSU~~ Dectris

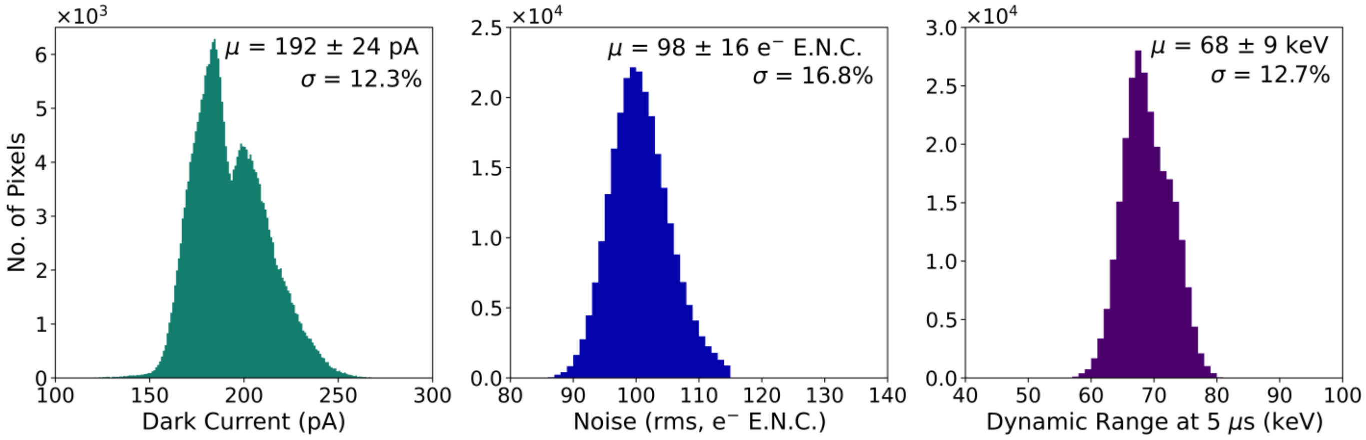

	Mean Dark Current (pA)	Mean Noise (rms e- E.N.C.)
TSU (2016)	391.0 (σ = 16.9 %)	115.93 (σ = 5.5 %)
TSU (2017)	201.6 (σ = 17.3 %)	101.65 (σ = 9.4 %)

Mo Fluorescence Flat Field

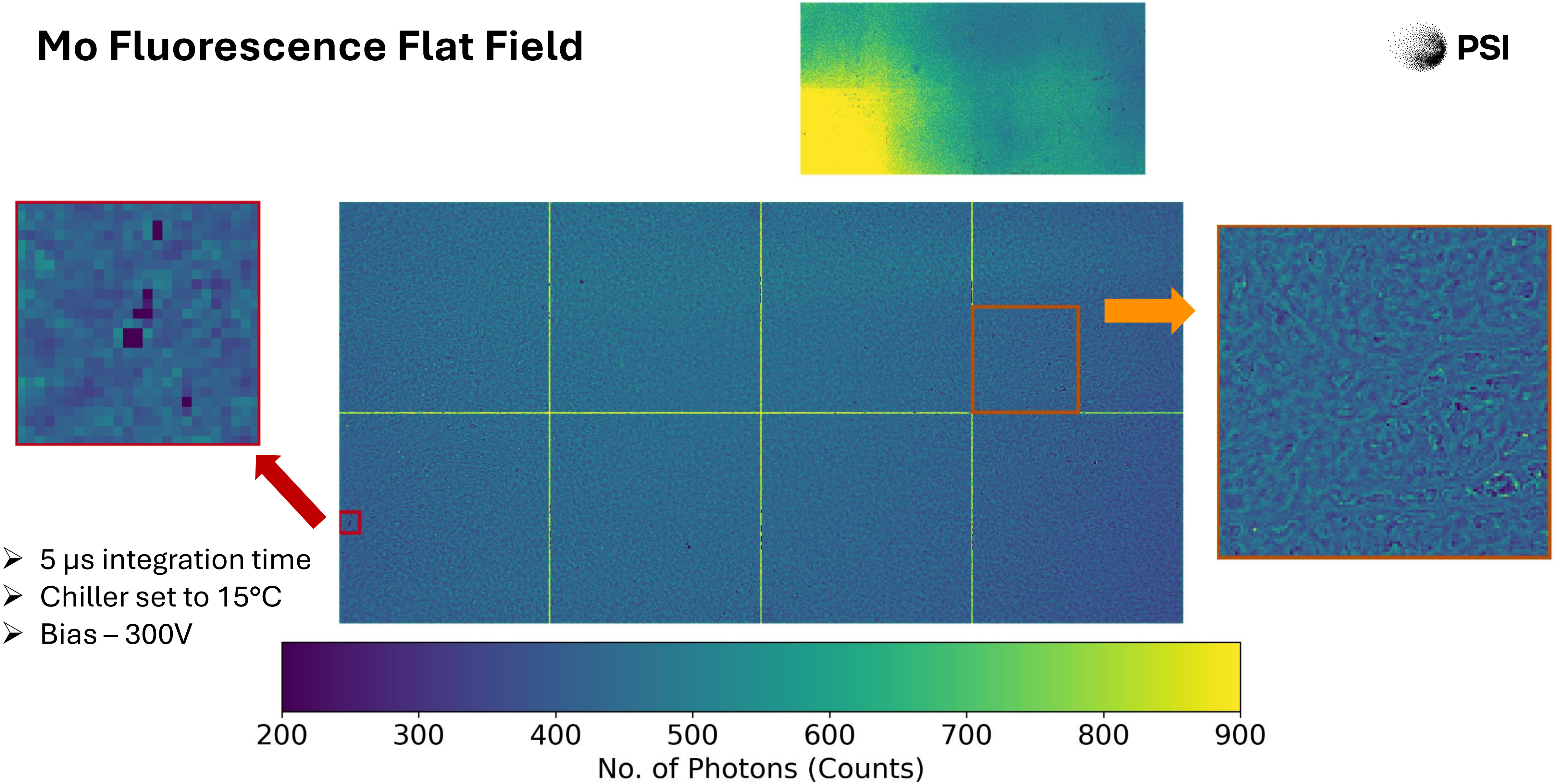

- 5 µs integration time
- Chiller set to 15°C
- Bias – 300V

Energy Resolution

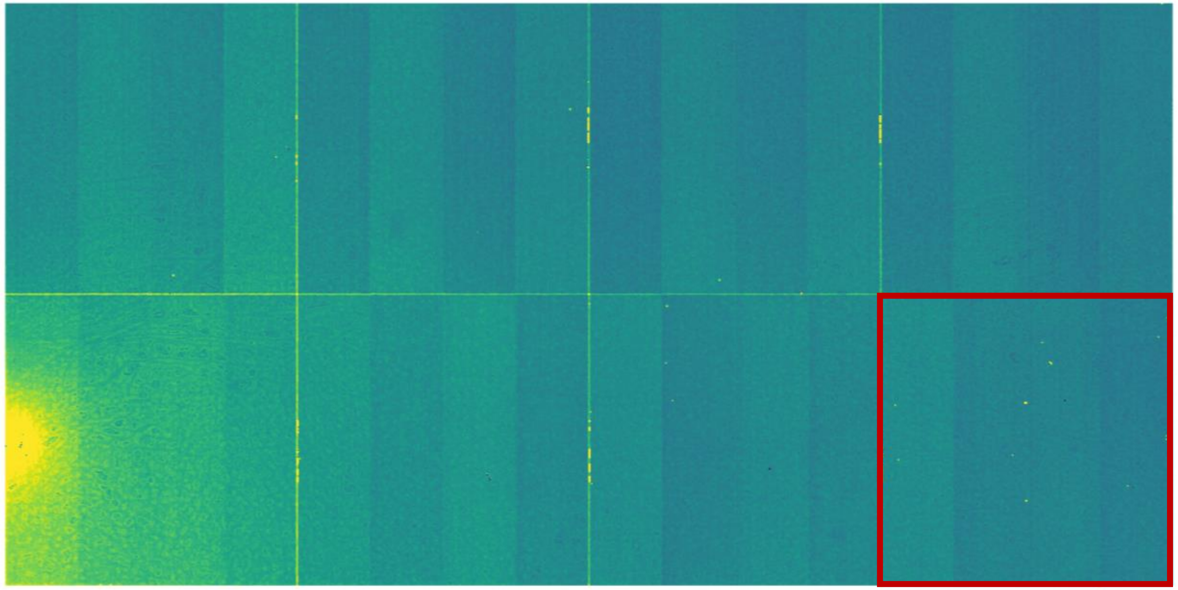

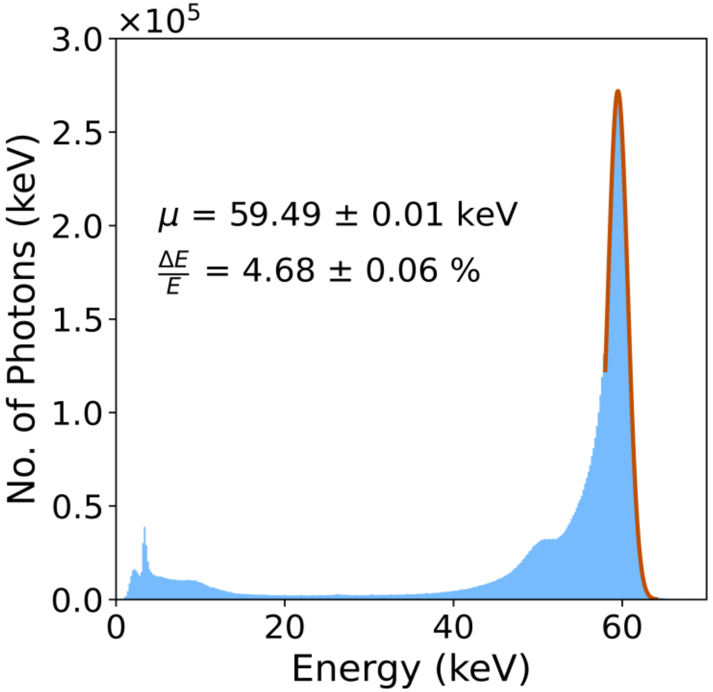

2016 TSU - 6.9%
2017 TSU - 4.3%

Hecht Measurements

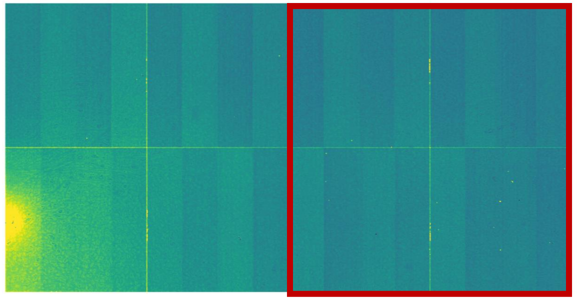

$$Q(U) = Q_0 \cdot \underbrace{\left[\exp\left(-\frac{(d-D)\cdot d}{\mu\cdot\tau\cdot(U-U_0)}\right)\right]}_{\text{Charge traping}} \cdot \underbrace{\left[\frac{\mu\cdot\tau\cdot(U-U_0)}{D\cdot d}\cdot\left[1-\exp\left(-\frac{D\cdot d}{\mu\cdot\tau\cdot(U-U_0)}\right)\right]\right]}_{\text{Signal induction}}$$

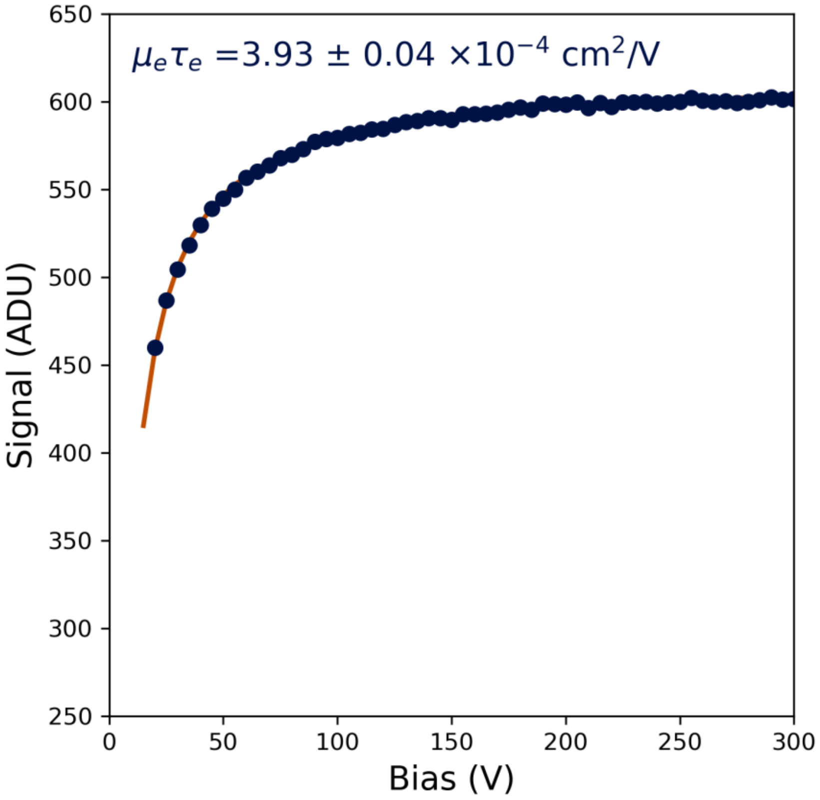

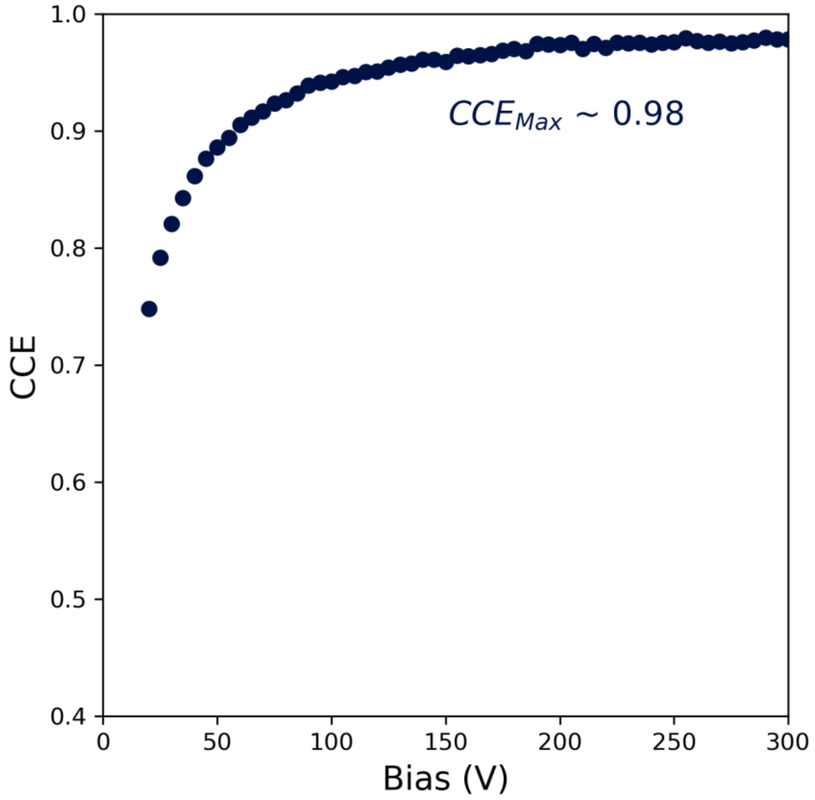

2016 TSU - 1.83 × 10^{-4} cm^2/V
2017 TSU - 4.73 × 10^{-4} cm^2/V

Interpolation with GaAs

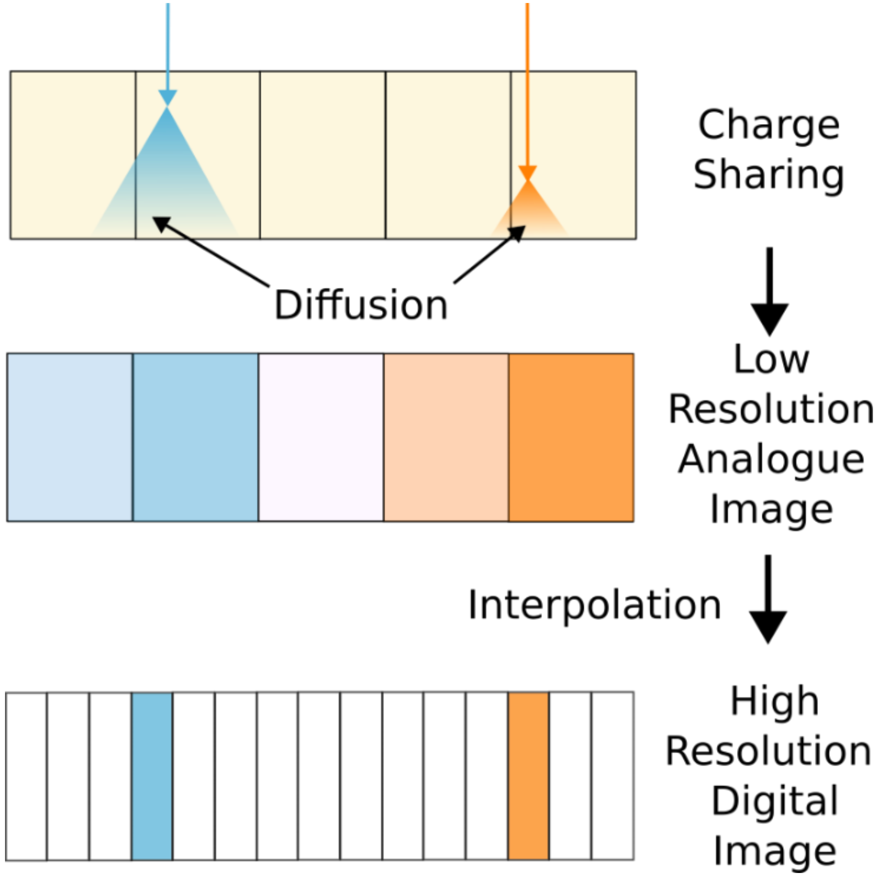

JUNGFRAU

- 75 µm physical pixel pitch
- Interpolation requires charge sharing on the order of a pixel pitch
- Challenging for thinner Si sensors

MÖNCH

S. Chiriotti et al., *JInst*, (2022)

25 µm Physical Pixel Pitch

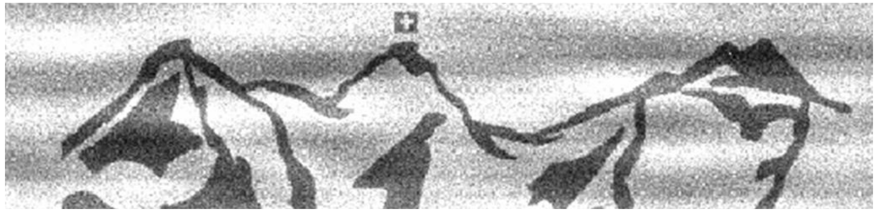

2.5 µm Interpolated Pixel

Swiss Flag 25 µm Wide, Cross 7µm Wide

PSI Center for Photon Science

High-Z Discussion

Afterglow

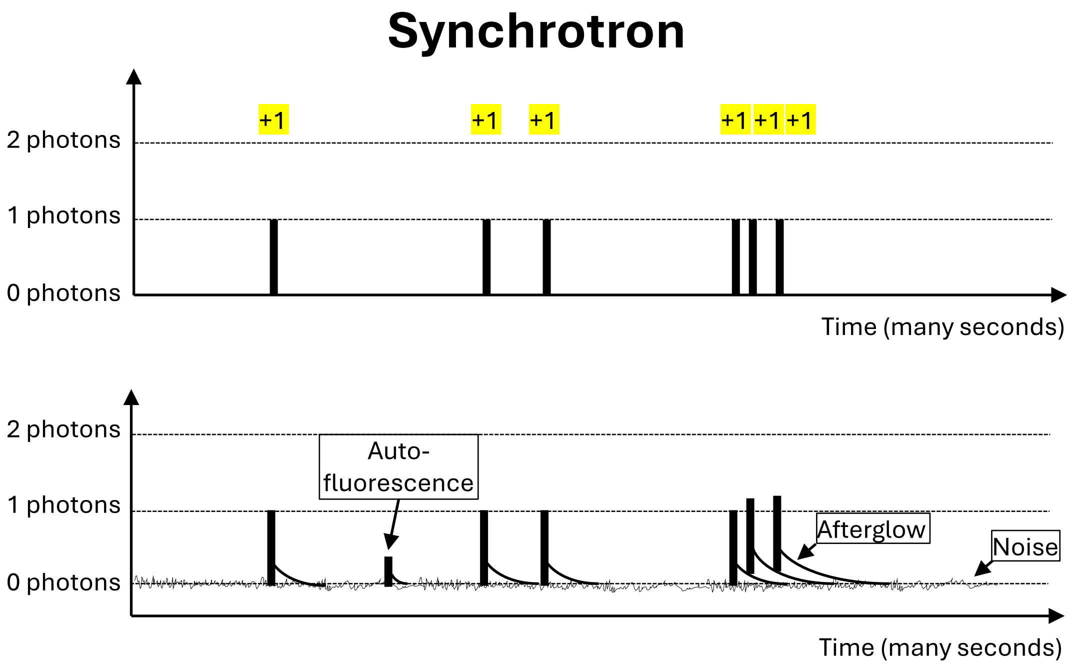

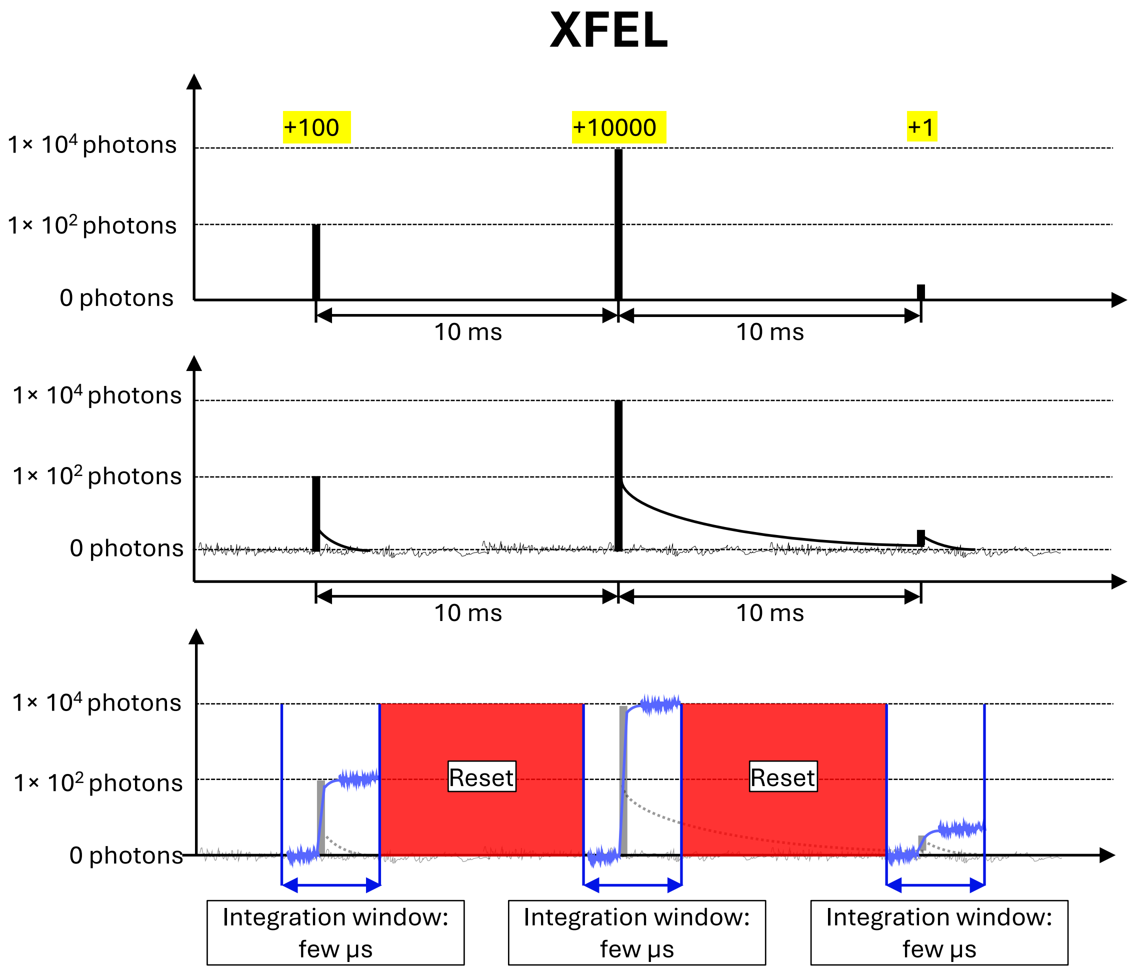

- CZT has very minimal afterglow
  - Would work at synchrotrons with photon counting
  - or XFELs with resets
- GaAs & CdTe suffer much more from this problem
  - Photon counting might still be the way forward

Which Material Wins?

CZT is the obvious choice

- Leakage current/afterglow, signal stability all comparable with silicon
- Should work well with charge integrating detectors at FELs
- Yield (including defect rate) needs to be further studied)
- < 1.5mm thick not currently possible
  - Charge sharing results in larger pixel sizes
  - Not suitable for photon counting unless pixels are grouped together in 2x2 150 μm super pixels

GaAs:Cr could be an alternative for photon counting

- High dark current is less of a concern
- Better commercial availability (full 500 μm thick modules)
- Uniformity is still a concern however

	Absorption efficiency	Signal stability	Afterglow	Spectral resolution capability	Dark current	Noise	Availability
Silicon	-	++	++	++	+	+	++
CdZnTe High Flux type	++	++	++	+	++	++	+
CdZnTe Spectroscopic type	++	+	+	+	++	++	+
CdTe e^- Schottky type	++	--	o	o	+	+	+
CdTe Ohmic tye	++	--	--	-	-	--	+
GaAs:Cr	+	o	o	+	--	-	+

Courtesy of D. Greiffenberg

PSI Center for Photon Science

Introduction to PSI

- Science at PSI
- User Facilities – SLS, SwissFEL, etc.
- Photon Science Detector Group – How we support user facilities

High-Z Characterisation at PSI

- Overview of High-Z materials
- GaAs
- CZT

High-Z Future & Applications

- **Photon Science**
- **Medical Physics**
- **Astronomy**

New CZT Assemblies

CZT + JF1.2

- Testing **dynamic gain switching with electrons**

Full CZT Module (2x Quads) + JF1.2

- 0.5M **uniformity** and **pilot experiments** at beamlines
- Expected later this year

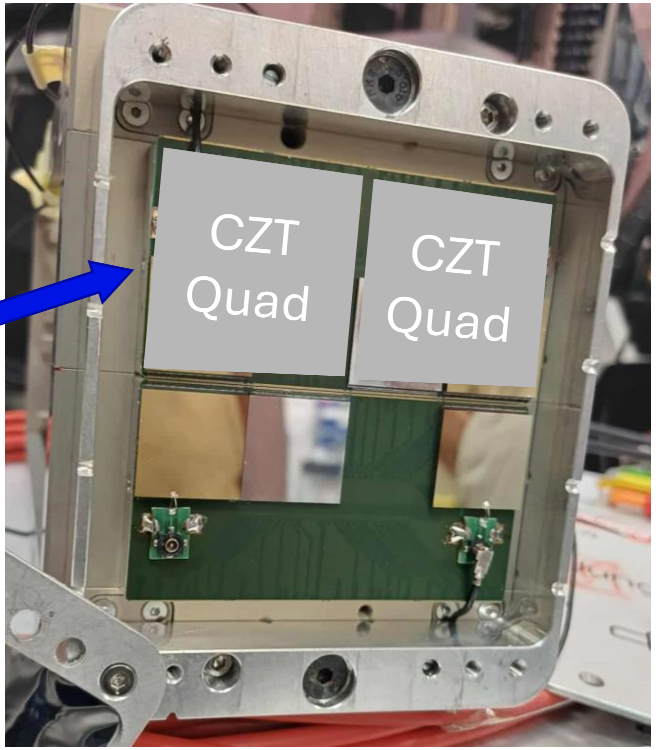

CZT + **Matterhorn**

- Photon counting with high-Z
- MH optimised for high count rates (20 MHz/Pixel)
- Aims to **mitigate afterglow** with thresholding and fast shaping
- **Higher bias** and **thinner sensors** are preferred (GaAs?)
- Initially **larger pixels** for CZT (**150 µm pitch**)
- First MH1.0 wafers expected at the end of the year

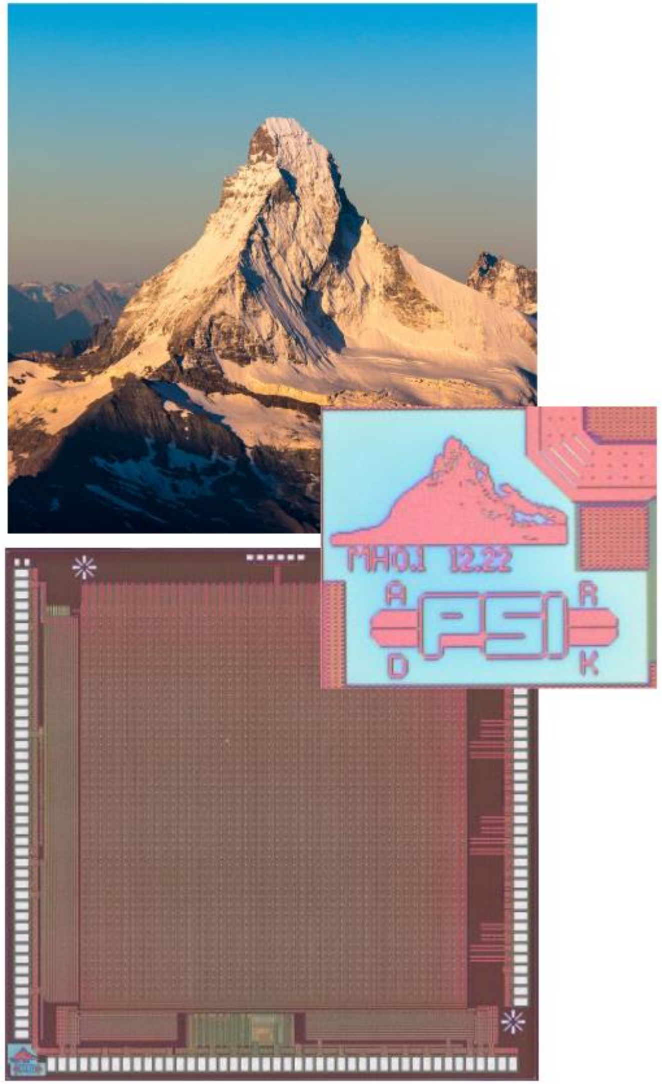

E. Fröjdh, 2023 [12]

Further Characterisation Planned

Planer CZT Crystals

- From Redlen (CA) and JX Advanced Metals (JP)
- More in-depth characterisation
  - Electrical properties (depletion)
  - Decoupling of μ and τ
  - Edge scanning with a laser

GaAs is considered for electron microscopy

- Electrons are absorbed in their entirety (not MIP-like)
  - But not before they scatter within the sensor
  - Higher absorption efficiency is preferred to reduce track length
- Short track lengths mean charge spread is dominated by diffusion
  - Simpler to interpolate
  - (For longer track lengths, interpolation would require machine learning)

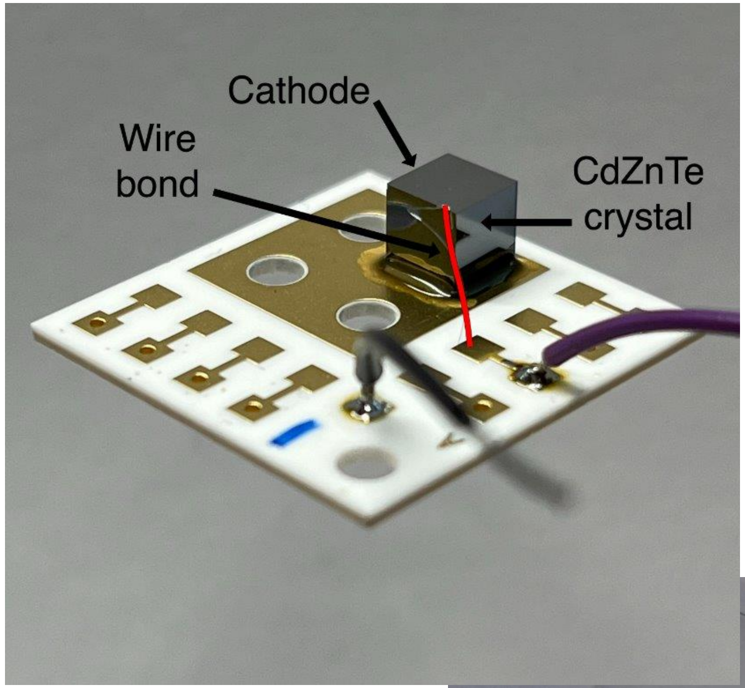

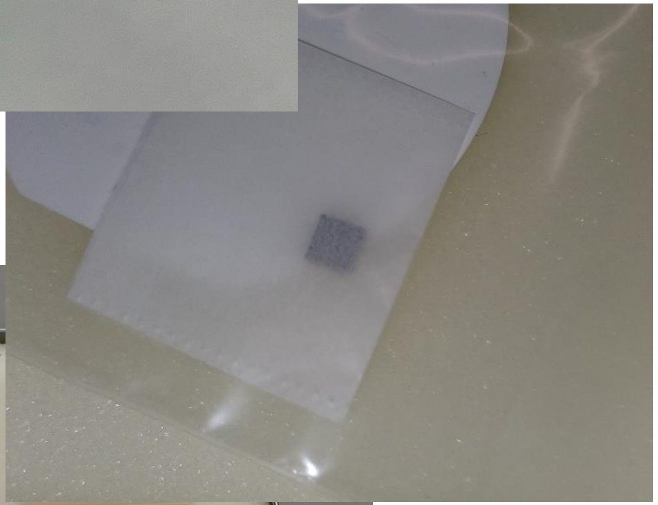

Medical Applications

- WidePIX (Based on Medipix)
  - 1mm CdTe
  - Multichannel “color” radiographs
  - Correction required for “veiny” structure

- Photon Counting Computed Tomography (PCCT)
  - CdTe
  - Offers better temporal discrimination between photons

- CdTe is often favoured over CZT
  - Cheaper and easier to make large area detectors
  - CZT also relatively new to the industry

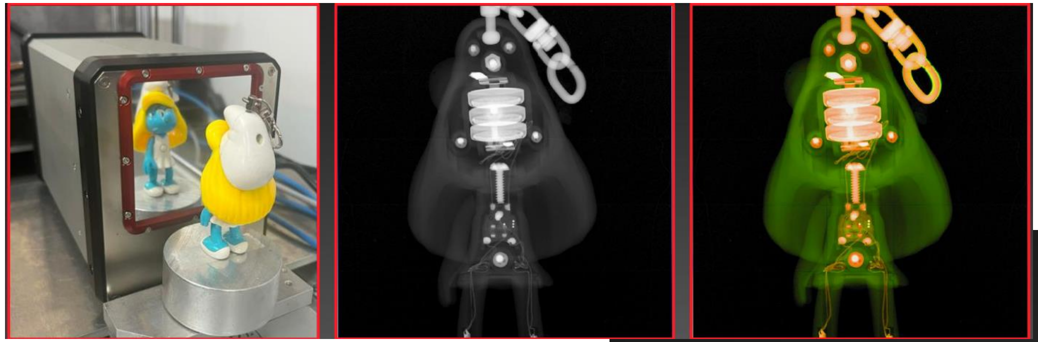

Z. Melníková, et al [13]

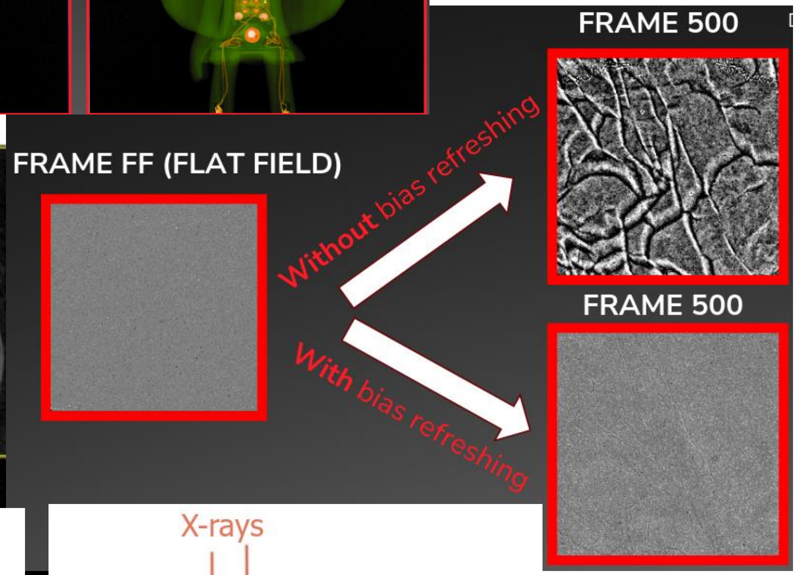

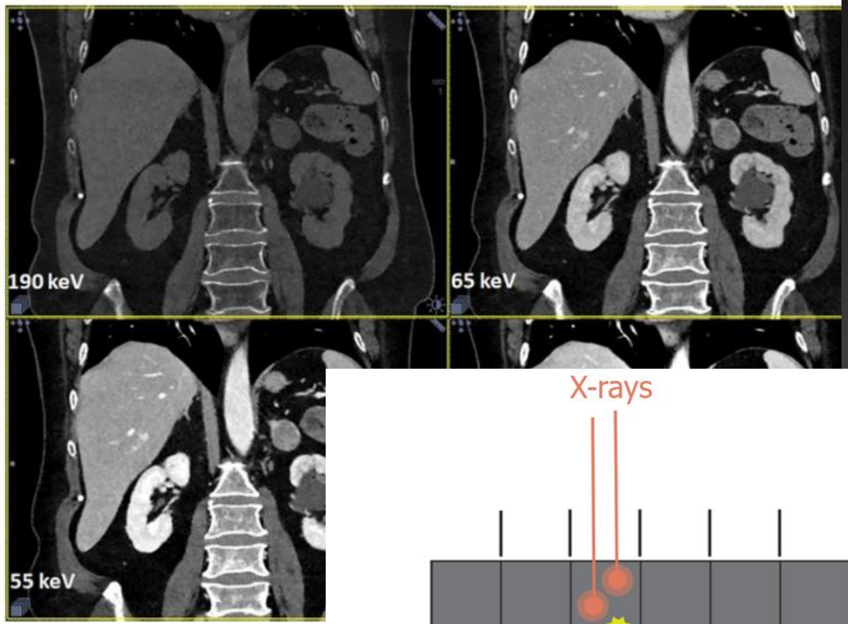

T. Flohr, et al [14]

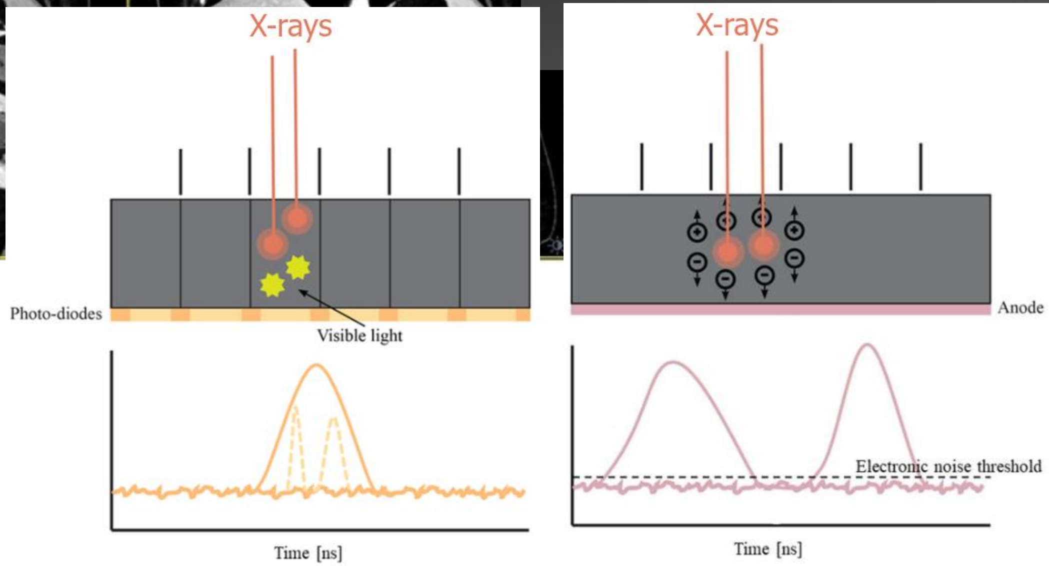

F. Maddaloni et al [15]

Energy Integrating Detectors

Photon Counting Detectors

Medical Applications

- SANTIS and EIGER from Dectris (PSI spinoff)
  - GaAs (~500 μm thick)
  - High resolution/sensitivity phase contrast imaging
  - Small pixel size and large sensitive area is desirable
  - Can provide the same SNR but with a higher resolution (compared to scintillation-based detectors)

- CZT "Gamma Camera" for SPECT
  - Imaging with radioisotopes: ^{99m}Tc and ^{123}I
  - Better contrast and energy resolution than previous CdTe detectors

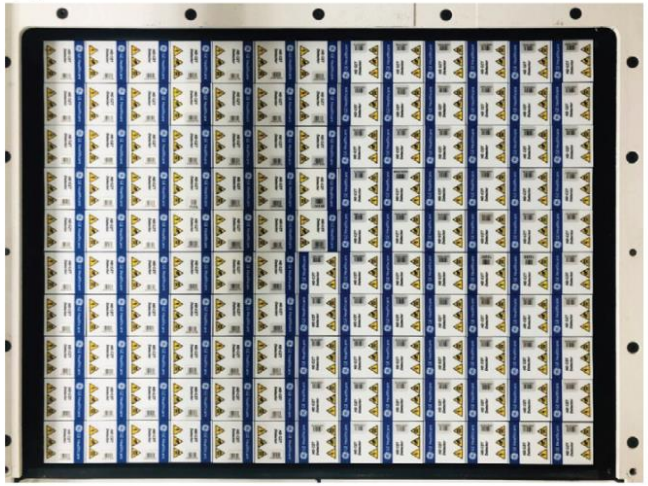

J. Scholz, et al [16]

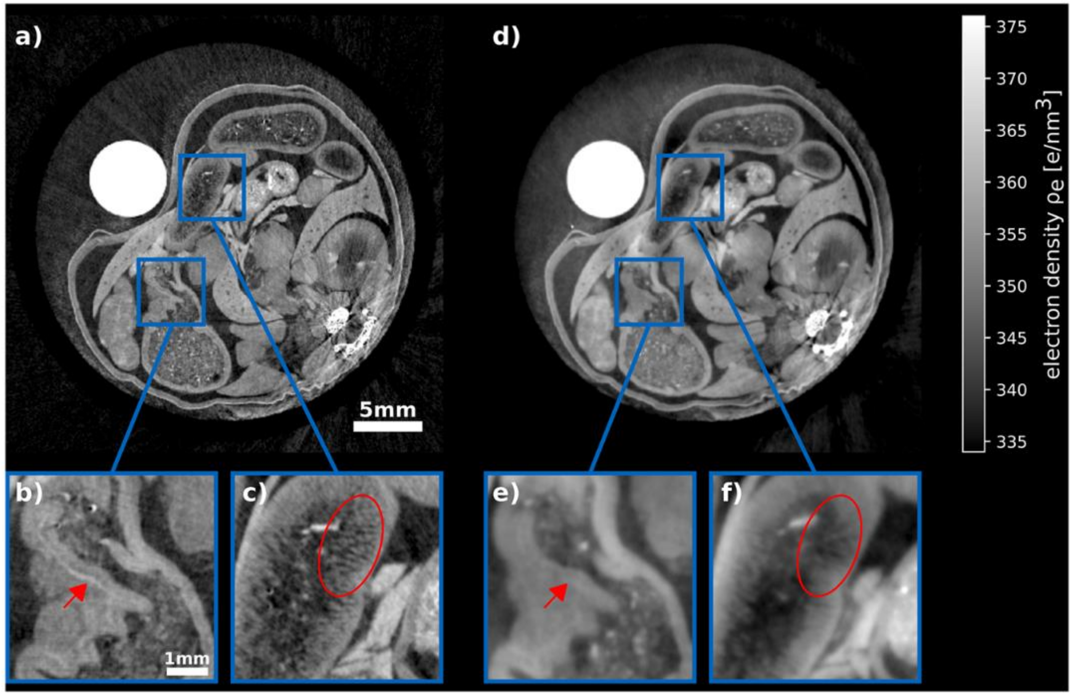

T. Ito, et al [17]

Astronomy Applications

Many CZT detectors used in space/upper atmosphere

- Low leakage current of CZT is ideal when power requirements and cooling are key
  - Rules out GaAs (Also has a lower absorption efficiency)

- CdTe performs worse than CZT in most metrics
  - Veiny/defect structure of CdTe is not ideal
  - Can also afford CZT's smaller active area

Name	Cystal Size	Material	Electrode Config.	Year Launched	Notes
PoRTIA	$2.54 \times 2.54 \times 0.19$ cm^3 $1.2 \times 1.2 \times 0.5$ cm^3	CZT	planar	1995	balloon[7]
CfA/CalTech	$2.54 \times 2.54 \times 0.19$ cm^3	CZT	planar	1995	balloon[8]
HEXIS	$1.2 \times 1.2 \times 0.3$ cm^3	CZT	cross strip/planar	1997	balloon[9]
InFocμs	$2.7 \times 2.7 \times 0.2$ cm^3	CZT	pixelated	2001	balloon[10]
ISGRI: Integral	$0.4 \times 0.4 \times 0.2$ cm^3	CdTe	planar	2002	[11]
BAT: Swift	$0.4 \times 0.4 \times 0.2$ cm^3	CZT	planar	2005	[2]
GRaND: Dawn	$1 \times 1 \times 0.7$ cm^3	CZT	coplanar	2007	[12, 13]
HEX: Chandrayaan-1	$4 \times 4 \times 0.2$ cm^3	CZT	planar	2008	[14]
AAUSat-2	$1 \times 1 \times 0.4$ cm^3	CZT	pixelated	2008	[15]
ProtoEXIST	$1.95 \times 1.95 \times 0.5$ cm^3	CZT	pixelated	2009-	balloon[16]
RT-2: Koronas-Foton	$3.96 \times 3.95 \times 0.5$ cm^3	CZT	pixelated	2009	[4]
NuSTAR	$2 \times 2 \times 0.2$ cm^3	CZT	pixelated	2012	[17]
X-Calibur	$2 \times 2 \times 0.2$ cm^3 $2 \times 2 \times 0.5$ cm^3 $2 \times 2 \times 0.8$ cm^3	CZT	pixelated	2014-	balloon[18]
CZTI: AstroSat	$3.9 \times 3.9 \times 0.5$ cm^3	CZT	pixelated	2015	[3]
BeEagleSat	$2 \times 2 \times 0.5$ cm^3	CZT	cross strip	2017	[19]
EPEx	$2 \times 2 \times 0.5?$ cm^3	CZT	pixelated	2018	balloon[20]
ASIM	$2 \times 2 \times 0.5$ cm^3	CZT	pixelated	2018	[21]
STIX: Solar Orbiter	$1 \times 1 \times 0.1$ cm^3	CdTe	variable pixelation	2020	[22]
OrionEagle	$2 \times 2 \times 1.5$ cm^3	CZT	pixelated	2021	balloon[23]
BADG3R	$2 \times 2 \times 0.6$ cm^3	CZT	cross strip	2022	balloon[24]
VZLUSAT-2	$1.4 \times 1.4 \times 0.2$ cm^3	CdTe	pixelated	2022	[25]
Sharjah-Sat 1	$2.54 \times 2.54 \times 0.5$ cm^3	CZT	pixelated	2023	[26, 27]
ComPair	$0.6 \times 0.6 \times 2$ cm^3	CZT	virtual Frisch grid	2023	balloon[28, 29]
SVOM:ECLAIRs	$0.4 \times 0.4 \times 0.1$ cm^3	CdTe	Schottky-type	s2024	[31]
MASS-Cube	$2 \times 2 \times 1.5$ cm^3	CZT	pixelated	s2024	[30]
TERI	$4 \times 4 \times 1.5$ cm^3	CZT	pixelated	s2025	this work
AXIS	$2 \times 2 \times 0.5?$ cm^3	CZT	pixelated	s2026	[32]
COSI	$8 \times 8 \times 1.5$ cm^3	HPGe	cross strip	s2027	[33]
Daksha	$3.9 \times 3.9 \times 0.5$ cm^3	CZT	pixelated	concept	[34]
ASTENA	$0.5 \times 2 \times 2$ cm^3	CZT	strip-drift	concept	[35, 36]
MeVCube	$2 \times 2 \times 1.5$ cm^3	CZT	pixelated	concept	[37]
AMEGO	$0.8 \times 0.8 \times 4$ cm	CZT	virtual Frisch grid	concept	[38]
GECCO	$0.8 \times 0.8 \times 3.2$ cm	CZT	virtual Frisch grid	concept	[39]
HSP	$2 \times 2 \times 0.3$ cm^3	CZT	pixelated	concept	[40]

D. Shy, et al [18]

Astronomy Applications

D. Shy, et al [18]

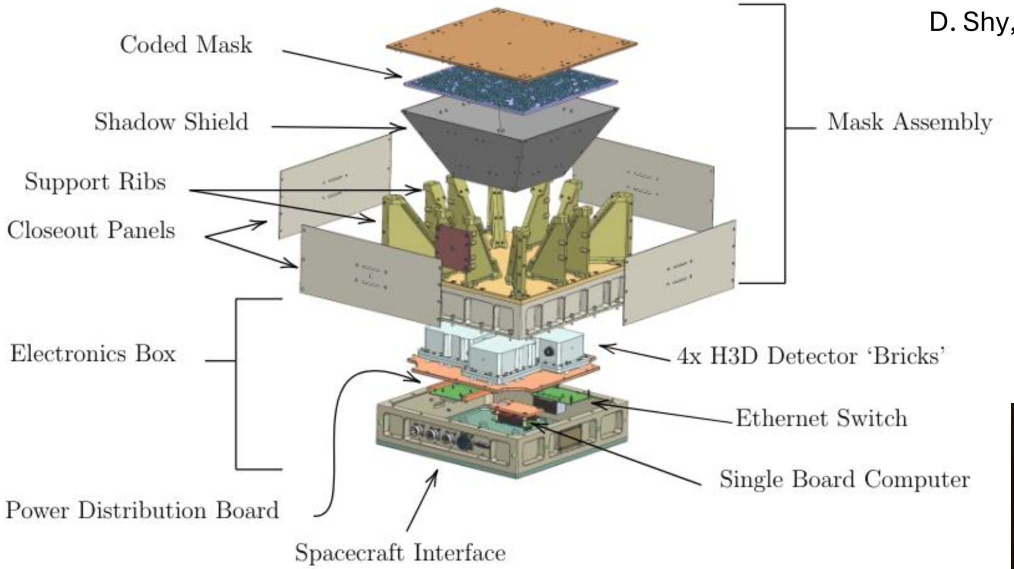

ESA [20]

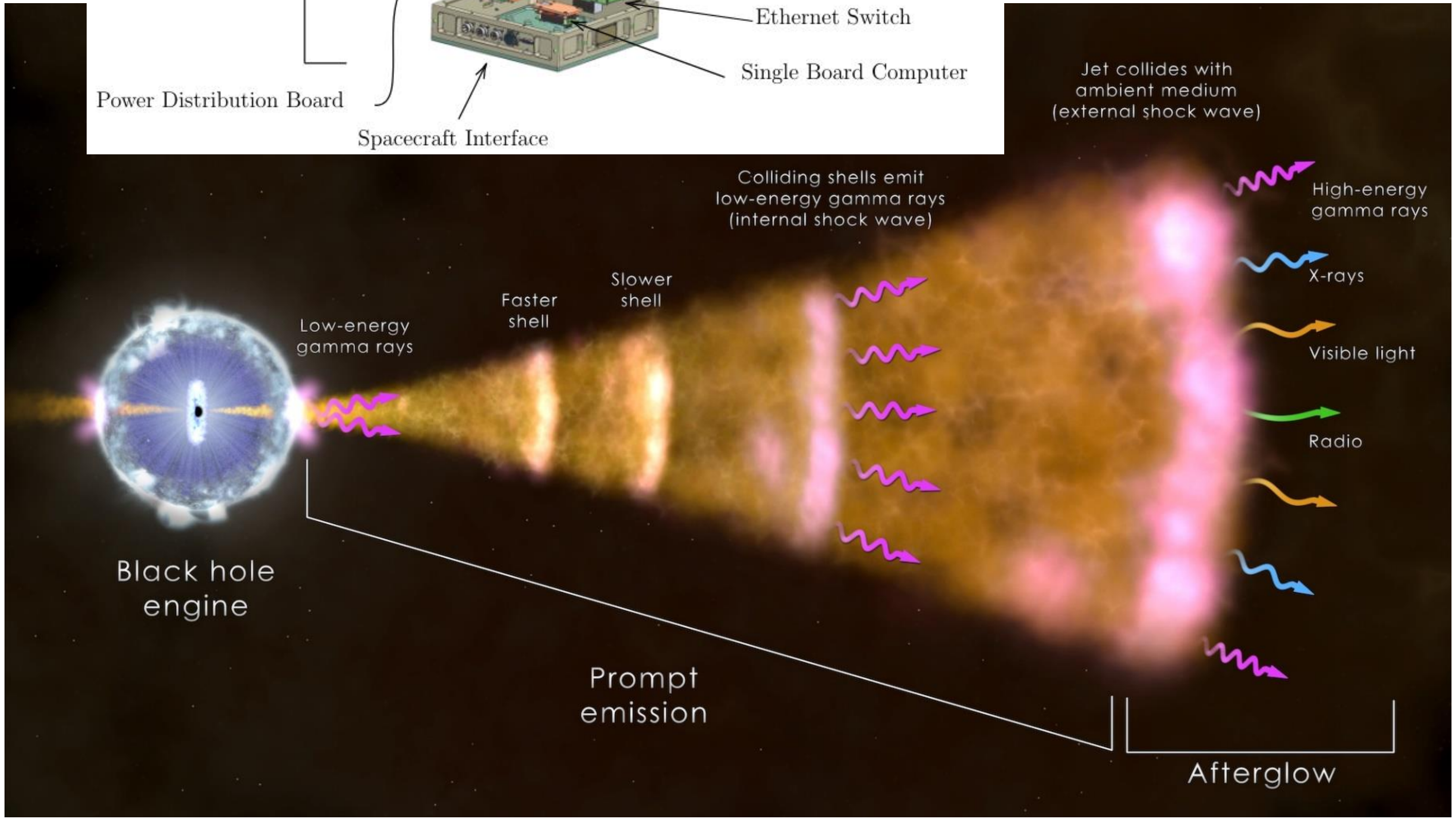

India's AstroSat launched in 2015

- CZT based detector
- Measured the polarisation of gamma ray bursts [19]

TERI is another example launched in 2025

- Goal is test CZT's long term viability and space [18]
- Also aimed at the MeV range, key for the study of astrophysical jets
- 15 mm CZT from Redlen [21]
- Up to 50 mm has also been characterised. 25 mm shows < 1% energy resolution at 662 keV [22]

PSI Center for Photon Science

Outlook and Summary

Summary

PSI continues to develop cutting edge detectors for photon science applications

- Jungfrau & Matterhorn represent the latest in charge-integrating and photon-counting technology

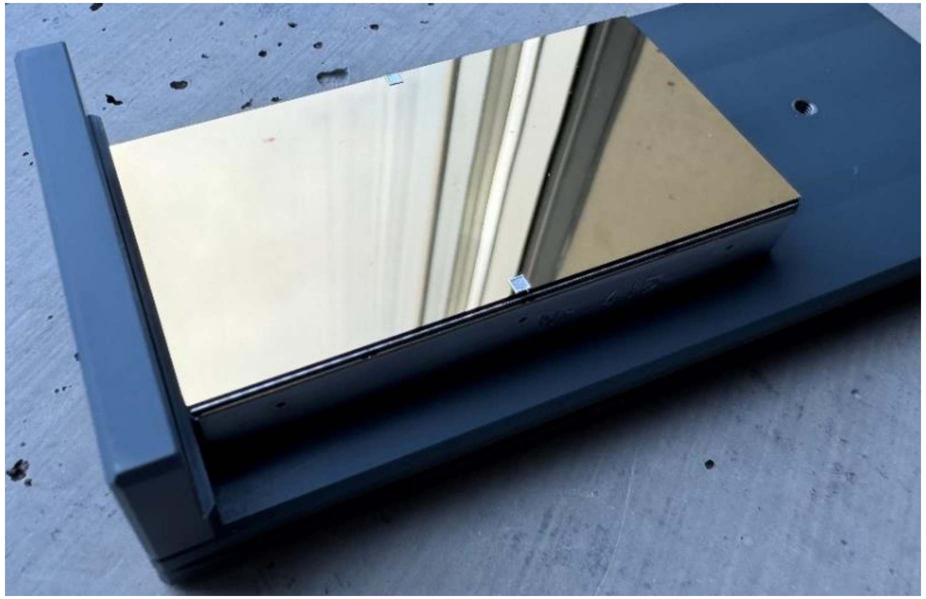

High-Z has a bright and brilliant future in photon science

- Already well established for high energy photon detection in medical physics and astronomy
- Thin, large area sensors are key and more work is still be to done!
- Characterisation work continues at PSI, aiming to unlock high-Z’s full potential
- Full module pilot experiments expected soon to demonstrated feasibility to users

Thank You!

V. Kedych, M. Müller, P. Sieberer, K. Ferjaoui, M. Brückner, E. Fröjdh, J. Heymes, C. Lopez-Cuenca,
K. Moustakas, C. Ruder, J. Mulvey, S. Silletta, V. Hinger, A. Mozzanica, M. Carulla, X. Xie,
R. Dinapoli, A. Bergamaschi, S. Li, D. Thattil, J. Zhang, A. Mazzoleni, V. Gautam, D. Mezza, T. King, B. Schmitt.
Not pictured: S. Ebner, D. Greiffenberg, S. Hasanaj, K.A. Paton, C. Posada Soto, M Hürst.

K.A.P. has received funding from the EU's Horizon 2020 MSCA grant. No. 884104 (PSI-FELLOW-III-3i)

References

[1] M. Böge, 'First Operation of the Swiss Light Source', Proceedings of EPAC 2002, Paris, France, 2002

[2] E P. Mithcell, et al, "Demystifying the Synchrotron Trip: A First-Time User's Guide." *Structure,* **7**, no. 5, May 1999, R111–R121. https://doi.org/10.1016/S0969-2126(99)80063-X

[3] M. Böge, et al, 'Commissioning and First Operation of SLS 2.0, the New Swiss Light Source', in Proceedings of IBIC 2025, paper MOCI01

[4] Paul Scherrer Institute. "SwissFEL Accelerator." SwissFEL – Swiss X-ray Free Electron Laser. Accessed October 6, 2025. https://www.psi.ch/en/swissfel/accelerator

[5] P. G. Jung, et al, "Microdome-Grooved Gd_2O_2S:Tb Scintillator for Flexible and High Resolution Digital Radiography." *Optics Express,* **18**, no. 14 (2010): 14850–14858. https://doi.org/10.1364/OE.18.014850

[6] A. Mozzanica, et al, 'Prototype characterization of the JUNGFRAU pixel detector for SwissFEL', *JINST*, **9**, (2014), C05010

[7] B. Thomas et al, 'Characterisation of Redlen high-flux CdZnTe', 2017, *JINST*, **12,** C12045

[8] K. A. Paton, 'Studying a new variety of GaAs:Cr with the JUNGFRAU charge integrating detector', *HiZPAD Workshop*, London, United Kingdom, 2025

[9] A. Mozzanica et al, 'Characterization results of the JUNGFRAU full scale readout ASIC', 2016, *JINST*, **11**, C02047

[10] M. Veale, "Solid-State Radiation Detectors: Chapter 3" (1st ed.), 2015, *CRC Press*

[11] D Greiffenberg et al, Energy resolution and transport properties of CdTe Timepix-Assemblies 2011 JINST 6 C01058

[12] E. Fröjdh, et al, 'A look at single photon counting detectors for SLS2.0', *The 13th International Conference on Position Sensitive Detectors (PSD13)*, Oxford, United Kingdom, 2023

References

[13] Z. Melníková, et al, “Large-Area CdTe Detector for X-ray Imaging and Overcoming Crystal Imperfections in CdTe Sensors”, International Workshop On Radiation Imaging Detectors (iWorid), Bratislava, Slovakia, 2025

[14] T. Flohr, et al, “Photon-counting CT review”, *Physica Medica*, **79**, 126–136, 2020

[15] F. Maddaloni et al, “Spatial resolution characteristics of a clinical Photon-Counting Computed Tomography scanner”, International Workshop On Radiation Imaging Detectors (iWorid), Bratislava, Slovakia, 2025

[16] J. Scholz, et al, “Biomedical x-ray imaging with a GaAs photon-counting detector”, *APL Photonics*, **5**(10), 106108, 2020, https://doi.org/10.1063/5.0023819

[17] T. Ito, et al, “Experimental evaluation of the GE Discovery 870 CZT clinical SPECT/CT system”, *Journal of Applied Clinical Medical Physics*, **22(1**), 1–13, 2021, https://doi.org/10.1002/acm2.13158

[18] D. Shy, et al, “Development of the cadmium zinc TElluride Radiation Imager (TERI)”. *arXiv preprint* arXiv:2408.04559, 2024, https://doi.org/10.48550/arXiv.2408.04559

[19] T. Chattopadhyay, et al, “Hard X-Ray Polarization Catalog for a Five-year Sample of Gamma-Ray Bursts Using AstroSat CZT Imager”, *The Astrophysical Journal*, 936:12 (13pp), 2022 September 1

[20] European Space Agency, 2023, Gamma-ray Burst Illustration, March 28, 2023, https://www.esa.int/ESA_Multimedia/Images/2023/03/Gamma-ray_burst_illustration

[21] Y. Zhu, Z. He, “Performance of Larger-Volume 40x40x10 and 40x40x15 mm3 CdZnTe Detectors”, *IEEE Transactions on Nuclear Science*, VOL. 68, NO. 2, February 2021

[22] A. E. Bolotnikov et al, “CdZnTe position-sensitive drift detectors with thicknesses up to 5 cm”, Appl. Phys. Lett. 108.093504, 2016

PSI Center for Photon Science

Extra Slides

Photon Science Applications

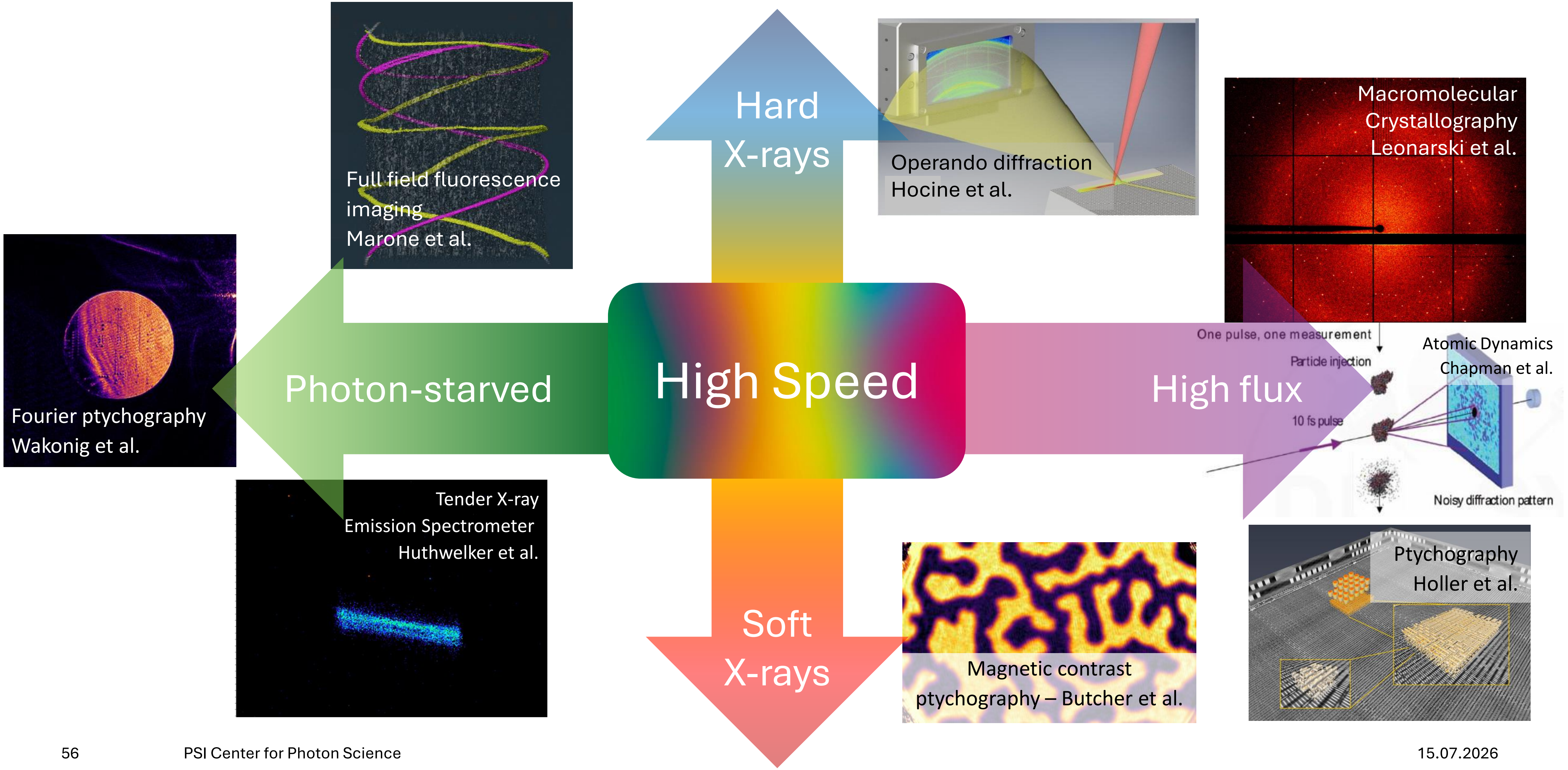

Courtesy of A. Bergamaschi

More Material Properties

	Atomic Number, Z	Auto-fluorescence [keV]	Density [g/cm^3]	Band Gap Energy (@RT) [eV]	e^-h^+ Pair Creation Energy [eV]	Resistivity [Ω·cm]	Electron μ·τ [cm^2/V]	Hole μ·τ [cm^2/V]	Afterglow Performance
Silicon	14	1.7	2.33	1.12	3.6	$< 10^4$	> 1	> 1	Near Perfect
$Cd_{0.9}Zn_{0.1}Te$	48, 30, 52	23, 27	5.78	1.57	4.6	10^{10}	$10^{-3}..10^{-2}$	10^{-5}	Pretty Good
CdTe	48, 52	23, 27	5.85	1.44	4.4	10^9	3×10^{-3}	2×10^{-4}	Not Ideal
GaAs:Cr	31, 33	10	5.32	1.43	4.2	$\sim 10^9$	$< 5 \times 10^{-4}$	$\sim 5 \times 10^{-7}$	Not Ideal

Courtesy of D. Greiffenberg

I-V Characteristics

Spectroscopic CZT (JF1.1 m401)

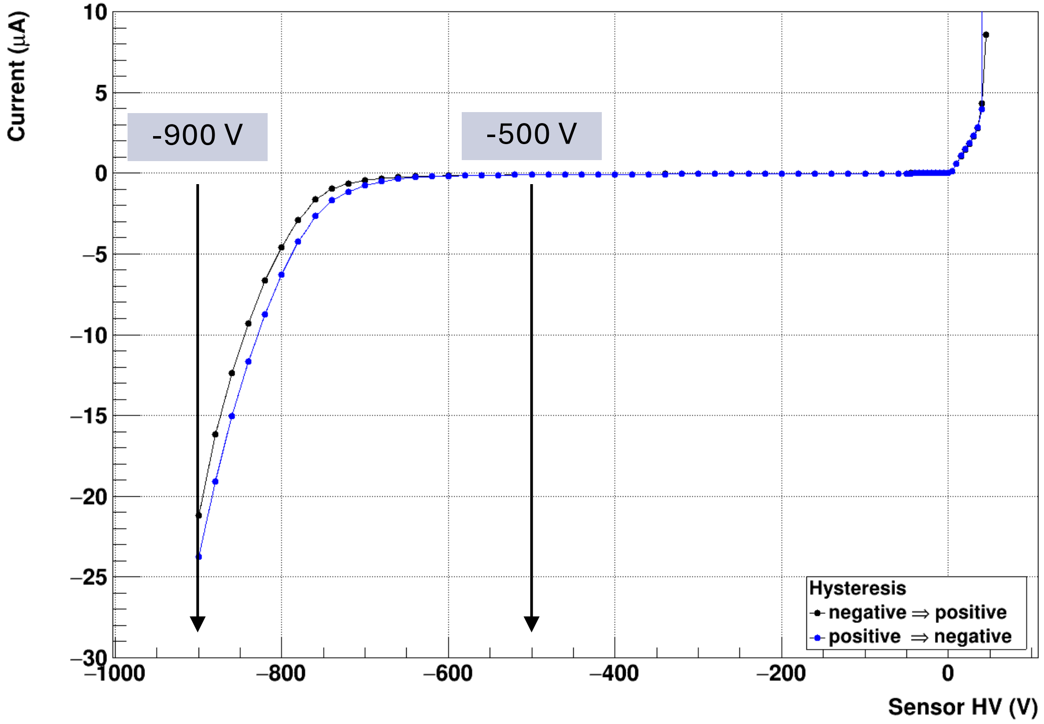

High Flux CZT (JF1.1 m343)

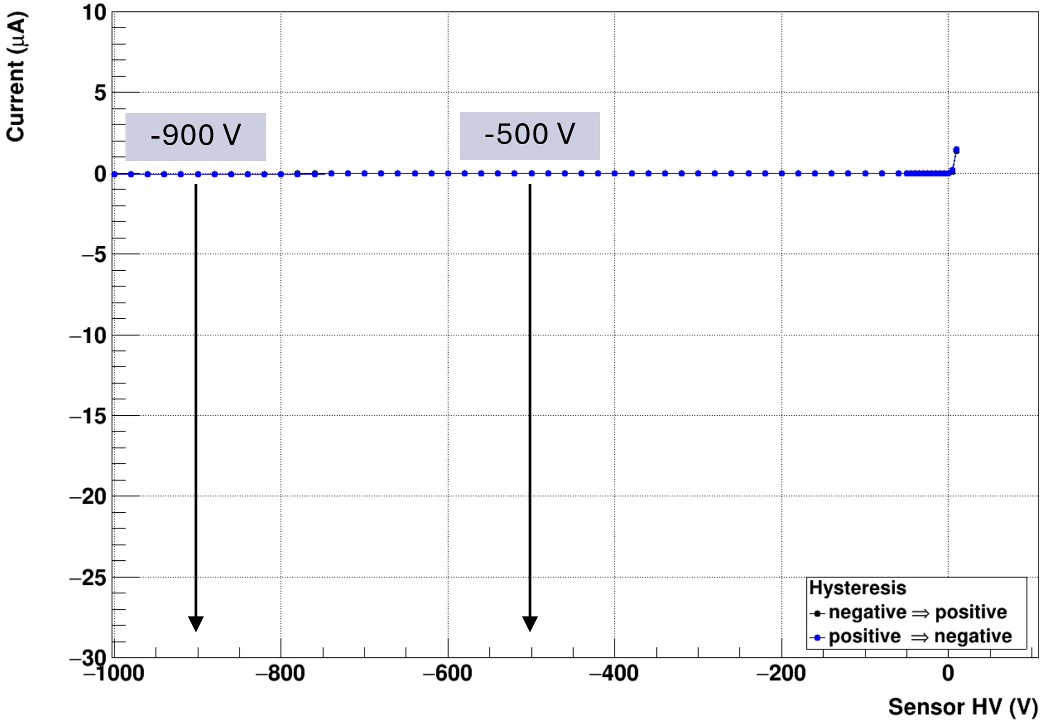

- **Surprise:**
  → **Each contact combintation** (Pt/CdZnTe/Au or Au/CdZnTe/Au) is **recifying**!
  → In **CdTe**, Pt/CdTe/Au or Au/CdTe/Au make **quasi-ohmic contacts**.
- **Comment on yield:**
  5x Assemblies received (JF1.1 + 3x CZT High Flux/2x CZT spectroscopic)
  → 2x Assemblies unusable (Both put JF1.1 in saturation in G2)
  → 1x CZT High Flux died after applying -900 V (according to specs)
  → 2x Assemblies alive (m401 CZT Spectroscopic + m343 CZT High Flux)

Leakage Current

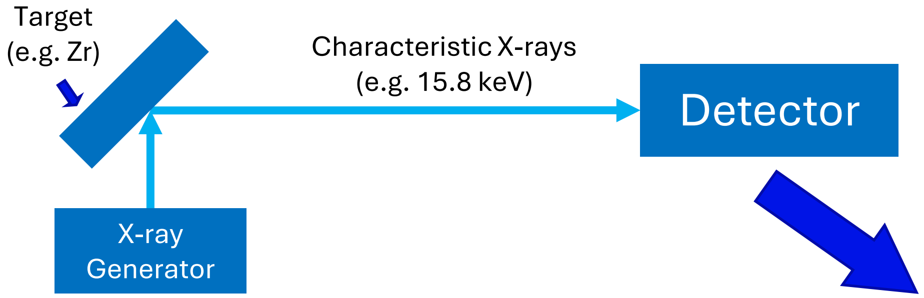

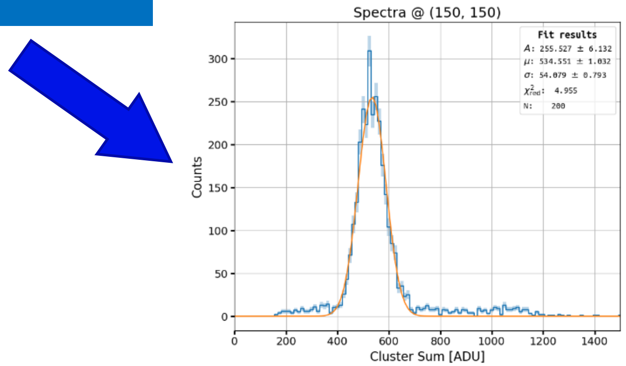

Integration Time (IT) Scan per pixel

- Measure the raw ADC values (ADU) a different integration times.

Apply **gain calibration**

- ADU → keV → e⁻ → Q
- Average e-h pair creation energy: ~ 4.43 eV
- 100 ADU (~ 3 keV) at 475 µs IT

Fit linear region (avoiding initial dip)

- Extract the leakage current (dQ/dt) from the gradient (E/t)

Note: Initial fall in ADU before 25 µs where it becomes linear

- Believed to be dominance of electronic effects
- Usually operated at a fixed integration time

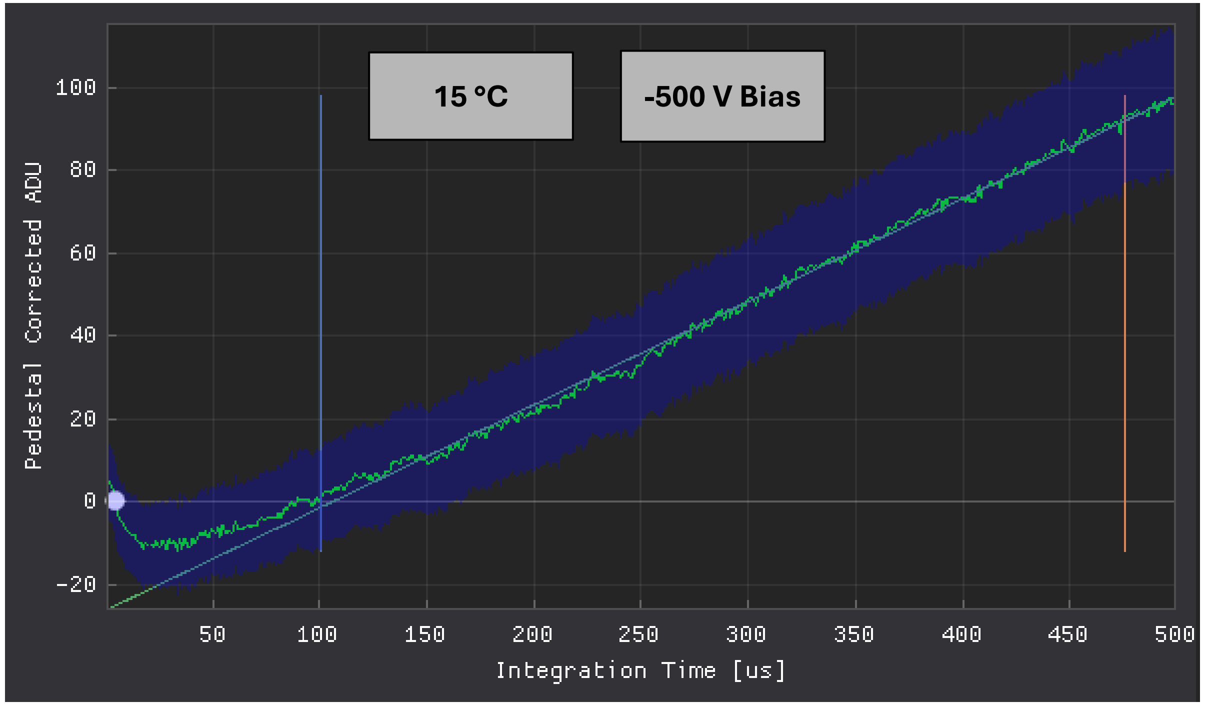

Scratches

Microscope scan

- **Different** Redlen CZT sensor (96x96 pixels)
- Scratches visible over the entire pixel array
- More scratches visible when zoomed in

clusters map

- Shows many more scratches
- More clusters found along scratches

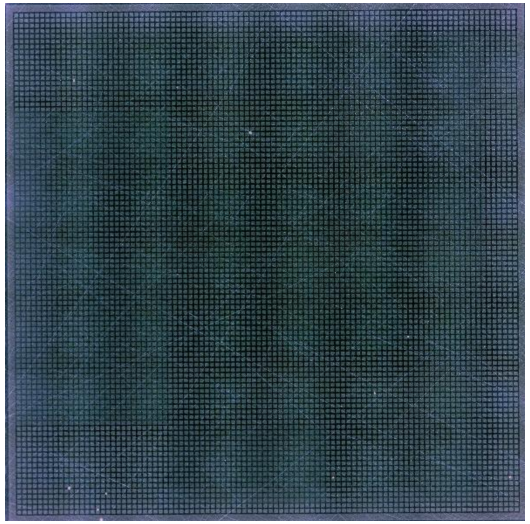

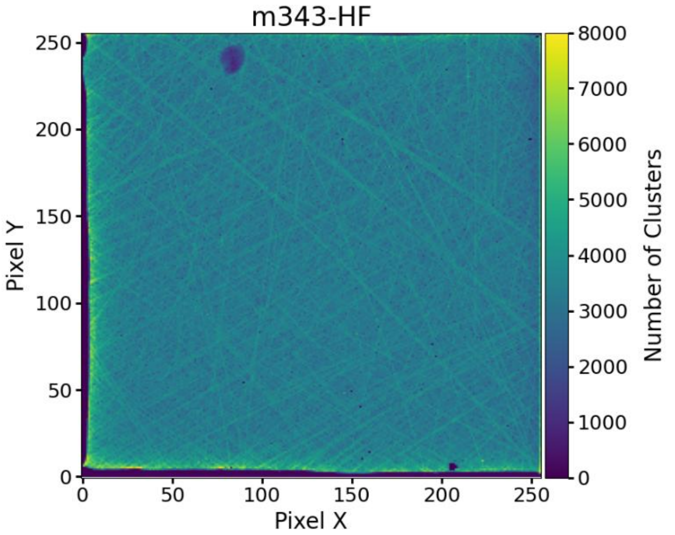

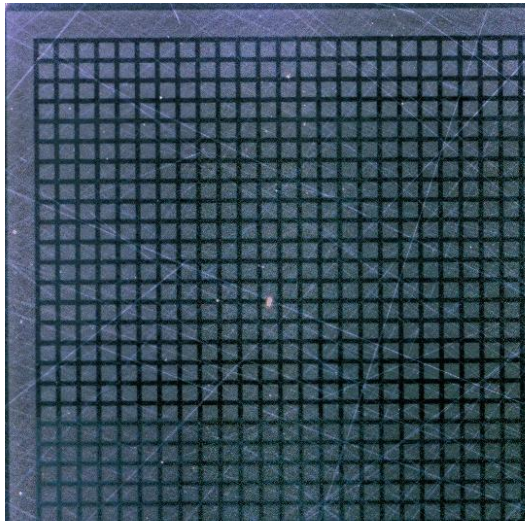

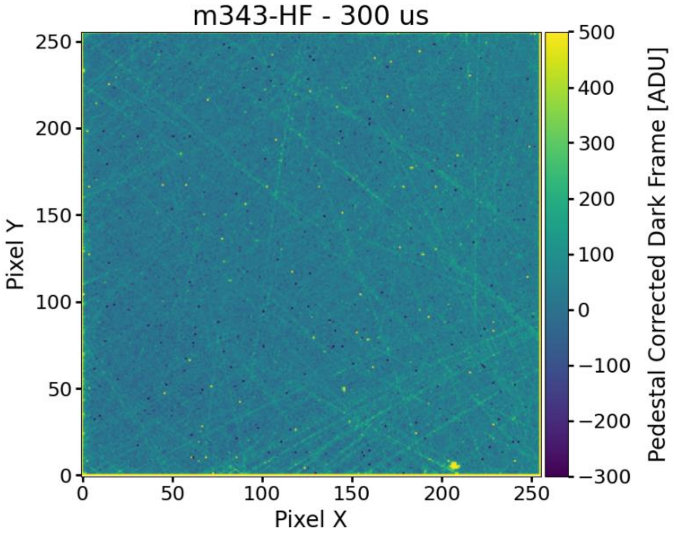

Clusters From Calibration

Healthy # of clusters

Details more apparent

- Defect structure in SP
- Many more scratches than in IT scan

Reduced # due to:

- Scratch on backside
- HV Solder

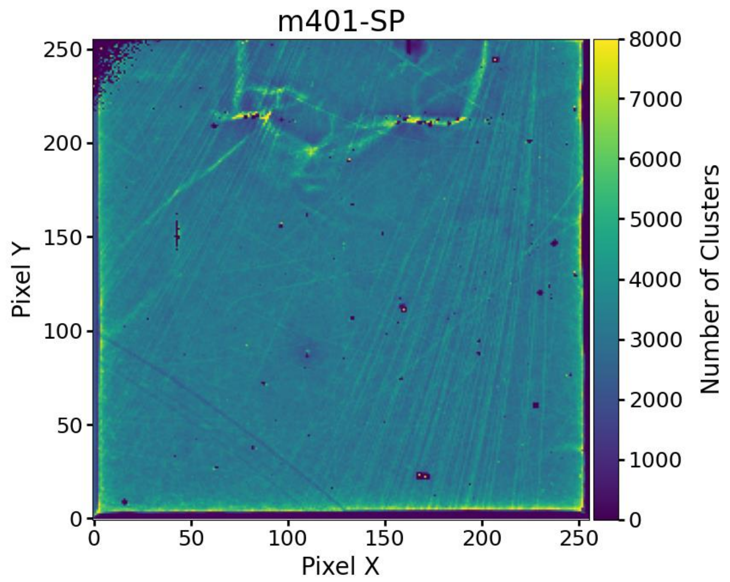

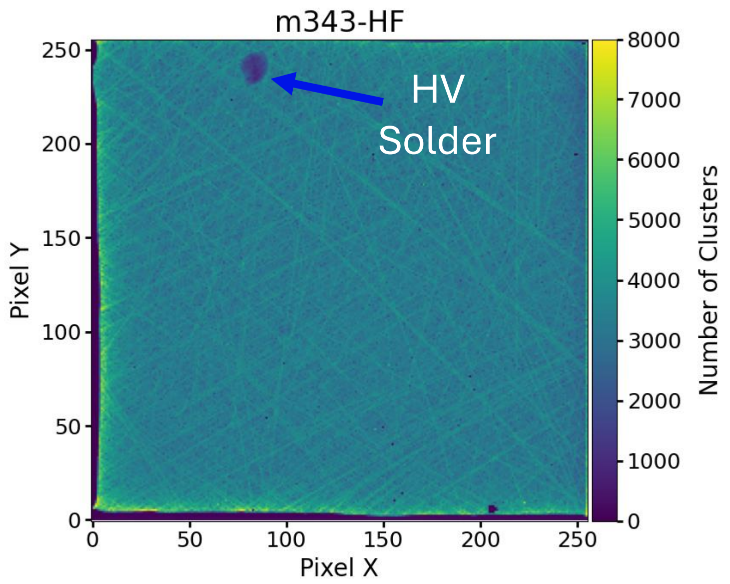

Energy Resolution

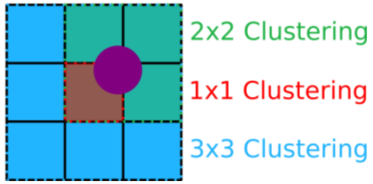

15 °C | **-500 V Bias** | **5 µs Int. Time**

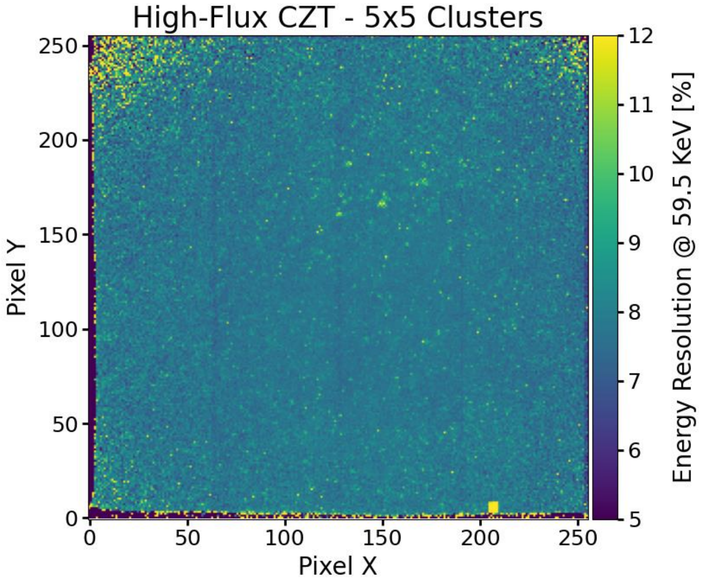

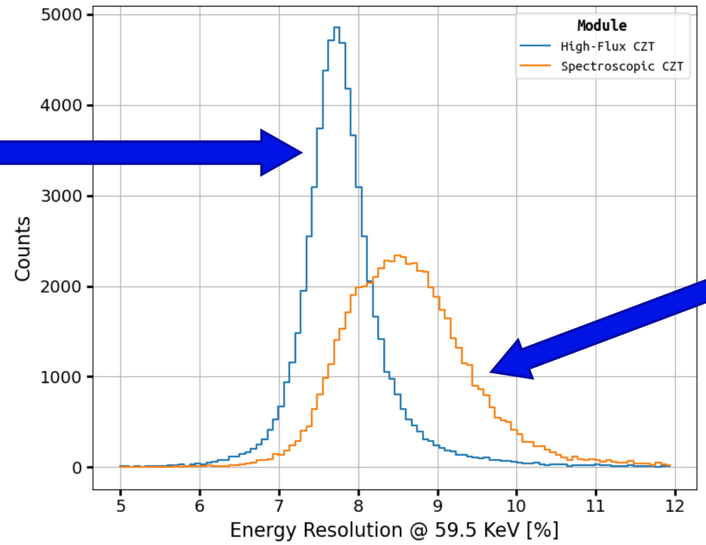

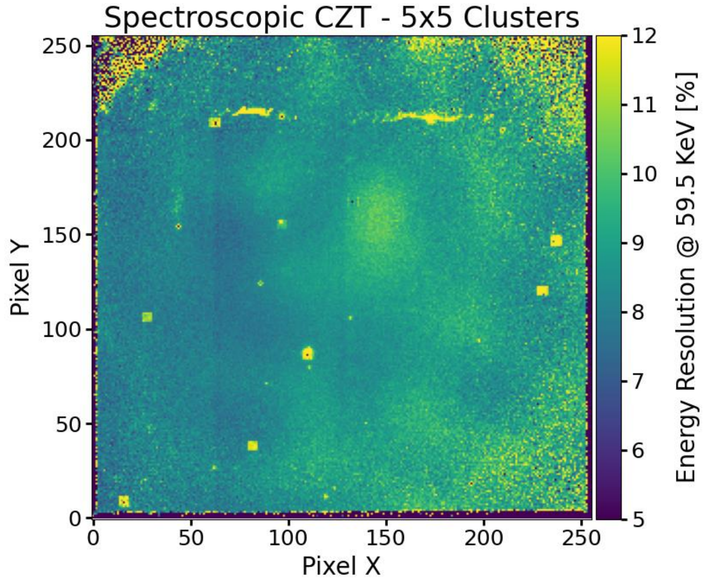

Energy Resolution with **5x5 clusters**

- **High-Flux is better than Spectroscopic**

Spectroscopic is also less uniform

- Corners likely due to low statistics

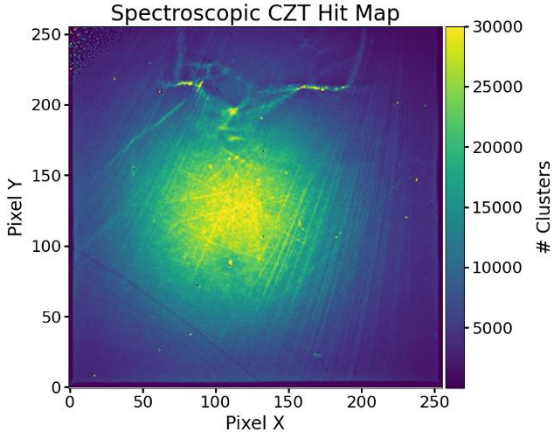

Interpolation with CZT

Spectroscopic CZT

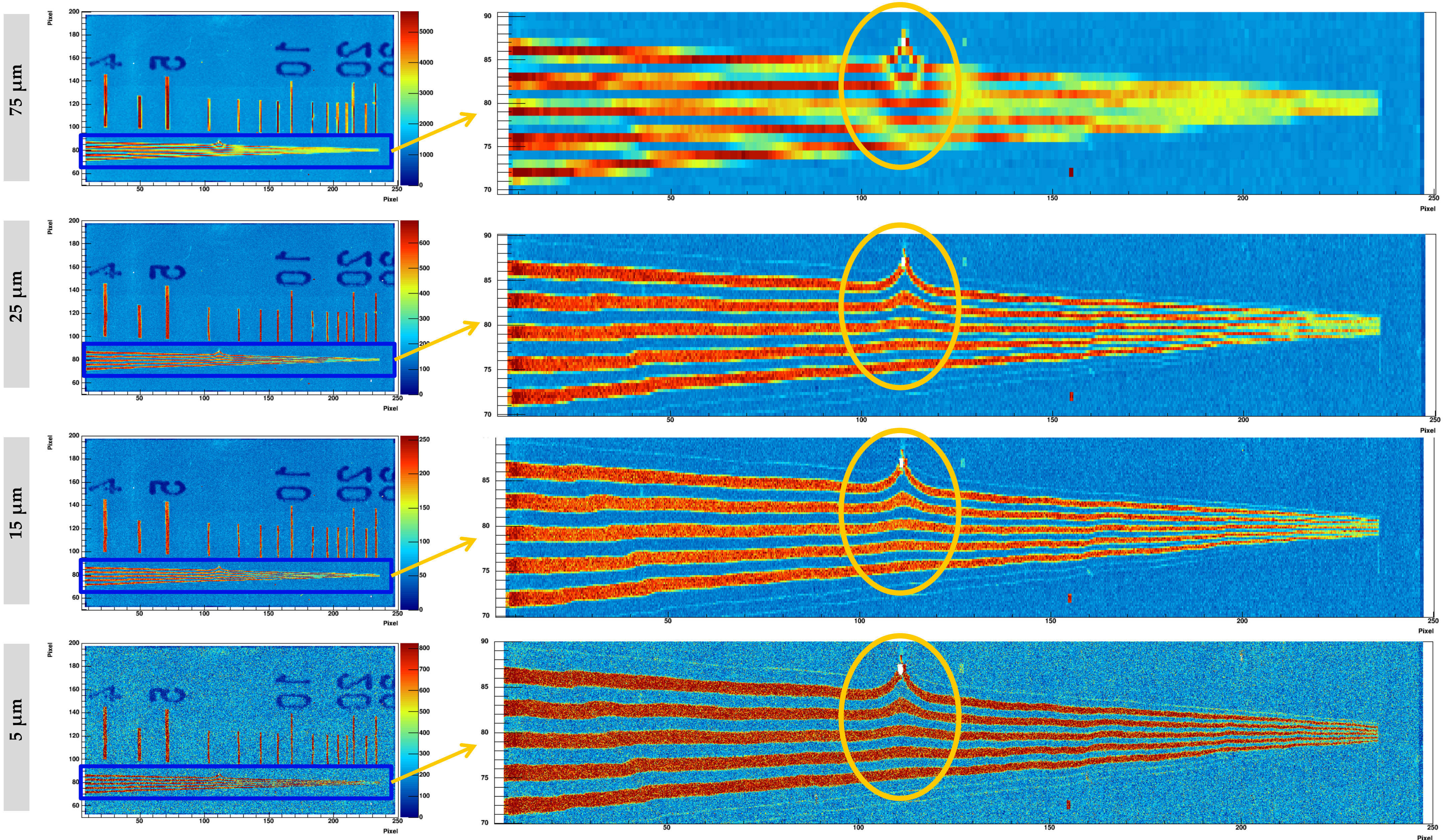

Courtesy of
D. Greiffenberg

A Minor Blemish...

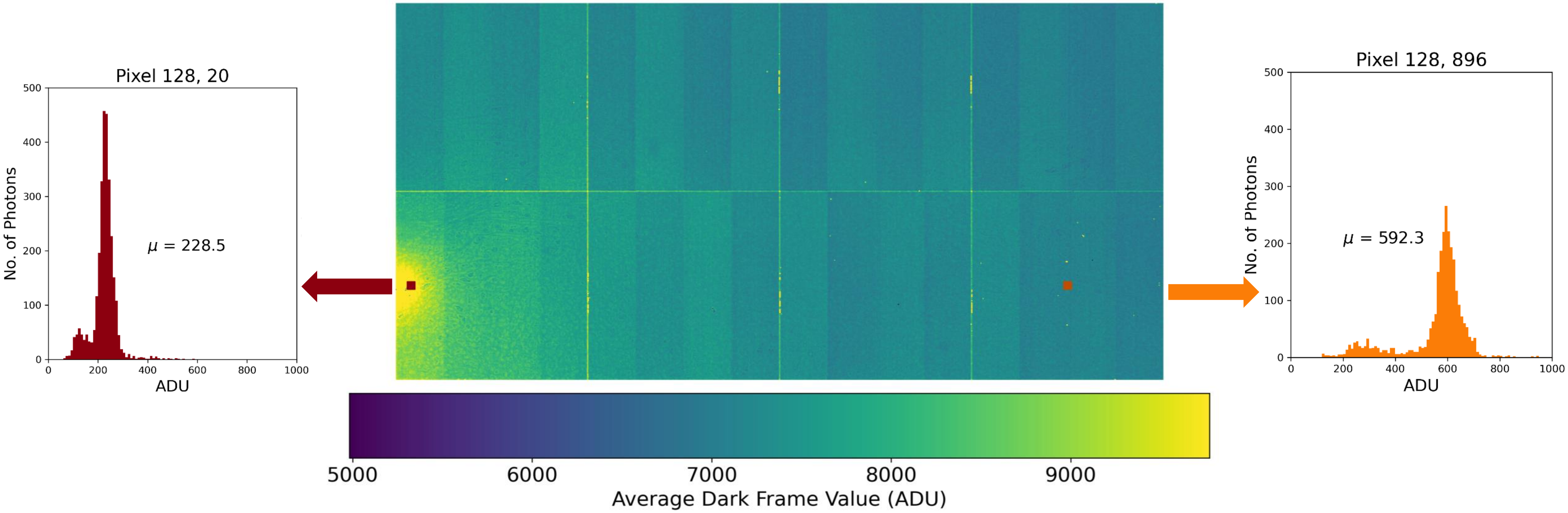

IT Scan

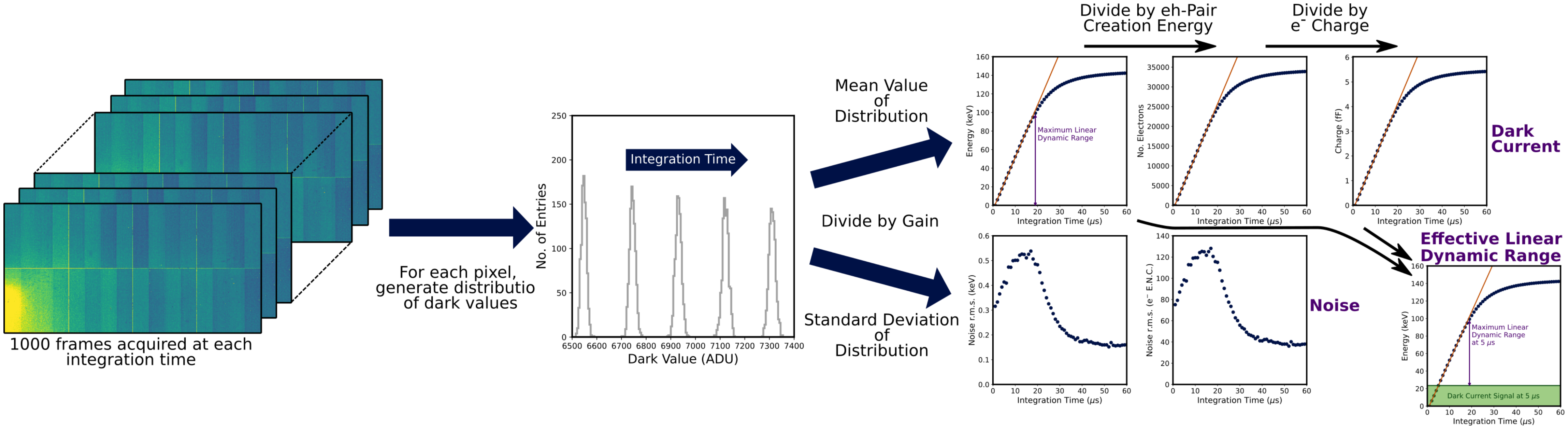

Courtesy of K. A. Paton

Hecht Measurements

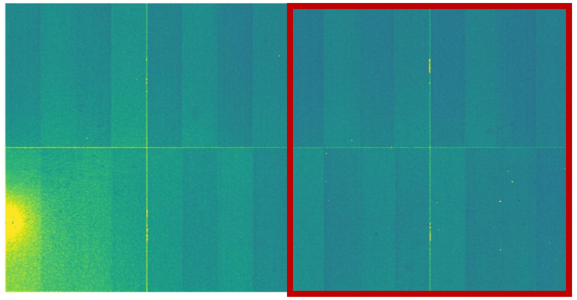

$$Q(U) = Q_0 \cdot \underbrace{\left[\exp\left(-\frac{(d-D)\cdot d}{\mu\cdot\tau\cdot(U-U_0)}\right)\right]}_{\text{Charge traping}} \cdot \underbrace{\left[\frac{\mu\cdot\tau\cdot(U-U_0)}{D\cdot d}\cdot\left[1-\exp\left(-\frac{D\cdot d}{\mu\cdot\tau\cdot(U-U_0)}\right)\right]\right]}_{\text{Signal induction}}$$

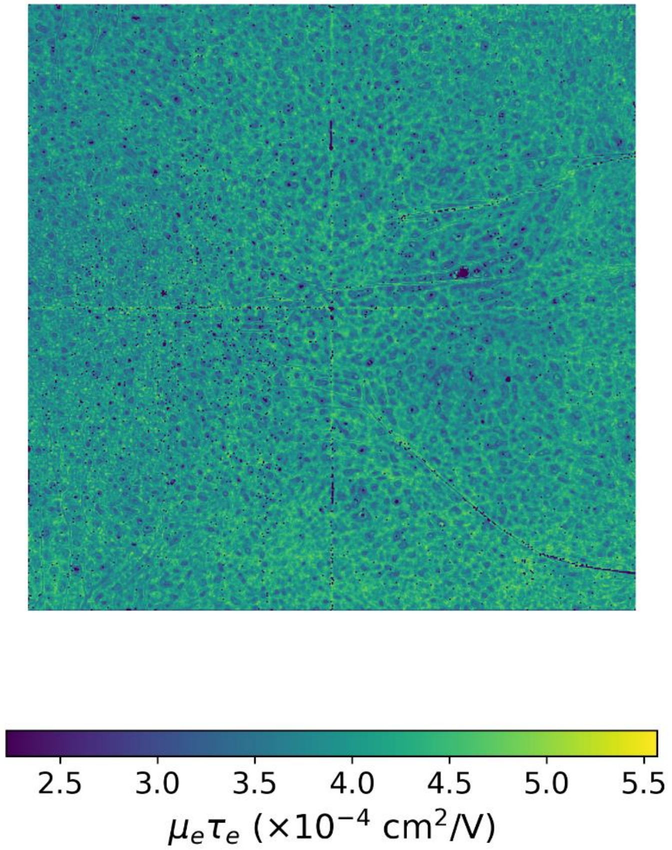

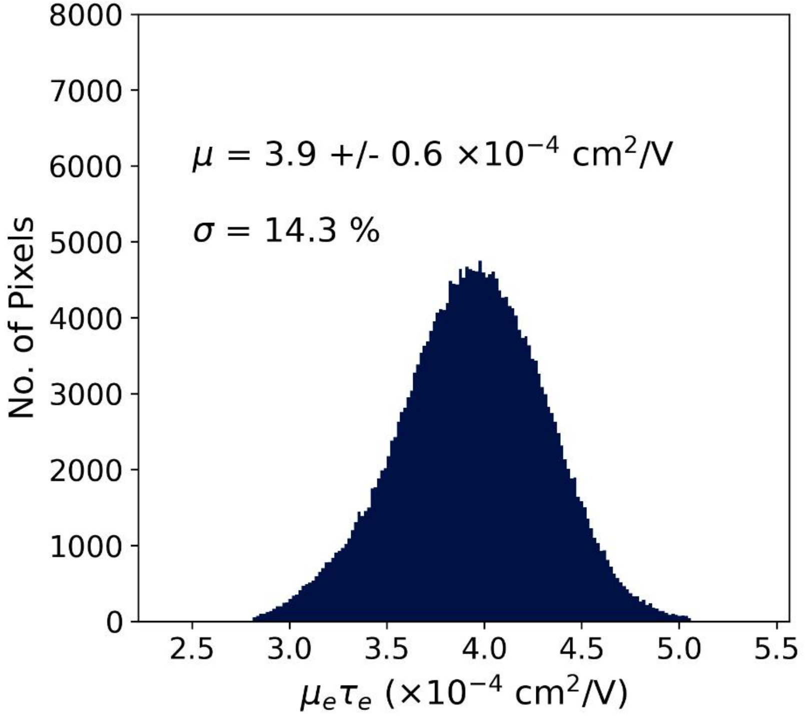

2016 TSU - 1.83 × 10^{-4} cm^2/V

2017 TSU - 4.73 × 10^{-4} cm^2/V

Interpolation with GaAs

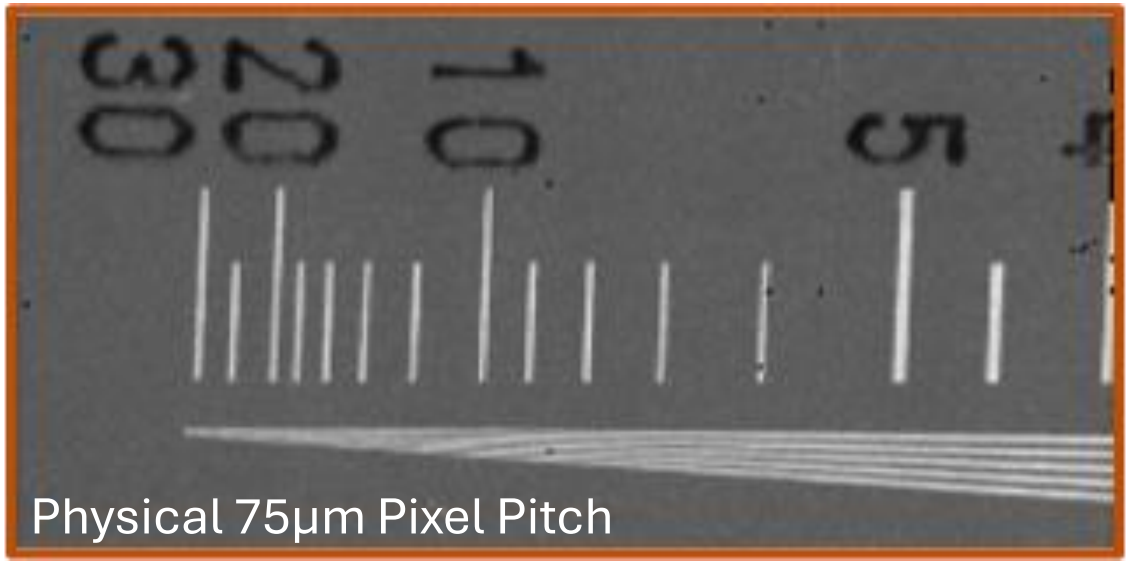

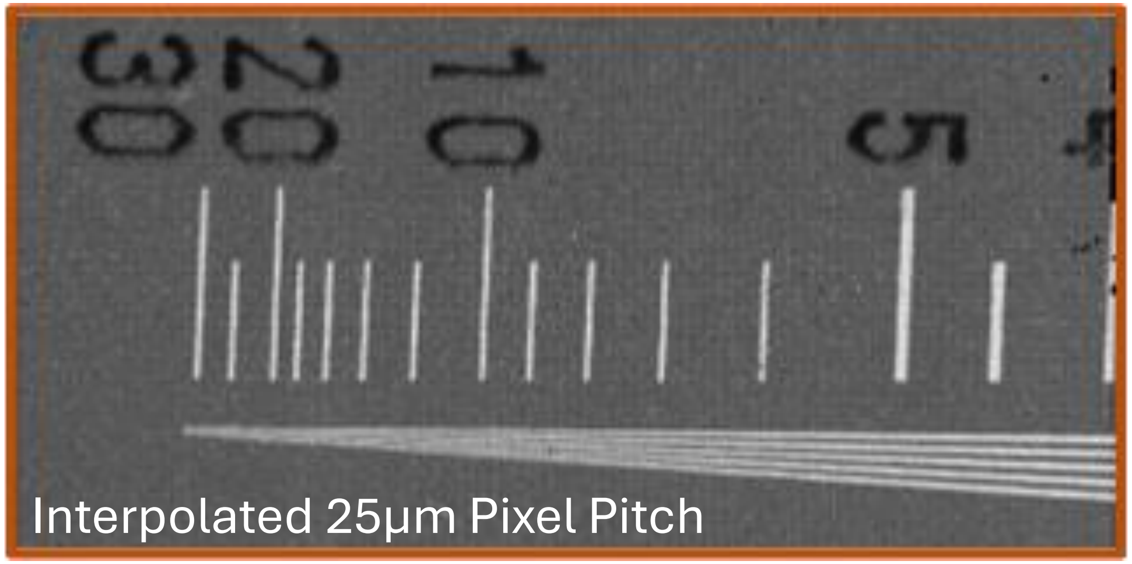

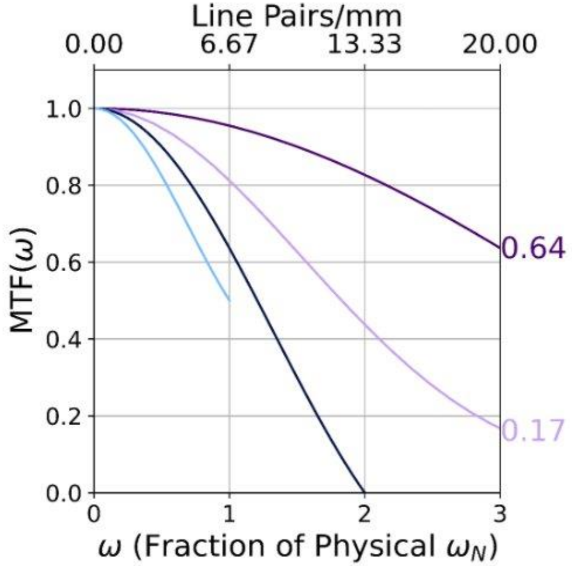

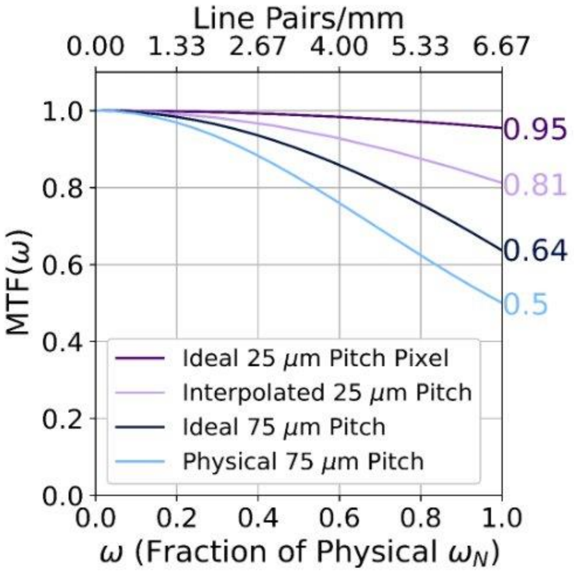

Imaging

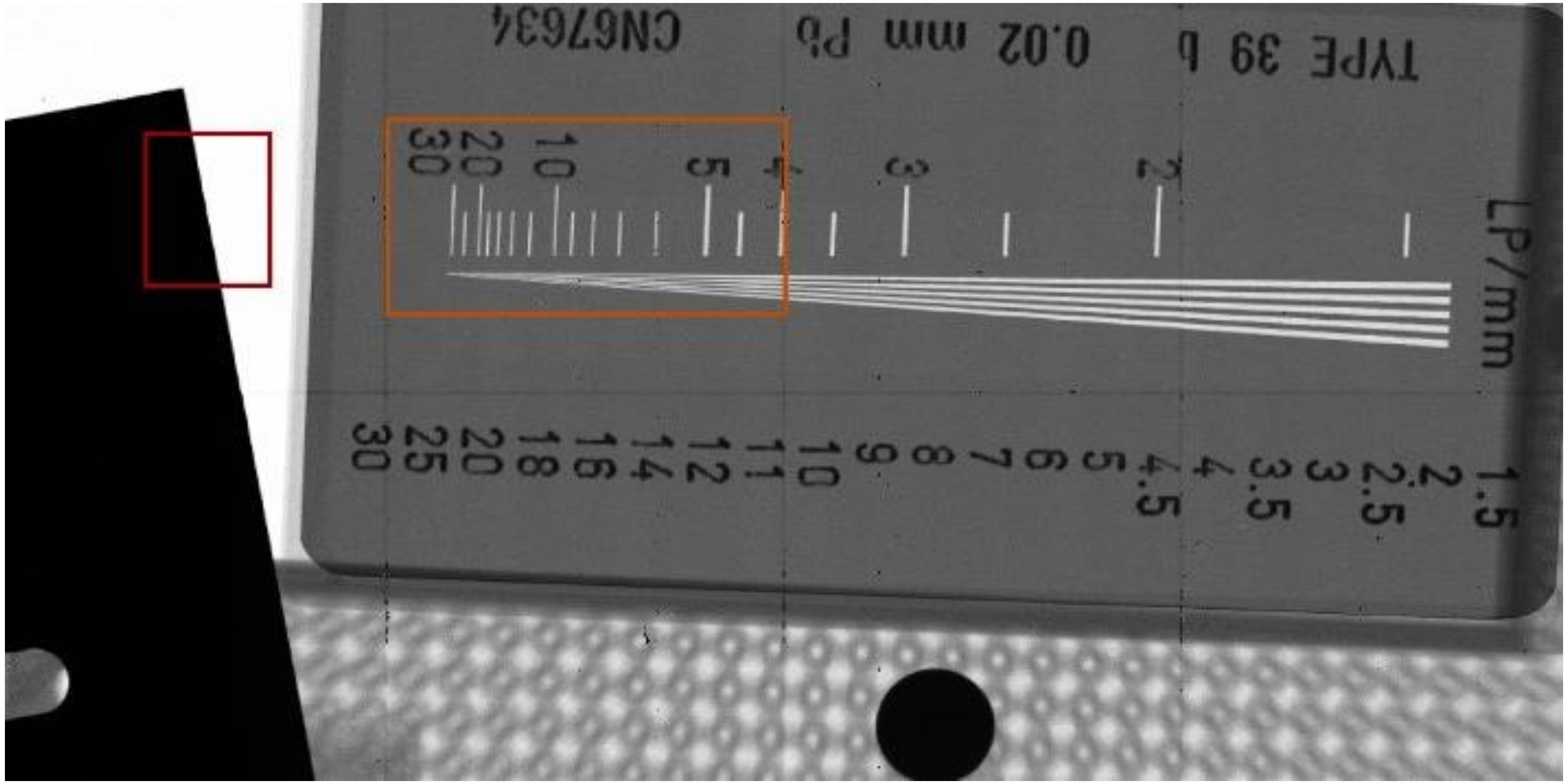

- Hamamatsu microfocused X-ray tube
- 40 kV peak voltage
- 30 uA current
- Flat field corrected (~ 2 h for each dataset)

Imaging

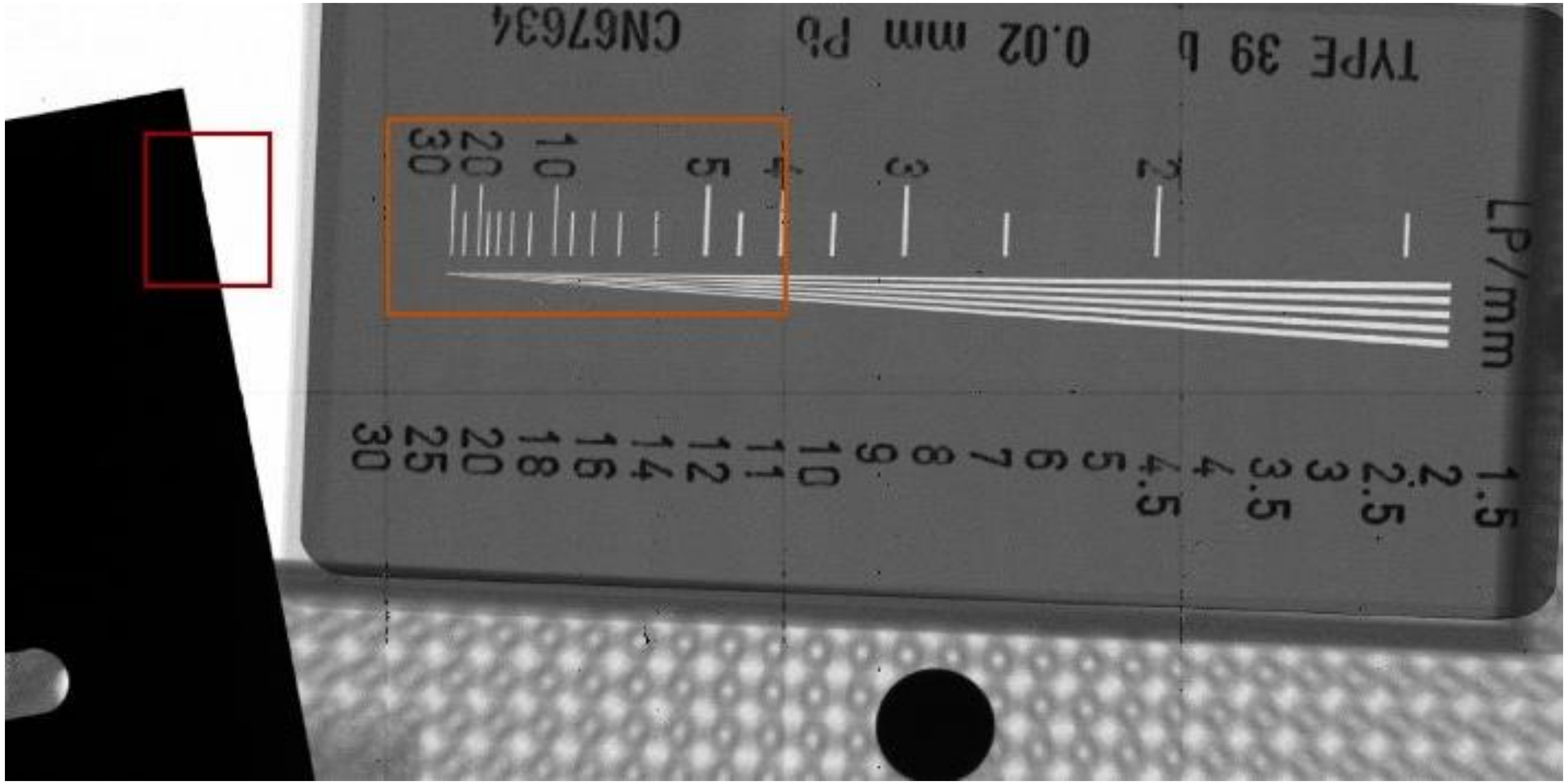

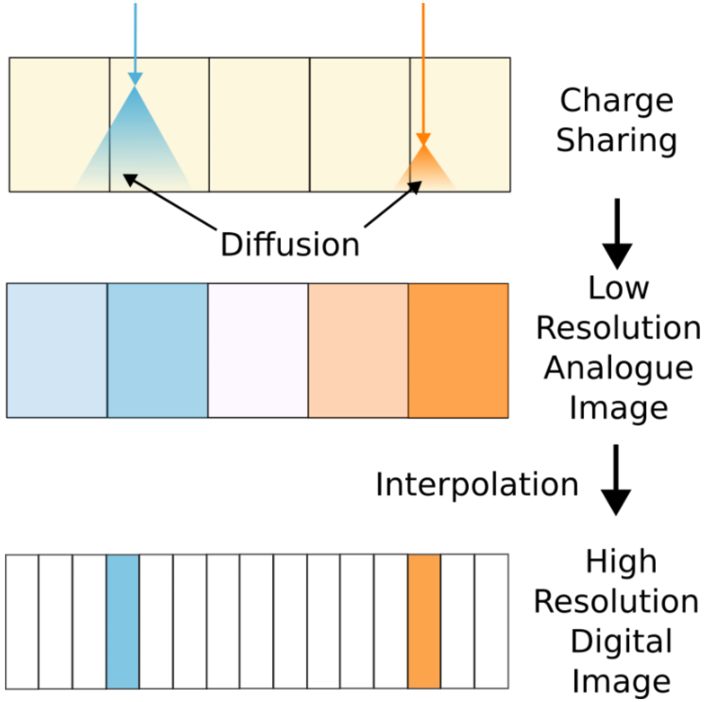

See S. Cartier et al, JInst (2014) for more details

Results Summary

PSI

	Leakage Current Per Pixel [pA]	Noise [keV]	$\mu_e \cdot \tau_e$ [$x10^{-3}$ cm^2/V]	Energy Resolution at 60 keV [%]
Silicon	~ 2	0.23	> 1 **	Can't detect 60 keV
CZT High Flux	0.18	0.28	10	5.8
CZT Spectroscopic	0.49	0.29	14	6.5
CdTe Schottkey	~ 0.76	~ 0.5	1.9 *	5.6 *
GaAs:Cr	190	0.41	0.39	4.68

* Measured with Time-Pix rather than JUNGFRAU [11]

** For both electrons and holes

Papers

GaAs:Cr

D. Greiffenberg et al., JInst, (2017)

D. Greiffenberg et al., Sensors (2021)

CdTe

M . Markus et al., JInst (2022)

Signal Stability

D. Greiffenberg et al. Jinst (2025)

Afterglow

Coming Soon™

CZT

Coming Soon™

X-RAY SENSORS

1st Joint X-ray Sensor Workshop
From Soft to Hard X-rays
ETH Zurich (Switzerland)
12.-16. January 2026

SOFT X-RAY DETECTORS
12-14 JANUARY 2026

Bridging Science and Detection Technology for Soft X-ray Applications

HiZPAD
15-16 JANUARY 2026

High-Z Pixel Array Detectors for Photon Science

Webpage:
https://indico.psi.ch/e/XRaySensors2026